



AFRL-RX-TY-TR-2011-0024

**BENDING AND SHEAR INTERACTION
BEHAVIOR OF UPGRADED CONVENTIONAL
COLD-FORMED STEEL CONNECTIONS TO
PROTECT AGAINST MODERATE BLAST
EVENTS**

Bryan Bewick
Airbase Technologies Division
Air Force Research Laboratory
139 Barnes Drive, Suite 2
Tyndall Air Force Base, FL 32403-5323

Hani Salim and Brett Agee
University of Missouri-Columbia
Department of Civil and Environmental Engineering
E2509 Lafferre Hall
Columbia, MO 65211-2200

Contract No. FA4819-10-C-0007

January 2011

DISTRIBUTION A: Approved for public release; distribution unlimited.
88ABW-2011-4144, 27 July 2011.

**AIR FORCE RESEARCH LABORATORY
MATERIALS AND MANUFACTURING DIRECTORATE**

NOTICE AND SIGNATURE PAGE

Using Government drawings, specifications, or other data included in this document for any purpose other than Government procurement does not in any way obligate the U.S. Government. The fact that the Government formulated or supplied the drawings, specifications, or other data does not license the holder or any other person or corporation; or convey any rights or permission to manufacture, use, or sell any patented invention that may relate to them.

This report was cleared for public release by the 88th Air Base Wing Public Affairs Office at Wright Patterson Air Force Base, Ohio and is available to the general public, including foreign nationals. Copies may be obtained from the Defense Technical Information Center (DTIC) (<http://www.dtic.mil>).

AFRL-RX-TY-TR-2011-0024 HAS BEEN REVIEWED AND IS APPROVED FOR PUBLICATION IN ACCORDANCE WITH ASSIGNED DISTRIBUTION STATEMENT.

**BEWICK.BRYAN.
T.1290370414**

Digitally signed by BEWICK.BRYAN.T.1290370414
DN: c=US, o=U.S. Government, ou=DoD, ou=PKI,
ou=USAF, cn=BEWICK.BRYAN.T.1290370414
Date: 2011.04.25 16:12:47 -05'00'

BRYAN T. BEWICK
Work Unit Manager

**RICHLIN.DEBRA.L.
.1034494149**

Digitally signed by RICHLIN.DEBRA.L.1034494149
DN: c=US, o=U.S. Government, ou=DoD, ou=PKI,
ou=USAF, cn=RICHLIN.DEBRA.L.1034494149
Date: 2011.04.26 15:36:02 -05'00'

DEBRA L. RICHLIN, DR-III
Acting Chief, Airbase Engineering
Development Branch

**RHODES.ALBERT
.N.III.1175488622**

Digitally signed by
RHODES.ALBERT.N.III.1175488622
DN: c=US, o=U.S. Government, ou=DoD, ou=PKI,
ou=USAF, cn=RHODES.ALBERT.N.III.1175488622
Date: 2011.07.25 12:04:19 -05'00'

ALBERT N. RHODES, PhD
Chief, Airbase Technologies Division

This report is published in the interest of scientific and technical information exchange, and its publication does not constitute the Government's approval or disapproval of its ideas or findings.

REPORT DOCUMENTATION PAGE

*Form Approved
OMB No. 0704-0188*

The public reporting burden for this collection of information is estimated to average 1 hour per response, including the time for reviewing instructions, searching existing data sources, gathering and maintaining the data needed, and completing and reviewing the collection of information. Send comments regarding this burden estimate or any other aspect of this collection of information, including suggestions for reducing the burden, to Department of Defense, Washington Headquarters Services, Directorate for Information Operations and Reports (0704-0188), 1215 Jefferson Davis Highway, Suite 1204, Arlington, VA 22202-4302. Respondents should be aware that notwithstanding any other provision of law, no person shall be subject to any penalty for failing to comply with a collection of information if it does not display a currently valid OMB control number.

PLEASE DO NOT RETURN YOUR FORM TO THE ABOVE ADDRESS.

1. REPORT DATE (DD-MM-YYYY)			2. REPORT TYPE		3. DATES COVERED (From - To)	
4. TITLE AND SUBTITLE					5a. CONTRACT NUMBER	
					5b. GRANT NUMBER	
					5c. PROGRAM ELEMENT NUMBER	
6. AUTHOR(S)					5d. PROJECT NUMBER	
					5e. TASK NUMBER	
					5f. WORK UNIT NUMBER	
7. PERFORMING ORGANIZATION NAME(S) AND ADDRESS(ES)					8. PERFORMING ORGANIZATION REPORT NUMBER	
9. SPONSORING/MONITORING AGENCY NAME(S) AND ADDRESS(ES)					10. SPONSOR/MONITOR'S ACRONYM(S)	
					11. SPONSOR/MONITOR'S REPORT NUMBER(S)	
12. DISTRIBUTION/AVAILABILITY STATEMENT						
13. SUPPLEMENTARY NOTES						
14. ABSTRACT						
15. SUBJECT TERMS						
16. SECURITY CLASSIFICATION OF:			17. LIMITATION OF ABSTRACT	18. NUMBER OF PAGES	19a. NAME OF RESPONSIBLE PERSON	
a. REPORT	b. ABSTRACT	c. THIS PAGE			19b. TELEPHONE NUMBER (Include area code)	

TABLE OF CONTENTS

LIST OF FIGURES	iii
LIST OF TABLES	v
LIST OF EQUATIONS	v
1. EXECUTIVE SUMMARY	1
2. INTRODUCTION	2
2.1. General	2
2.2. Objective	3
2.3. Approach	4
2.4. Scope	4
3. LITERATURE REVIEW	5
3.1. Objectives	5
3.2. General	5
3.3. Idealizing Blast Loads	6
3.4. Cold Formed Steel Properties	6
3.5. Bolted Angle Connection	6
3.6. Hybrid Connection and Steel Sheet Walls	7
3.7. Web Crippling Tests	8
3.8. Dynamic Modeling	9
3.9. Unified Facilities Criteria (UFC)	10
4. EXPERIMENTAL EVALUATION	11
4.1. Objective	11
4.2. Short-Beam Experimental Set-Up	11
4.3. Short-Beams Experimental Matrix	14
4.4. Analytical Predictions	15
4.4.1. Web Crippling	17
4.4.2. Shear of Stud	21
4.4.3. Lateral Torsional Buckling	21
4.4.4. Tilting and Bearing of Screw	22
4.4.5. Screw Pullout	22
4.4.6. Screw Pullover	23
4.5. Coupon Tension Tests	23
5. TEST RESULTS	25
5.1. General	25
5.2. Results	25
5.3. Trends	26
5.3.1. Maximum Capacity	27
5.3.2. Toughness	30
5.4. Short-Beam Failure Modes	33
5.4.1. Failure Mode 1	33
5.4.2. Failure Mode 2	34
5.4.3. Failure Mode 3	35
5.4.4. Failure Mode 4	37
5.5. Discussion	38
6. FULL-LENGTH BEAM SAMPLES	41
6.1. Objective	41

6.2.	Experimental Set-Up.....	41
6.3.	Results.....	44
6.4.	Discussion.....	44
7.	CONCLUSIONS AND RECOMMENDATIONS	49
7.1.	Conclusions.....	49
7.2.	Recommendations.....	49
8.	REFERENCES	51
	Appendix A: Short-Beam Data	52
	Appendix B: Full Length Beam Data	103
	Appendix C: Allowable Response Limits (developed by US Army Corps of Engineers, PDC).....	129
	LIST OF SYMBOLS, ABBREVIATIONS, AND ACRONYMS	130

LIST OF FIGURES

Figure	Page
1. Threat Level Gap	2
2. Conventional Steel Stud Wall ^[3]	3
3. Conventional Steel Stud Wall Connection	4
4. Blast Wave Propagation ^[6]	5
5. Blast Wave Parameters ^[6]	6
6. BREW Steel Stud Connection Detail ^[10]	7
7. Steel Stud System Heavily Stiffened ^[1]	8
8. Resistance Curve of Heavily Stiffened Sample ^[1]	8
9. Loading Scenarios for AISI Web Crippling Tests ^[13]	9
10. Beam Idealized as a Single-Degree-of-Freedom System ^[15]	10
11. UFC Support Deflection Angle	10
12. Short-Beam Test Loading Frame Drawing	11
13. Short-Beam Test Loading Diagram	12
14. Deflection Measurement Locations	12
15. Typical Short-Beam Sample Prior to Testing	13
16. Typical Connection Detail	13
17. Coupon Testing Extensometer	23
18. Coupon Testing MTS Set-up	23
19. Sample Tension Test Stress–Strain Curve	24
20. Maximum Strength vs. Number of Screws	27
21. Maximum Strength vs. Stud Gauge	28
22. Maximum Strength vs. Track Gauge	28
23. Maximum Strength vs. Length of Track Flange	29
24. Maximum Strength vs. Size of Screw	29
25. Toughness vs. Number of Screws	30
26. Toughness vs. Size of Screw	31
27. Toughness vs. Stud Gauge	31
28. Toughness vs. Track Gauge	32
29. Toughness vs. Length of Track Flange	32
30. Crippling of Stud	33
31. Screw Pulling Out	33
32. Typical Load–Displacement Plot of Failure Mode One	34
33. Stud Crippling at Mid-Span	34
34. Screws after Shearing Due to Torsional Load	35
35. Typical Load–Displacement Plot of Failure Mode Two	35
36. Failure of Track Flange	36
37. Typical Load–Displacement Plot of Failure Mode Three	36
38. Tension Development	37
39. Typical Load–Displacement Plot of Failure Mode Four	37
40. Load–Deflection Plots for One and Six Screws	38
41. Load–Deflection Plots for Two, Four and Six Screws	39
42. Load–Deflection Plots for 1.5-in and 3-in Flanges	39
43. Load–Displacement Plots for 14- and 16-gauge Track	40
44. Ten-foot 16-point Loading Tree Diagram	41

45.	Ten-foot Sample Deflection Measurement Locations	41
46.	Ten-foot Sample Support.....	42
47.	Ten-foot Sample Prior to Testing	43
48.	Ten-foot Sample Deflection Gauge Locations	43
49.	Failure of Track-to-Floor Connection.....	45
50.	Load–Displacement Plots for #8, #10, and #12 Screws	45
51.	Load vs. Displacement for 1 and 2 #10 Screws.....	46
52.	Load–Displacement Plot for 1.5-in and 3-in Flanges	47
53.	Toughness vs. Number of Screws Comparison (All Samples).....	47
54.	Toughness vs. Number of Screws Comparison (Similar Samples)	48
55.	Toughness vs. Size of Screw Comparison.....	48

LIST OF TABLES

Table		Page
1.	Experimental Matrix for Tests with 6-inch Studs.....	14
2.	Analytical Predictions.....	15
3.	Tension Testing Data.....	17
4.	Tension Testing Summary.....	24
5.	Web Crippling Response (20-gauge Samples).....	25
6.	Web Crippling Response (16-gauge Samples).....	26
7.	Web Crippling Response (12-gauge Samples).....	27
8.	Strength Increase Comparison.....	38
9.	Ten-foot Sample Matrix.....	42
10.	Ten-foot Samples Results.....	44

LIST OF EQUATIONS

Equation		Page
1	6
2	9
3	9
4	17
5	21
6	21
7	21
8	21
9	21
10	21
11	21
12	21
13	22
14	22
15	22
16	23

1. EXECUTIVE SUMMARY

The cost of building a structure which is able to withstand blast events has caused many owners to forego added protection unless the threat is extremely high. If small changes to conventional design can be made that significantly increase the capabilities of a structure, many buildings will be able to provide this protection. One material being used to accomplish this is cold-formed steel. The high ductility and strength along with a vast array of upgradeable conventional construction details combine to make steel a very efficient material. Previous research has studied the behavior of steel to a great extent and can model the reaction to many loading scenarios, but blast event loading has not been sufficiently studied with these details.

The Air Force Research Laboratory (AFRL) has been conducting a research program to evaluate the effectiveness and feasibility of modifying conventional steel stud track wall systems to more effectively utilize the strength and ductility of the material without significantly increasing the cost of construction. The objective of this research is to focus on the web crippling behavior of enhanced conventional connections in order to quantify the bending and shear interaction of the proposed connection details in comparison with typical steel stud connection details. The approach is to evaluate the strength of various modifications to the standard connection detail for steel stud wall systems. All of the proposed modifications were selected to be a moderate change to traditional details, so that any strength increase would be practically implemented.

Results from tests of lighter-gauge samples show that tensile membrane action is fairly easily obtained and can be very useful in blast design. Engineers working with moderate blast threat levels should look into light-gauge steel stud systems and evaluate their effectiveness in their individual applications. By utilizing this extra capacity the material can be more efficiently used and will result in less wasted material. Heavier-gauge stud wall systems still have untapped strength that would drastically improve the practicality of using steel stud wall systems for blast design. Other connection methods should be pursued that carry a large amount of shear without a large amount of time or resources needed to install. These connections could begin to develop more capacity in the samples quickly. The Unified Facilities Criteria (UFC) limits should be re-evaluated based on the results of this project and the desired levels of protection. Development of a design guide to predict the response based on the connection design is recommended.

2. INTRODUCTION

2.1. General

Considering blast events when designing a structure is becoming increasingly important to prevent the loss of life that such a threat can cause. Unlike the over-designed concrete bunkers of previous generations, modern design is attempting to utilize all materials and components of a structure more efficiently. The cost of building a structure to resist blast events has caused many owners to forego the added protection unless the threat is extremely high. The gap between Department of State and Department of Defense research and design and that of typical wind loading, as shown in Figure 1, creates an area where blast resistant buildings are not constructed because a lack of knowledge. If small changes to conventional design can be made that significantly increase the capabilities of the structure, many buildings will be able to provide enhanced blast protection.

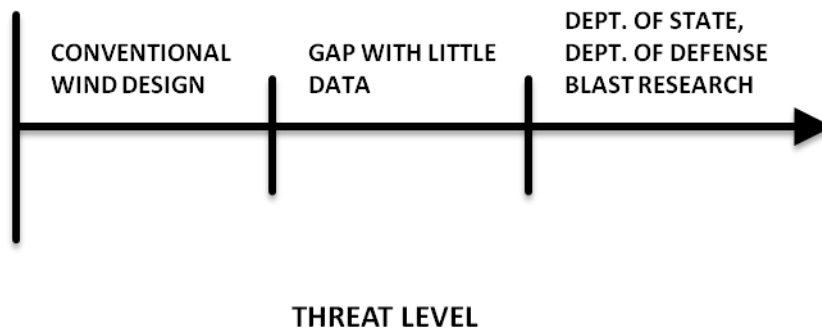


Figure 1. Threat Level Gap

One material being used to accomplish this is cold-formed steel. Its high ductility and strength along with a vast array of upgradeable conventional construction details combine to make steel a very efficient material^[1]. Previous research has studied the behavior of steel to a great extent with models for the reaction to many loading scenarios, but blast event loading has not been sufficiently studied with these details. The current project aims to evaluate small changes to conventional construction that can increase blast resistance. Tests were conducted by AFRL at Tyndall AFB in Florida to look individually at the bending, rotation, and tension response of the stud-track connection^[2]. By separating these failure mechanisms the individual capacities of each one can be found and compared to find the most efficient method of upgrading the connection. The task of this research was to evaluate the web crippling action (WCA) capacity of the connection details. This report is focused on finding small changes to typical wall construction that could significantly increase the web crippling and shear capacities and the cost effectiveness of having a moderately blast-resistant structure.

Cold-formed steel studs have inherent desirable properties for blast protection, such as strength and ductility. To be able to fully utilize these properties, the members and connections need to be efficiently designed to prevent any premature failures. Conventionally constructed steel stud walls are generally designed for wind loads, and thus the studs are not designed to undergo large deformations and support rotations as is normally expected in blast design. As a consequence,

conventional end connections are relatively weak and control the failure under blast loads. Therefore, the overall objective of the project is to measure the capacity of conventional connections and to modify their design to improve their resistance and rotation capacities. The project hopes to utilize conventional construction practices of using a track and screwed connections with efficiently designed track and screw layouts and quantities to enhance the flexural and tension membrane resistance of the stud wall. Because of this the axial, bending, rotational rigidity, and shear response of the connection needed to be investigated using these improved conventional connection details.

2.2. Objective

The objective of this research is to evaluate the effectiveness and feasibility of modifying conventional steel stud track wall systems (Figs. 2 and 3) to more effectively utilize the strength and ductility of the material without significantly increasing the cost of construction. The steps involved in this process are noted below:

- Consider previous research on similar topics
- Develop trial connection details that may increase strength
- Design a laboratory-scale quasi-static method for evaluating connection details
- Evaluate strength and ductility of these details



Figure 2. Conventional Steel Stud Wall^[3]

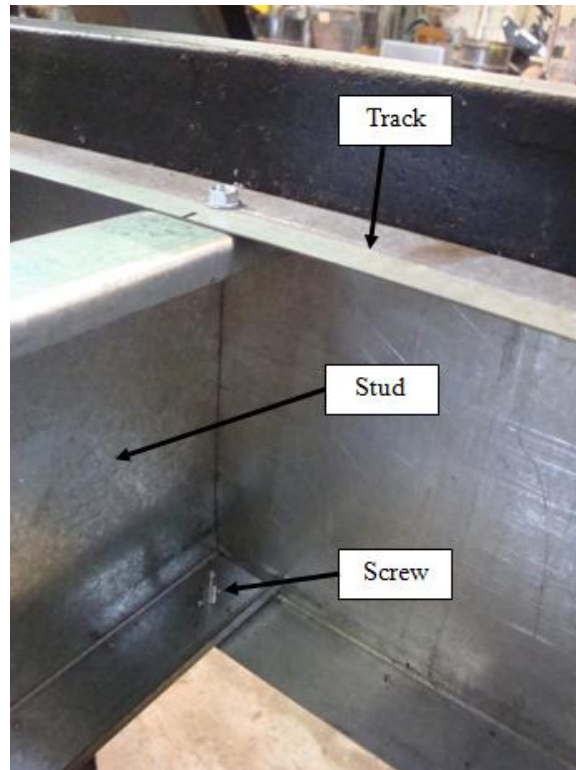


Figure 3. Conventional Steel Stud Wall Connection

2.3. Approach

The approach of this research is to evaluate the strength of various modifications to the standard connection detail for steel stud wall systems. The study begins by using 4-ft samples to isolate shear failures because the failure mode of typical wall systems is a shear failure near the connection. Three samples are included in the test matrix that are representative of current typical construction practice to serve as controls. Although the shear and moment diagrams will not be comparable to the full span tests, the shear failure will be very similar and will most likely control the full-span tests. Based on observations and evaluations of the short-beam samples, the next phase will be to predict the failure mode of standard 10-ft samples and test a small group of these samples to confirm the results.

2.4. Scope

This report begins with a brief review of applicable previous research in Section 3 followed by a description of the first phase of tests consisting of short-beam samples in Section 4. Also included in Section 4 are the equations on which the predictions are based. Section 5 tabulates the results and describes the trends observed, which are used in Section 6 to develop a test matrix of full-length beam samples. The test setup and results for the full-length samples are also in Section 6. Finally Section 7 provides conclusions based on this effort and recommendations for future work. In addition, load–displacement plots and pictures documenting the testing are provided in Appendices A and B and the Unified Facilities Criteria (UFC) rotation limit table is in Appendix C.

3. LITERATURE REVIEW

3.1. Objectives

This section presents a brief overview of blast design and some strategies that have been evaluated in the past both in general and for cold-formed steel. The design of blast-resistant structures has been an increasingly significant area as the threat of terrorist attacks to government and military facilities has increased over history. Protection levels vary depending on the importance of the structure. For example a hospital may require full functionality after a blast event while an office building may be designed to allow damage that would need to be repaired so long as the inhabitants are safe. These lower levels of protection—which allow significant deflections and inelastic yielding—are very efficient with their material usage and can be used in many more buildings.

3.2. General

Biggs^[4] describes a blast as a “circular shock front propagating away from the burst.” The impulse from this shock wave travels in all directions and will curve around objects to create overpressures on all surfaces nearby (Figure 4). Part of the energy of the blast is released as thermal radiation and part of it is transmitted to the ground as a shock wave^[5]. The wave has a large peak pressure and then quickly dissipates into a negative-pressure phase (Figure 5). The area under this curve is the impulse of the blast. The impulse has an associated energy that is converted into kinetic energy when it is applied to a surface, which in turn creates a momentum, which then loads the rest of the structure while it tries to impede the motion of the surface. One measure of blast resistance is toughness, defined as the area under the load–deflection or resistance curve. Toughness correlates to the amount of energy that a system can absorb during a blast event.

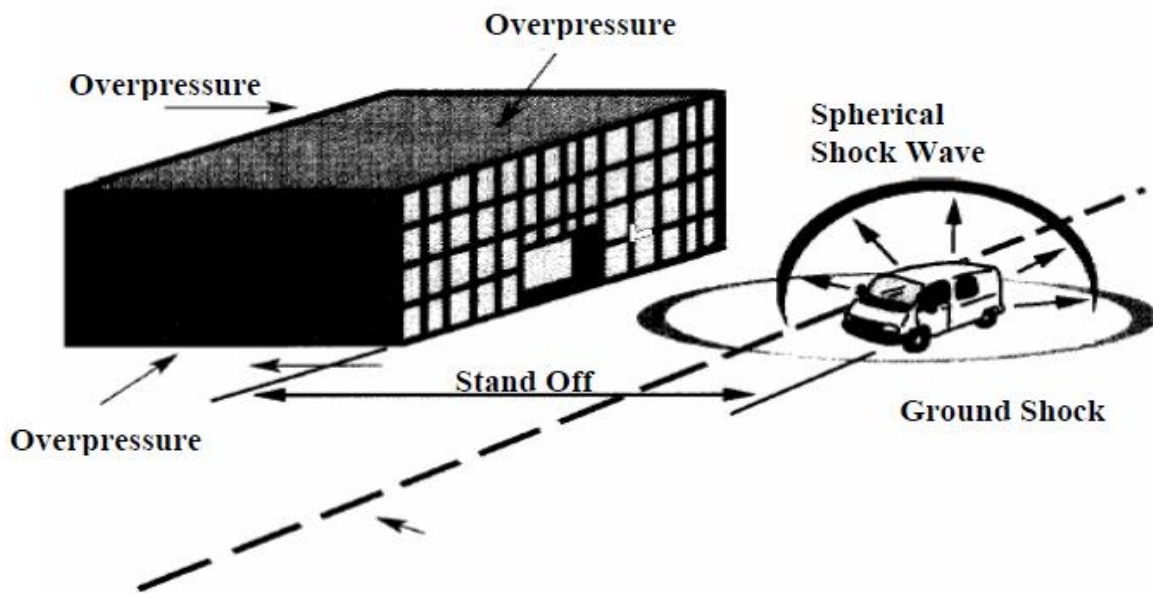


Figure 4. Blast Wave Propagation^[6]

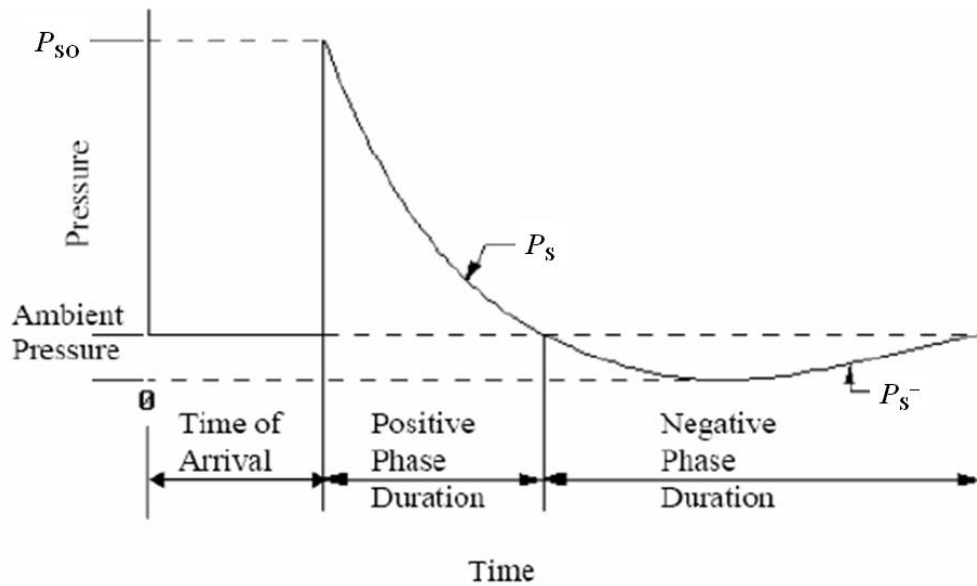


Figure 5. Blast Wave Parameters^[6]

3.3. Idealizing Blast Loads

The most common method of analyzing blast loads is using a triangular load history diagram^[7]. This involves a peak pressure, P_{so} , and a time duration of the blast, t_d . The pressure decreases linearly from the peak pressure to zero in the time of duration. A more accurate method of analyzing the blast wave is an exponential equation given as Equation 1.

$$P(t) = P_{SO} \left(1 - \frac{t}{t_d}\right) e^{-bt/t_d} \quad (1)$$

Where:

- P = pressure
- P_{SO} = peak pressure
- t = time
- t_d = time duration
- b = constant

3.4. Cold Formed Steel Properties

Cold-formed steel is a unique classification of steel that has been worked by rolling it into sheets and then bending those sheets into structural shapes so as to align the sub materials for better strength^[8]. With this working process, ductility is lost but strength is gained. The strength and ductility of steel are still very apparent in cold-formed sections. These attributes can be very useful for light-gauge applications such as framing^[9].

3.5. Bolted Angle Connection

Earlier research performed by Dinan in 2000 focused on significantly increasing the capacity of steel stud wall systems^[10]. This research included the Blast Resistant Exterior Wall (BREW) series, which focused on Department of Defense and Department of State threat levels. The project focused on finding a way to develop tensile membrane behavior in steel studs. The connection was heavily over-designed to keep the studs from failing at the connections. Steel sheet was added to the front of the wall to tie everything together and to prevent shrapnel from the explosion entering the building. The connection detail tested is shown in Figure 6. This project resulted in very high capacity and toughness, but is also very expensive and time consuming to construct.

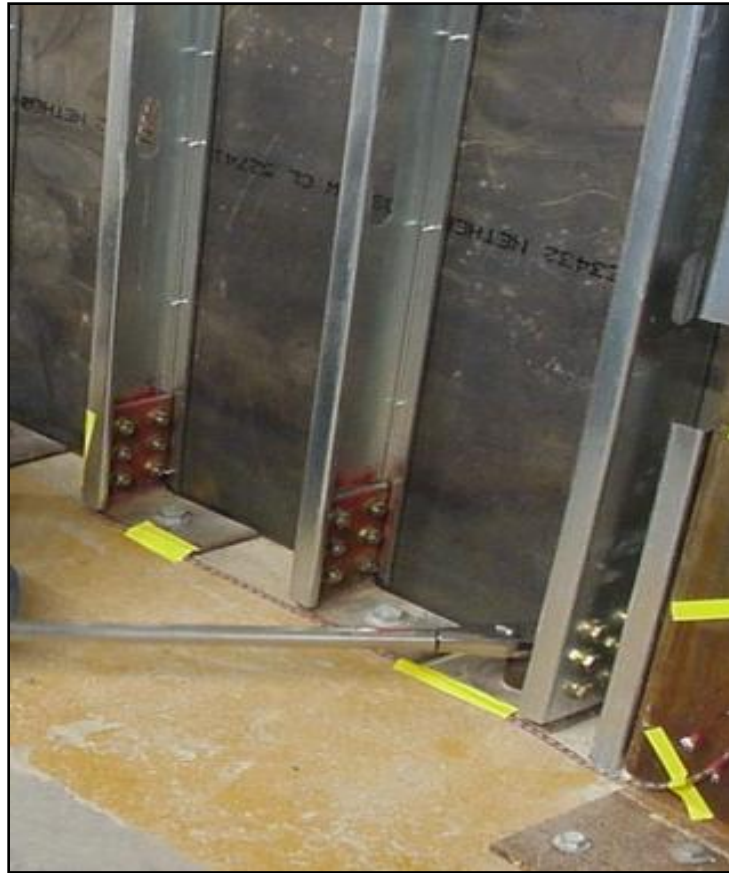


Figure 6. BREW Steel Stud Connection Detail^[10]

3.6. Hybrid Connection and Steel Sheet Walls

More recently, research with a similar goal to this project's (although for a higher threat level) consisted of supporting the stud system by a bearing angle and attaching a steel sheet to the front of the wall^[11] as seen in Figure 7. This significantly increased the pressure carried and changed the failure mode. Rather than failing at the connection, the plastic neutral axis was moved to the sheet side of the studs resulting in tension of the entire cross section of the stud^[11]. This failure was much more ductile and allowed for very high deflections as shown in Figure 8, but also came at a higher cost. The feasibility of this type of construction is restricted to high threat levels predominantly seen in military applications. Finding a way to use this tensile strength of the

studs without such a costly connection would drastically improve the feasibility of steel stud use for blast design^[11].



Figure 7. Steel Stud System Heavily Stiffened^[1]

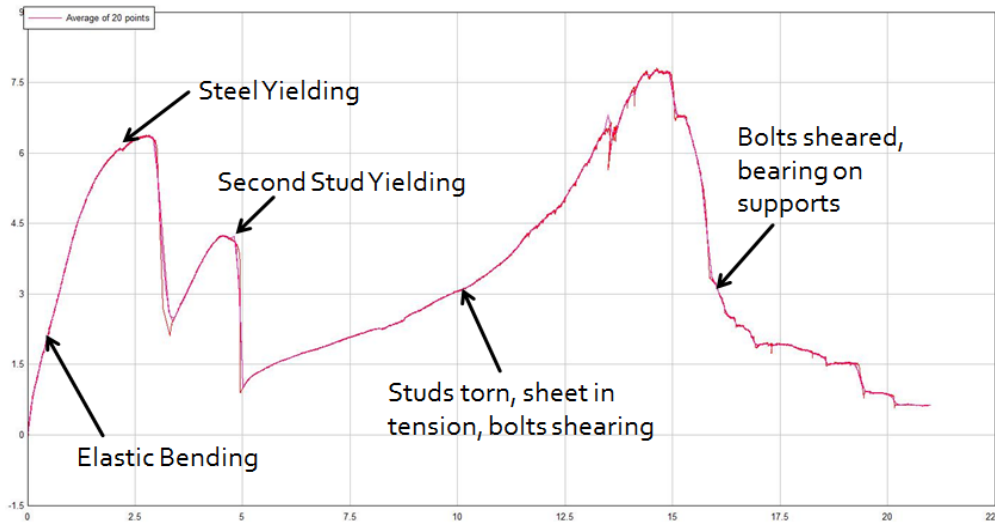


Figure 8. Resistance Curve of Heavily Stiffened Sample^[1]

3.7. Web Crippling Tests

Tests similar to the research performed in this report were conducted to design for flexural loads^[12]; however, some key differences make these data unreliable for blast loads. Previous web crippling research^[12] was aimed at creating code equations for the cold-formed steel design manual^[13]; therefore it focused on beam-type web crippling. This included mid-span supports and end-of-span supports but was restricted in its support conditions^[12]. The studs were loaded from one side and then from both sides but were not pinned to the loading member and avoided any tension development in the connection^[14]. Some examples of previous research loading

scenarios can be seen in Figure 9. While this research was valuable for most situations it cannot be applied to steel stud track systems

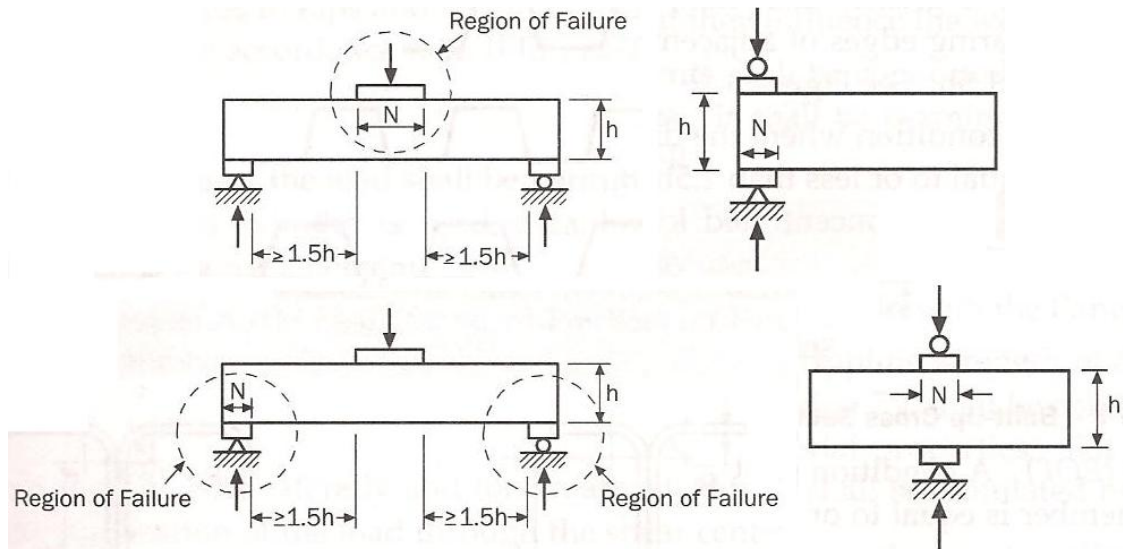


Figure 9. Loading Scenarios for AISI Web Crippling Tests^[13]

3.8. Dynamic Modeling

To design against blast events it is important to understand some basics of structural dynamics. The equation of motion $M\ddot{y} + c\dot{y} + ky = F(t)$ (2) relates the motion of an object to the time history of the force acting on it. In the case of blasts only the initial deflection is important and structural members are expected to respond well beyond elastic response, thus damping can be neglected^[15]. In addition, the k value representing stiffness can be substituted with the resistance function for non-linear systems, resulting^[16] in $M\ddot{u} + R = F(t)$ (3). Figure 10 shows how a beam can be idealized as a spring-mass system, which can then be modeled using a single-degree-of-freedom dynamic model^[4]. The use of static load-deflection curves to model live blast behavior by using this equation has been well documented^[17]. By applying a dynamic strength increase factor to the static resistance function, the response can be modeled and deflections can be predicted^[10]. Therefore, this project focused on developing the static resistance function of the modified conventional steel stud wall system.

$$M\ddot{y} + c\dot{y} + ky = F(t) \quad (2)$$

Where:

- M = mass
- c = damping coefficient
- k = stiffness
- y = deflection at a specified point
- $F(t)$ = load as a function of time, t

$$M\ddot{u} + R = F(t) \quad (3)$$

Where:

R = static resistance function

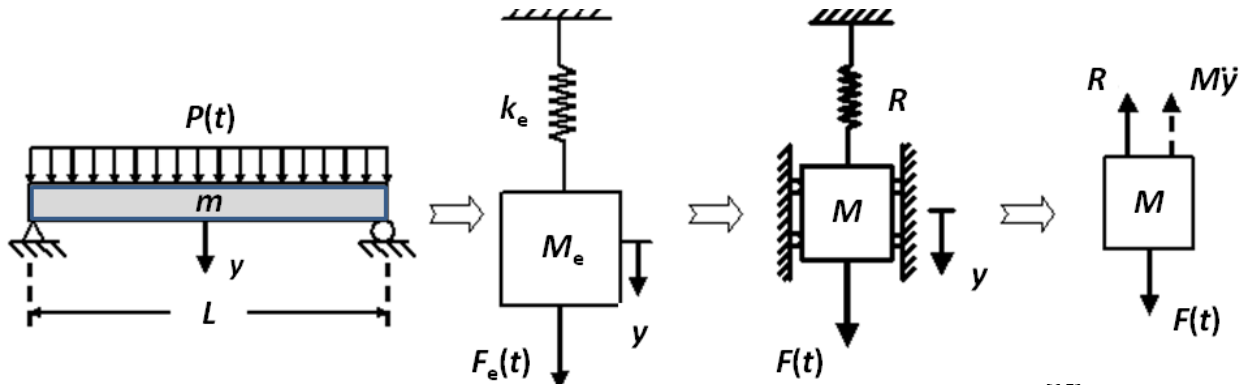


Figure 10. Beam Idealized as a Single-Degree-of-Freedom System^[15]

3.9. Unified Facilities Criteria (UFC)

The UFC is a set of documents that sets standards for blast design and serves as the code for federal buildings. The current method of regulating blast design is for the deflection angle at the support to be limited to $0.5^\circ - 2^\circ$ based on the amount of damage allowed (Appendix C). This angle is shown in Figure 11. These values are based on the elastic bending characteristics and design using weak connections. This project aims at evaluating the applicability of these limits both for conventional details and the upgraded details.



Figure 11. UFC Support Deflection Angle

4. EXPERIMENTAL EVALUATION

4.1. Objective

The short-beam tests in this section are designed to evaluate the web crippling action seen on steel stud track walls. Shortening the span to 4 ft allows the shear diagram to control the response and the moment diagram will not be as significant. This is important because steel stud wall systems with traditional connection details typically fail at the connection in a shear failure mode. This project focused on evaluating the stud-to-track connection using short-beam tests, full-length beam tests, and coupon testing of the stud and track materials. The short-beam and coupon tests are described in Sections 4 and 5, and the full-length beam testing is described in Section 6.

4.2. Short-Beam Experimental Set-Up

This phase of the project tested a 4-ft sample loaded at four points and restrained by a track section bolted to a rigid frame. As part of this test series, three samples that are representative of typical construction practice were included to serve as control tests. The constants for all samples tested were that two 33-ksi 6-in studs were attached to the track spaced at 16 in on center. The 6-in track was bolted to the rigid frame by three (3) ½-in diameter bolts spaced at 16 in on center with the middle bolt located in the center of the two studs. The loading points were 10 in apart. The parameters varied among the samples and are described in Table 1. The parameters were the number and size of screws attaching the studs to the track, the size and thickness of the track, and the thickness of the stud. In addition to these samples, four samples with no bracing were tested to compare the effectiveness of the bracing. Figure 12 and Figure 13 show the loading frame model and the location of the loading points. Figure 14 shows the displacement measurement locations and Figure 15 and Figure 16 show a sample installed in the frame ready to be tested.

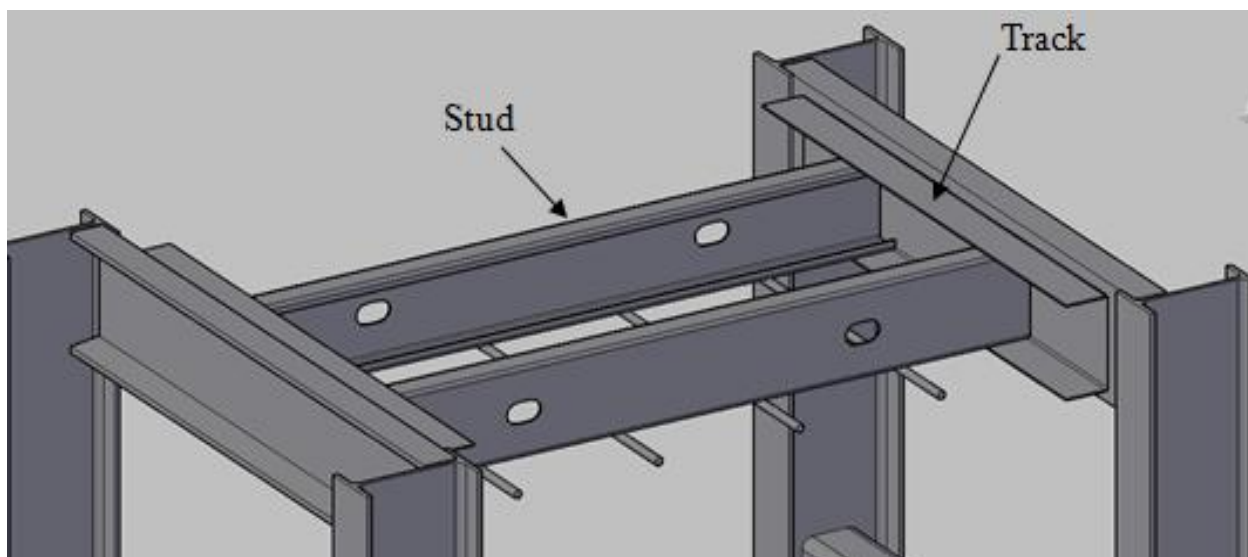


Figure 12. Short-Beam Test Loading Frame Drawing

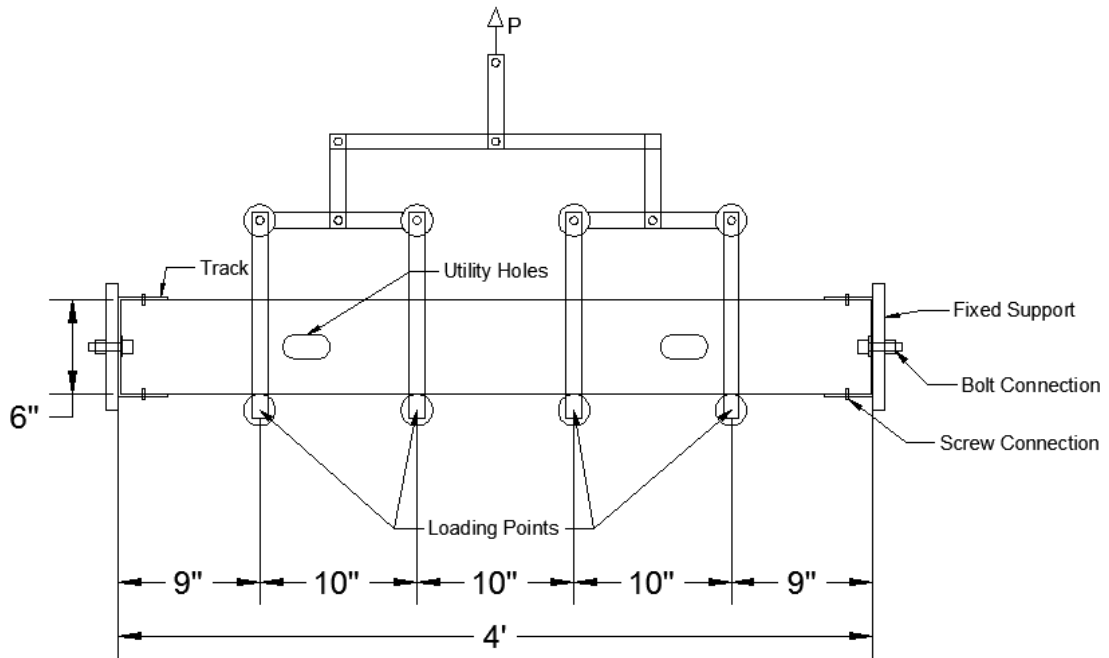


Figure 13. Short-Beam Test Loading Diagram

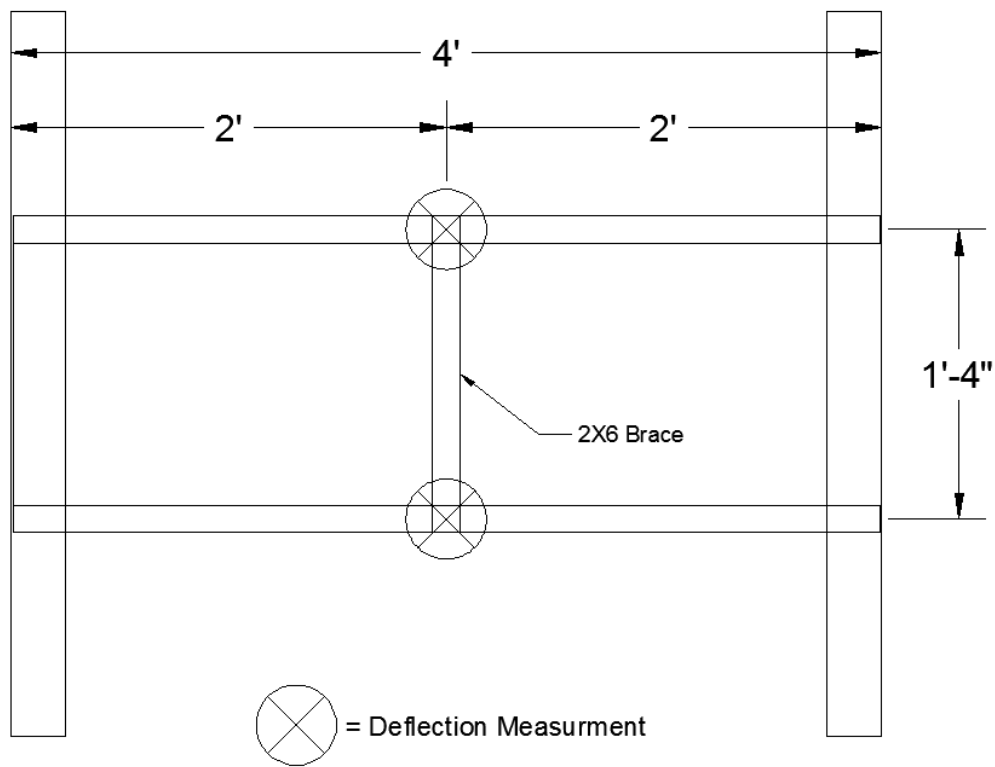


Figure 14. Deflection Measurement Locations

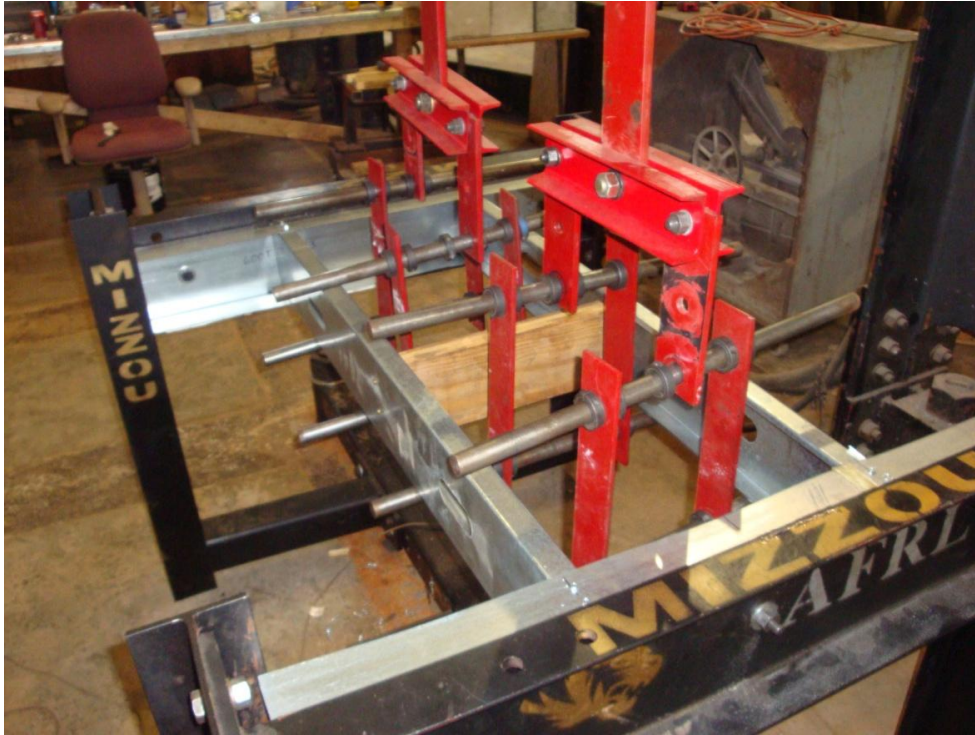


Figure 15. Typical Short-Beam Sample Prior to Testing



Figure 16. Typical Connection Detail

4.3. Short-Beams Experimental Matrix

The 4-ft beam data are shown in Table 1. The matrix was reduced prior to the testing, resulting in two different numbering systems. The web crippling action (WCA) number is the original sample number that is maintained to correspond to other testing at AFRL^[2]. The sample number is the reference number for this report. In Table 1, the stud column shows the type of studs used in each sample. For each sample two 4-ft-long stud sections were used. The track column shows the size and thickness of the track used in each sample. Samples 8, 27 and 42 are control tests, which are similar to standard construction practice. Screw spacing is a variable that was not considered in this test series. The screw configurations are based on the American Iron and Steel Institute standards^[18, 19] for spacing and were centered horizontally and vertically on the specimens.

Table 1. Experimental Matrix for Tests with 6-inch Studs

Sample #	WCA Label	Stud (33 ksi)	Track (33 ksi) (gauge)	Flange (in)	Screw	Qty of Screws
1	WCA 2	600S137-33 (20 ga)	20	3	#8	2
2	WCA 5	600S137-33 (20 ga)	20	3	#10	2
3	WCA 7	600S137-33 (20 ga)	20	3	#12	2
4	WCA 10	600S137-33 (20 ga)	18	3	#8	2
5	WCA 13	600S137-33 (20 ga)	18	3	#10	2
6	WCA 15	600S137-33 (20 ga)	18	3	#12	2
7	WCA 17	600S137-33 (20 ga)	20	1.5	#8	2
8	WCA 18 (20-gauge stud control)	600S137-33 (20 ga)	20	1.5	#8	1
9	WCA 19	600S137-33 (20 ga)	20	1.5	#10	1
10	WCA 20	600S137-33 (20 ga)	20	1.5	#12	1
11	WCA 21	600S137-33 (20 ga)	18	1.5	#8	2
12	WCA 22	600S137-33 (20 ga)	18	1.5	#8	1
13	WCA 23	600S137-33 (20 ga)	18	1.5	#10	1
14	WCA 24	600S137-33 (20 ga)	18	1.5	#12	1
15	WCA 25	600S162-54 (16 ga)	16	3	#8	6
16	WCA 27	600S162-54 (16 ga)	16	3	#8	4
17	WCA 29	600S162-54 (16 ga)	16	3	#8	2
18	WCA 32	600S162-54 (16 ga)	16	3	#10	2
19	WCA 34	600S162-54 (16 ga)	16	3	#12	2
20	WCA 36	600S162-54 (16 ga)	14	3	#8	6
21	WCA 38	600S162-54 (16 ga)	14	3	#8	4
22	WCA 40	600S162-54 (16 ga)	14	3	#8	2
23	WCA 43	600S162-54 (16 ga)	14	3	#10	2
24	WCA 45	600S162-54 (16 ga)	14	3	#12	2
25	WCA 47	600S162-54 (16 ga)	16	1.5	#8	4
26	WCA 48	600S162-54 (16 ga)	16	1.5	#8	2
27	WCA 49 (16-gauge stud control)	600S162-54 (16 ga)	16	1.5	#8	1

28	WCA 50	600S162-54 (16 ga)	16	1.5	#10	2
29	WCA 51	600S162-54 (16 ga)	16	1.5	#10	1
30	WCA 52	600S162-54 (16 ga)	16	1.5	#12	2
31	WCA 53	600S162-54 (16 ga)	16	1.5	#12	1
32	WCA 54	600S162-54 (16 ga)	14	1.5	#10	2
33	WCA 55	600S162-54 (16 ga)	14	1.5	#10	1
34	WCA 56	600S162-54 (16 ga)	14	1.5	#12	2
35	WCA 57	600S162-54 (16 ga)	14	1.5	#12	1
36	WCA 58	600S200-97 (12 ga)	12	3	#10	6
37	WCA 60	600S200-97 (12 ga)	12	3	#10	4
38	WCA 62	600S200-97 (12 ga)	12	3	#10	2
39	WCA 65	600S200-97 (12 ga)	12	3	#12	2
40	WCA 67	600S200-97 (12 ga)	12	1.5	#10	4
41	WCA 68	600S200-97 (12 ga)	12	1.5	#10	2
42	WCA 69	600S200-97 (12 ga) (12-gauge stud control)	12	1.5	#10	1
43	WCA 70	600S200-97 (12 ga)	12	1.5	#12	2
44	WCA 71	600S200-97 (12 ga)	12	1.5	#12	1
45	WCA 91	600S137-33 (20 ga)	20	1.5	#10	1
46	WCA 92	600S137-33 (20 ga)	18	1.5	#10	1
47	WCA 93	600S162-54 (16 ga)	16	1.5	#10	1
48	WCA 95	600S200-97 (12 ga)	12	1.5	#10	1

4.4. Analytical Predictions

Using the 2008 edition of the Cold-Formed Steel Design Manual^[13] and the material properties gathered in Section 4.5 of this document, several limit states were formulated. Table 2 gives the calculated limit states which are based on the equations provided in Sections 4.4.1 through 4.4.6. These limit states provide a background of what the peak load would be if that failure mode were the only one present; however, interactions between these limits have an impact on the overall

Table 2. Analytical Predictions

Report Sample #	Web Crippling Min (kips)	Web Crippling Max (kips)	Screw Pullout/Pullover (kips)	Tilting and Bearing (kips)	Shear of Stud (kips)
1	0.41	1.42	3.86	8.76	1.97
2	0.41	1.42	4.47	9.43	1.97
3	0.41	1.42	5.08	10.05	1.97
4	0.41	1.42	3.86	8.76	1.97
5	0.41	1.42	4.47	9.43	1.97
6	0.41	1.42	5.08	10.05	1.97
7	0.31	1.10	3.86	8.76	1.97
8 (20-gauge stud control)	0.31	1.10	1.93	4.38	1.97

Report Sample #	Web Crippling Min (kips)	Web Crippling Max (kips)	Screw Pullout/Pullover (kips)	Tilting and Bearing (kips)	Shear of Stud (kips)
9	0.31	1.10	2.24	4.71	1.97
10	0.31	1.10	2.54	5.03	1.97
11	0.31	1.10	3.86	8.76	1.97
12	0.31	1.10	1.93	4.38	1.97
13	0.31	1.10	2.24	4.71	1.97
14	0.31	1.10	2.54	5.03	1.97
15	2.45	4.01	18.94	54.97	8.61
16	2.45	4.01	12.62	36.65	8.61
17	2.45	4.01	6.31	18.32	8.61
18	2.45	4.01	7.31	19.72	8.61
19	2.45	4.01	8.31	21.03	8.61
20	2.45	4.01	18.94	54.97	8.61
21	2.45	4.01	12.62	36.65	8.61
22	2.45	4.01	6.31	18.32	8.61
23	2.45	4.01	7.31	19.72	8.61
24	2.45	4.01	8.31	21.03	8.61
25	1.93	3.17	12.62	36.65	8.61
26	1.93	3.17	6.31	18.32	8.61
27 (16-gauge stud control)	1.93	3.17	3.16	9.16	8.61
28	1.93	3.17	7.31	19.72	8.61
29	1.93	3.17	3.66	9.86	8.61
30	1.93	3.17	8.31	21.03	8.61
31	1.93	3.17	4.16	10.51	8.61
32	1.93	3.17	7.31	19.72	8.61
33	1.93	3.17	3.66	9.86	8.61
34	1.93	3.17	8.31	21.03	8.61
35	1.93	3.17	4.16	10.51	8.61
36	6.59	11.20	39.42	125.21	24.16
37	6.59	11.20	26.28	83.48	24.16
38	6.59	11.20	13.14	41.74	24.16
39	6.59	11.20	14.94	47.45	24.16
40	5.30	9.08	26.28	83.48	24.16
41	5.30	9.08	13.14	41.74	24.16
42 (12-gauge stud control)	5.30	9.08	6.57	20.87	24.16
43	5.30	9.08	14.94	47.45	24.16
44	5.30	9.08	7.47	23.72	24.16
45	0.31	1.10	2.24	4.71	1.97
46	0.31	1.10	2.24	4.71	1.97
47	1.93	3.17	3.66	9.86	8.61
48	5.30	9.08	6.57	20.87	24.16

strength of the connection. For example the screw shear limit state will not accurately predict the failure load, even if that is the failure mode, because the track applies a compressive load to the stud, which will increase the shear capacity of the screw.

4.4.1. Web Crippling

The stud support is the location of maximum shear and therefore the most likely location of web crippling. The shear value in the short-beam tests is half the total load carried by the stud or a fourth of the total sample load. Web crippling is calculated by Equation 4^[13], which includes several constants that vary for load scenarios depending on conditions. Examples of variations in the conditions include fixed or pinned supports, whether the stud is fastened to the support or not, and the location of the loading point being near the end or interior to the span. For a conventionally constructed stud wall, the actual support conditions fall within all of these conditions. Therefore, for the purposes of predicting the failure response, several conditions were calculated and the maximum and minimum values are tabulated in Table 3.

$$P_n = Ct^2F_y \sin \theta \left(1 - C_R \sqrt{\frac{R}{t}} \right) \left(1 + C_N \sqrt{\frac{N}{t}} \right) \left(1 - C_h \sqrt{\frac{h}{t}} \right) \quad (4)$$

Where:

P_n = Nominal resistance

C = Coefficient from cold-formed steel design manual

t = Web thickness

F_y = Design yield stress

θ = Angle between plane of web and bearing surface

C_R = Bend radius coefficient from cold-formed steel design manual

R = Inside bend radius

C_N = Bearing Length coefficient from cold-formed steel design manual

N = Bearing length

C_h = Web slenderness coefficient from cold-formed steel design manual

h = flat dimension of web measured in plane of web

Table 3. Tension Testing Data

WCA #	Stud (S) or Track (T)	Width (in)	Thickness (in)	F_y (ksi)	F_u (ksi)	E (ksi)	Max Strain	Max Strain/Yield Strain
2	S	0.505	0.035	49	71	2733	8.9%	4.5
2	T	0.5055	0.048	58	72	2960	6.8%	3.4
5	S	0.505	0.038	47	66	4400	9.0%	4.5
5	T	0.504	0.0485	55	70	4062	4.2%	2.1
7	S	0.5045	0.0355	41	70	1816	12.8%	6.4
7	T	0.5015	0.0405	45	54	2485	11.5%	5.8
10	S	0.4985	0.0355	50	70	4572	8.0%	4.0
10	T	0.5085	0.05	50	67	2081	7.5%	3.7
13	S	0.5045	0.034	43	73	2397	13.2%	6.6
13	T	0.502	0.047	53	72	2574	8.3%	4.2
15	S	0.4945	0.036	47	71	3824	11.2%	5.6
15	T	0.5015	0.048	18	41	1491	17.3%	8.7

WCA #	Stud (S) or Track (T)	Width (in)	Thickness (in)	F_y (ksi)	F_u (ksi)	E (ksi)	Max Strain	Max Strain/Yield Strain
17	S	0.501	0.0345	46	72	2636	6.2%	3.1
17	T	0.502	0.036	49	69	3488	8.8%	4.4
18	S	0.501	0.032	53	79	2894	10.4%	5.2
18	T	0.5015	0.036	43	69	2234	12.6%	6.3
19	S	0.4975	0.0365	43	70	1658	13.9%	6.9
19	T	0.5025	0.0355	46	70	2244	11.7%	5.8
20	S	0.502	0.036	38	140	1431	14.1%	7.1
20	T	0.503	0.033	42	50	2573	11.4%	5.7
21	S	0.503	0.0575	29	43	1708	12.5%	6.3
21	T	0.5045	0.0535	54	79	1628	21.2%	10.6
22	S	0.5	0.0325	48	77	2494	12.0%	6.0
22	T	0.477	0.053	47	79	2307	9.3%	4.6
23	S	0.5005	0.0365	45	68	3542	10.0%	5.0
23	T	0.508	0.0555	47	75	2047	11.8%	5.9
24	S	0.4965	0.0345	50	73	2566	9.4%	4.7
24	T	0.5065	0.0465	13	41	6496	23.3%	11.6
25	S	0.504	0.0585	59	72	2309	2.4%	1.2
25	T	0.507	0.058	34	57	2601	16.0%	8.0
27	S	0.5085	0.059	56	72	2744	7.5%	3.7
27	T	0.5045	0.054	56	62	2747	6.6%	3.3
29	S	0.51	0.059	59	71	2960	5.1%	2.6
29	T	0.505	0.053	56	64	2441	10.4%	5.2
32	S	0.4985	0.0565	40	76	2551	9.7%	4.9
32	T	0.505	0.058	56	58	3237	8.6%	4.3
34	S	0.507	0.0565	58	75	2102	8.2%	4.1
34	T	0.51	0.056	37	48	2309	14.1%	7.1
36	S	0.507	0.0585	55	72	3037	7.3%	3.6
36	T	0.508	0.073	50	74	2519	10.5%	5.3
38	S	0.5025	0.0585	42	72	2346	9.3%	4.6
38	T	0.512	0.074	46	73	2023	5.9%	2.9
40	S	0.501	0.057	60	74	2789	6.0%	3.0
40	T	0.507	0.0695	51	78	2129	10.1%	5.1
43	S	0.501	0.058	62	73	2397	7.6%	3.8
43	T	0.5105	0.0715	33	75	2256	12.7%	6.3
45	S	0.501	0.0565	65	77	5361	3.7%	1.8
45	T	0.505	0.0655	52	67	2894	6.5%	3.3
47	S	0.4985	0.053	64	80	2981	7.1%	3.5
47	T	0.5025	0.0455	43	52	7993	12.4%	6.2
48	S	0.499	0.057	62	74	2588	6.6%	3.3
48	T	0.502	0.046	43	50	3957	15.2%	7.6
49	S	0.5015	0.059	62	72	3251	5.2%	2.6
49	T	0.505	0.046	34	51	2655	21.0%	10.5

WCA #	Stud (S) or Track (T)	Width (in)	Thickness (in)	F_y (ksi)	F_u (ksi)	E (ksi)	Max Strain	Max Strain/Yield Strain
50	S	0.507	0.0615	56	70	2592	6.6%	3.3
50	T	0.5005	0.0445	44	53	2096	12.3%	6.1
51	S	0.5045	0.0585	55	72	2888	7.5%	3.8
51	T	0.506	0.0475	39	50	2619	15.4%	7.7
52	S	0.5045	0.057	63	74	3175	4.8%	2.4
52	T	0.508	0.07	52	79	2360	8.7%	4.4
53	T	0.5055	0.057	48	49	4869	5.9%	2.9
53	S	0.5	0.058	27	43	1438	9.2%	4.6
54	S	0.5085	0.0595	26	71	2150	13.0%	6.5
54	T	0.5095	0.0715	49	63	3613	5.4%	2.7
55	S	0.497	0.0565	65	75	2555	28.8%	14.4
55	T	0.506	0.0715	52	65	2536	7.0%	3.5
56	S	0.4965	0.0585	46	75	2670	10.1%	5.0
56	T	0.508	0.0715	49	61	1990	7.9%	4.0
57	S	0.5	0.058	38	66	1968	18.2%	9.1
57	T	0.5035	0.0685	54	68	2412	6.6%	3.3
58	S	0.51	0.105	53	73	2088	8.8%	4.4
58	T	0.51	0.1045	44	56	4347	3.7%	1.8
60	S	0.514	0.0995	51	77	2546	9.3%	4.7
60	T	0.512	0.099	62	77	2236	4.5%	2.3
62	S	0.4965	0.102	36	75	2237	13.5%	6.7
62	T	0.5085	0.1	58	75	3428	5.6%	2.8
65	S	0.5145	0.098	64	78	2468	5.0%	2.5
65	T	0.5135	0.102	53	73	2846	8.2%	4.1
67	S	0.5185	0.101	59	75	3878	8.1%	4.0
67	T	0.513	0.1045	45	57	1591	4.3%	2.2
68	S	0.5135	0.101	46	76	2627	9.8%	4.9
68	T	0.513	0.104	34	50	2373	15.4%	7.7
69	S	0.5105	0.101	41	77	1776	12.0%	6.0
69	T	0.511	0.104	38	56	2112	9.9%	5.0
70	S	0.512	0.105	34	73	1783	11.5%	5.7
70	T	0.521	0.102	45	56	2682	3.5%	1.7
71	S	0.5175	0.101	45	75	2074	9.8%	4.9
71	T	0.5	0.0945	18	57	3119	0.4%	0.2
91	S	0.511	0.05	49	63	4225	3.6%	1.8
91	T	0.4995	0.0395	45	55	2639	6.3%	3.1
92	S	0.5045	0.0515	43	57	1564	13.7%	6.9
92	T	0.504	0.044	18	44	1251	23.7%	11.8
93	S	0.501	0.06	46	63	1896	7.5%	3.7
93	T	0.5025	0.053	43	51	2610	9.4%	4.7
95	S	0.476	0.097	58	80	3896	5.7%	2.9
95	T	0.513	0.096	52	75	1931	14.1%	7.0

4.4.2. Shear of Stud

The shear strength of webs of studs may also contribute to the overall capacity. The shear applied will be similar to that in the web-crippling limit state. Shear is defined per the equations below^[13]:

$$V_n = A_w F_v \quad (5)$$

$$\text{For } \frac{h}{t} \leq \sqrt{\frac{E k_v}{F_y}}$$

$$F_v = 0.6 F_y \quad (6)$$

$$\text{For } \sqrt{\frac{E k_v}{F_y}} < \frac{h}{t} \leq 1.51 \sqrt{\frac{E k_v}{F_y}}$$

$$F_v = \frac{0.6 t \sqrt{E k_v F_y}}{h} \quad (7)$$

$$\text{For } \frac{h}{t} > \sqrt{\frac{E k_v}{F_y}}$$

$$F_v = \frac{\pi^2 E k_v}{12(1-\mu^2) \left(\frac{h}{t}\right)^2} \quad (8)$$

Where:

- V_n = Nominal shear strength
- A_w = Area of web element
- F_v = Nominal shear stress
- E = Modulus of elasticity of steel
- k_v = shear buckling coefficient
- μ = Poisson's ratio

4.4.3. Distortional Buckling

The bracing used in these tests reduces the likelihood of distortional buckling but the possibility still exists in some samples. The load required to buckle the stud^[13] is given by Equation 9. Equations 10–13 define the terms.

$$P_n = \left(1 - 0.25 \left(\frac{P_{crd}}{P_y} \right)^{0.6} \right) \left(\frac{P_{crd}}{P_y} \right)^{0.6} P_y \quad (9)$$

$$P_y = A_g F_y \quad (10)$$

$$P_{crd} = A_g F_d \quad (11)$$

$$F_d = \alpha k_d \frac{\pi^2 E}{12(1-\mu^2)} \left(\frac{t}{b_o} \right)^2 \quad (12)$$

$$k_d = 0.05 \leq 0.1 \left(\frac{b_o D \sin \theta}{h_o t} \right) \leq 8.0 \quad (13)$$

Where:

A_g = Gross cross-sectional area

α = A value that accounts for the benefit of an unbraced length, L_m , shorter than L_{cr} , but can be conservatively taken as 1.0

= 1.0 for $L_m \geq L_{cr}$

= $(L_m/L_{cr})^{\ln(L_m/L_{cr})}$ for $L_m < L_{cr}$

b_o = Out-to-out web depth-

F_d = distortional buckling stress

h_o = Out-to-out flange width

4.4.4. Tilting and Bearing of Screw

As the stud deflects, the deformation causes a tensile force in the connection. This force must be carried by the screws and the track initially as a shear force in the screw and later as tilting and bearing. This failure mode combines screw pull-out and the forces involved with shear in the screw. The capacity can be found using Equation 14^[13].

Lesser of:

$$P_{ns} = 4.2\sqrt{t_2^3}dF_{u2} \quad (14)$$

$$P_{ns} = 2.7t_1dF_{u1}$$

$$P_{ns} = 4.2t_2dF_{u2}$$

Where:

P_{ns} = nominal shear strength per screw

t_1 = thickness of top sheet

t_2 = thickness of bottom sheet

d = screw diameter

F_{u1} = Ultimate stress of top sheet

F_{u2} = Ultimate stress of bottom sheet

4.4.5. Screw Pullout

If the track is light its rotation will exceed the stage of tilting and bearing and become a tensile force on the screw. The screw pullout failure mode occurs when the hole expands to the point that the threads of the screw pull out of the track. This limit state is given by Equation 15 and is multiplied times the total number of screws.

$$P_{not} = 0.85t_c dF_{u2} \quad (15)$$

Where:

P_{not} = nominal pull-out strength (resistance)

t_c = thickness

4.4.6. Screw Pullover

Similar to the limit state of pulling out the screw, pulling over the screw involves the tension forces developed in the screw after tilting and bearing. In this case, however, the screw develops a large enough force in the threads to deform the stud around the screws until the hole is large enough for the stud to go over the head of the screw.

$$P_{nov} = 1.5t_1d'_wF_{u1} \quad (16)$$

Where:

- P_{nov} = nominal pull-over strength (resistance)
- t_1 = thickness of sheet
- d'_w = washer diameter

4.5. Coupon Tension Tests

To find the delivered yield and ultimate strengths along with the modulus of elasticity for analytical predictions, coupons were cut from each stud and track section's web in the long direction in accordance with ASTM A370-10 and tested until they failed in tension^[18]. The set-up for this process was an MTS machine with an extensometer as shown in **Error! Reference source not found.** and **Error! Reference source not found.**.



Figure 17. Coupon Testing Extensometer



Figure 18. Coupon Testing MTS Set-up

The data gathered from this part of the project were used to compare the predicted failure modes with the delivered strengths as opposed to the specified strengths. A sample stress-strain curve is shown in Figure 19. The summary of the results can be found in Table 2 and all of the data points can be found in **Error! Reference source not found.** The delivered yield and ultimate

strengths were both almost 50% higher than the stamped (ordered) values but the modulus of elasticity was 9% lower than the expected value of 29,500 ksi.

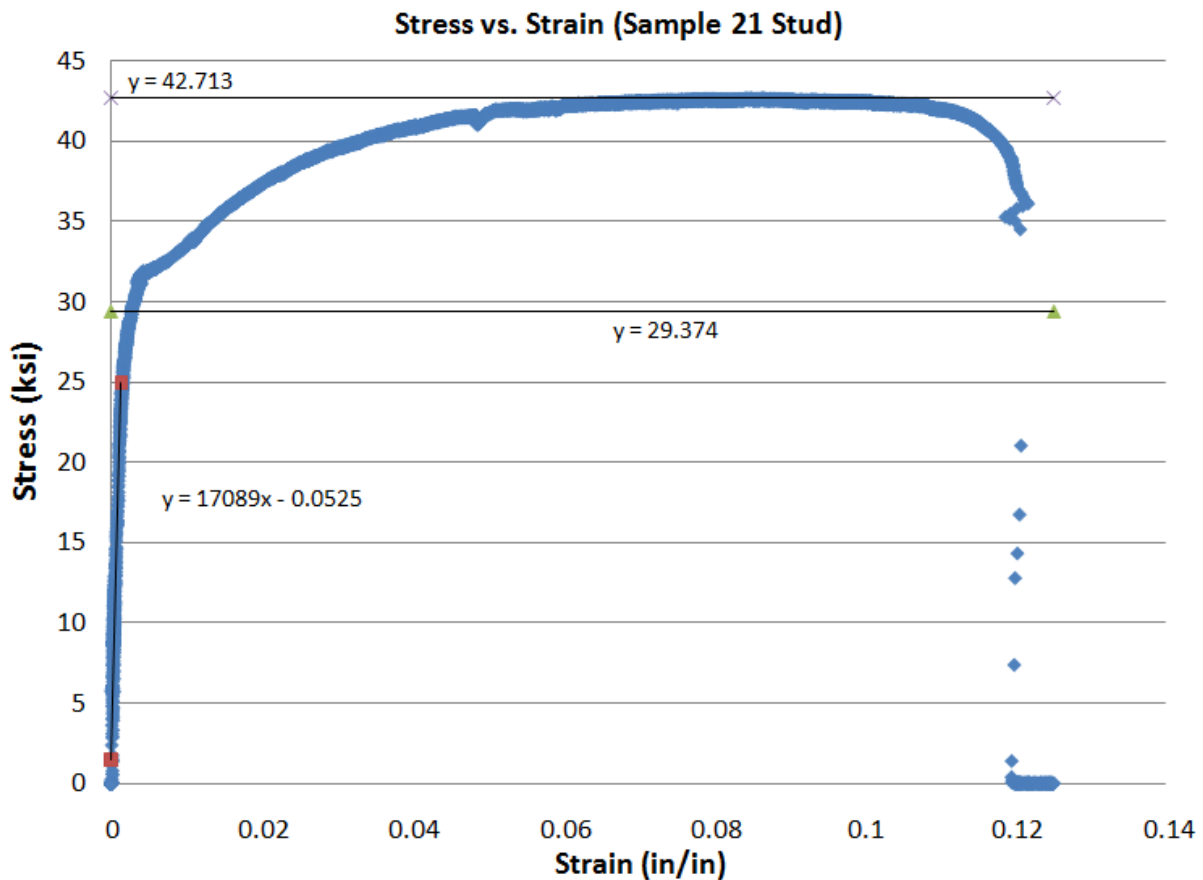


Figure 19. Sample Tension Test Stress–Strain Curve

Table 4. Tension Testing Summary

	F_y (ksi)	F_u (ksi)	E (ksi)
Stamped Value	33	45	29500
Average	47	67	26757
Percent Difference	42.9	49.9	-9.3
Standard Deviation	8.1	9.3	6480.8
Minimum	13	41	6496
Maximum	65	140	79938
Median	48	71	25490

5. TEST RESULTS

5.1. General

This section provides the results of the short-beam tests and describes the trends associated with them. Both the toughness and the peak load are compared and the experimental peak is compared to the analytical peak loads. The load–displacement plots are included in Appendix A and show the behavior of each sample as the displacement increased. The area under this load–displacement curve represents the energy, which is also tabulated in Table 5 through

Table 7. The energy-absorption capacity, represented by the area under the curve, is a good measure of the blast resistance provided by a wall system connection design.

5.2. Results

The tabulated peak loads are shown in Table 5 through

Table 7. The large range of analytical peaks shows that there is a large difference between the limit states that will all have an impact on the actual capacity because there are interactions between them all. The experimental peak is around the average of the minimum and maximum analytical peaks for the lighter-gauge samples and approaches 80% of the maximum value for the heavier-gauge samples. This is due to the connection's coming closer to a fixed state as opposed to the pinned counterpart in the case of the lighter-gauge samples. Control samples are included to show the current conventional connection details behavior. These controls are constructed by using a track with a 1.5-in flange and of the same gauge as the stud, and attaching the stud using one standard-size screw for that gauge at each face. The 20- and 16-gauge control samples use one #8 screw while the 12-gauge control sample uses one #10 screw on each flange. The experimental toughness (the area under the load–displacement curve) of the control samples is much less than the samples around the same type and size. The percent difference in both energy and peak load show that the

Table 5. Web Crippling Response (20-gauge Samples)

Report Sample #	Analytical Peak (kips)		Exp Peak (kips)	Percent Difference	Exp Energy (kip-in)	Percent Difference
	Maximum	Minimum				
1	8.76	0.41	3.0	36.4	7.2	75.6
2	9.43	0.41	2.8	27.3	4.3	4.9
3	10.05	0.41	2.9	31.8	17.7	331.7
4	8.76	0.41	2.9	31.8	7.8	90.2
5	9.43	0.41	2.8	27.3	7.5	82.9
6	10.05	0.41	2.9	31.8	17.6	329.3
7	8.76	0.31	2.9	31.8	10.5	156.1
8	4.38	0.31	2.2	0.0	4.1	-
9	4.71	0.31	2.3	4.5	2.7	-34.1
10	5.03	0.31	2.7	22.7	4.5	9.8
11	8.76	0.31	2.6	18.2	4.8	17.1
12	4.38	0.31	2.4	9.1	3.4	-17.1
13	4.71	0.31	2.3	4.5	5.2	26.8
14	5.03	0.31	2.7	22.7	4.5	9.0

modifications increased the capacity of the conventional details up to 450% and almost always by 30% or more. This shows the connection detail upgrades increased the blast-resistant properties of the conventional details. Load–deflection plots for these samples are shown in Appendix A.

Table 6. Web Crippling Response (16-gauge Samples)

Report Sample #	Analytical Peak (kips)		Exp Peak (kips)	Percent Difference	Exp Energy (kip-in)	Percent Difference
	Maximum	Minimum				
15	54.97	2.45	9.2	27.8	28.0	211.1
16	36.65	2.45	9.0	25.0	43.5	383.3
17	18.32	2.45	7.8	8.3	14.7	63.3

Report Sample #	Analytical Peak (kips)		Exp Peak (kips)	Percent Difference	Exp Energy (kip- in)	Percent Difference
	Maximum	Minimum				
18	19.72	2.45	7.5	4.2	49.4	448.9
19	21.03	2.45	8.6	19.4	30.9	243.3
20	54.97	2.45	9.0	25.0	28.7	218.9
21	36.65	2.45	9.0	25.0	16.2	80.0
22	18.32	2.45	8.4	16.7	10.5	16.7
23	19.72	2.45	8.8	22.2	16.5	83.3
24	21.03	2.45	9.1	26.4	31.7	252.2
25	36.65	1.93	8.2	13.9	15.9	76.7
26	18.32	1.93	8.5	18.1	22.5	150.0
27 (control)	9.16	1.93	7.2	0.0	9.0	-
28	19.72	1.93	7.4	2.8	34.0	277.8
29	9.86	1.93	7.1	-1.4	12.0	33.3
30	21.03	1.93	7.7	6.9	28.0	211.1
31	10.51	1.93	7.6	5.6	12.7	41.1
32	19.72	1.93	8.7	20.8	9.5	5.6
33	9.86	1.93	7.6	5.6	8.0	-11.1
34	21.03	1.93	7.4	2.8	21.5	138.9
35	10.51	1.93	7.3	1.4	10.4	15.6

5.3. Trends

The trends observed in the data are discussed in this section. The following figures compare the strength and toughness of all the samples by evaluating one variable at a time. Each line refers to a group of samples in which all other variables are constant so that the relative values can be observed. The results are compared graphically in a series of **Error! Reference source not found.** below. Specific observations of the trends are discussed next.

Table 7. Web Crippling Response (12-gauge Samples)

Report Sample #	Analytical Peak (kips)		Exp Peak (kips)	Percent Difference	Exp Energy (kip-in)	Percent Difference
	Maximum	Minimum				
36	125.21	6.59	20.4	20.7	24.1	5.2
37	83.48	6.59	19.5	15.4	18.2	-20.5
38	41.74	6.59	18.8	11.2	26.2	14.4
39	47.45	6.59	21.2	25.4	36.1	57.6
40	83.48	5.30	19.3	14.2	56.3	145.9
41	41.74	5.30	16.2	-4.1	13.7	-40.2
42 (control)	24.16	5.30	16.9	0.0	22.9	
43	47.45	5.30	20.8	23.1	45.3	97.8
44	24.16	5.30	16.5	-2.4	21.5	-6.1
45	4.71	0.31	4.4	100.0	4.6	12.2
46	4.71	0.31	4.1	86.4	5.4	31.7
47	9.86	1.93	6.6	-8.3	10.1	12.2
48	24.16	5.30	10.0	-40.8	8.0	-65.1

5.3.1. Maximum Capacity

Error! Reference source not found. shows that the number of screws helped increase capacity for each of the variations and that the effect is especially large on the lighter-gauge studs. This is because the lighter-gauge studs buckled earlier and relied more on the screws to help develop a tensile membrane behavior,

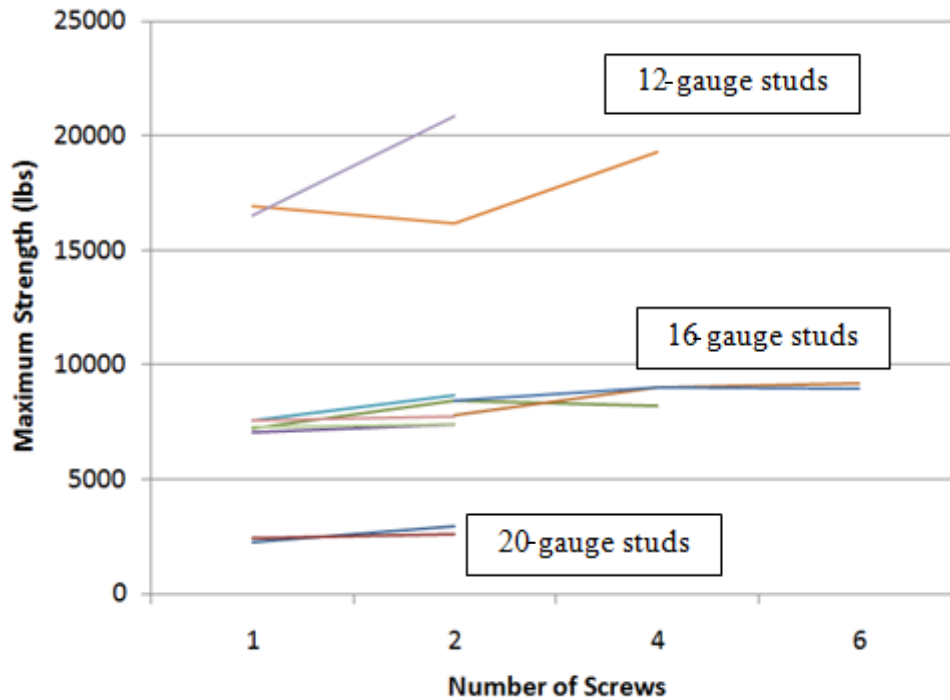


Figure 20. Maximum Strength vs. Number of Screws

whereas the thicker sections relied more on the track itself to resist the deflections. **Error! Reference source not found.** shows that the largest contributing factor to strength was the thickness of the stud. This is expected as increasing the stud gauge increases all the limit states and also is the most expensive of all the modifications.

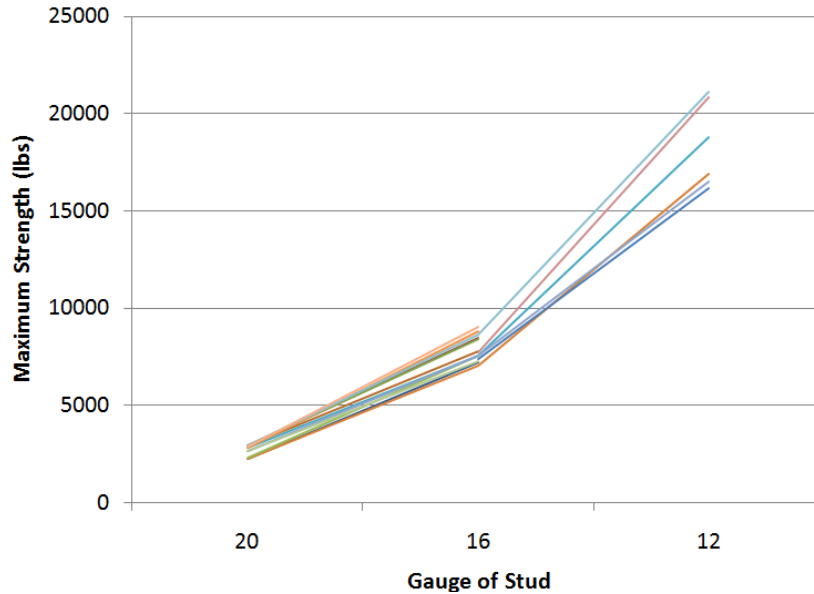


Figure 21. Maximum Strength vs. Stud Gauge

Error! Reference source not found. and Figure 23 show that the track gauge being the same as or one gauge lower than the stud and the length of the track did not make a statistically important difference. Having extra room for the same number of screws did not make a difference because block shear was never an issue.

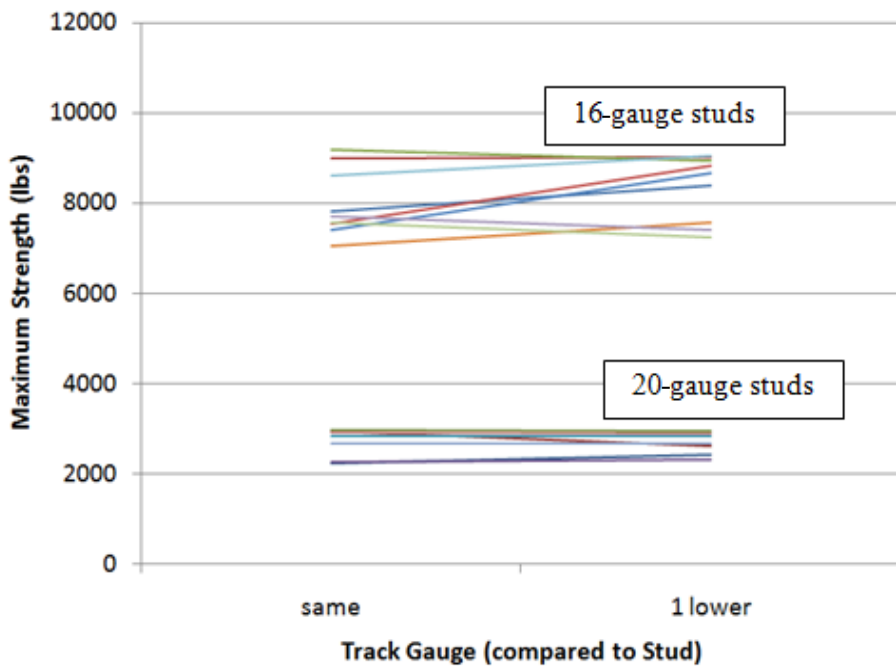


Figure 22. Maximum Strength vs. Track Gauge

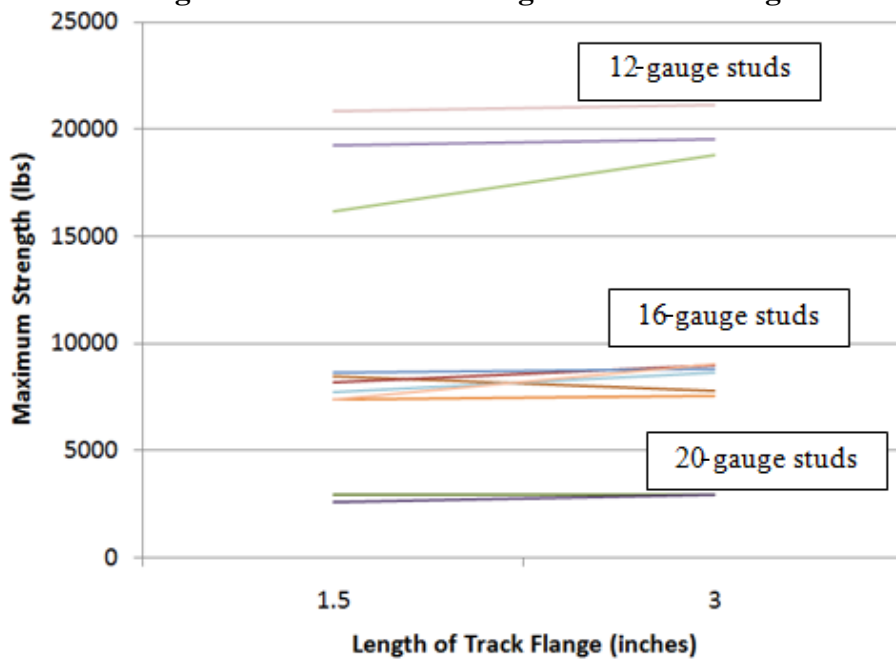


Figure 23. Maximum Strength vs. Length of Track Flange

Perhaps once the full length spans develop tensile membrane behavior the track will show some block shear failures and the length of the track will have more of an impact. **Error! Reference source not found.** shows that the size of the screws made a small difference in the lighter-gauge samples but had a much larger impact with the 12-gauge samples. This is due to the shear

failures of the screws with the 12-gauge samples and the pullout and pullover failures in the other samples. The cross sectional area

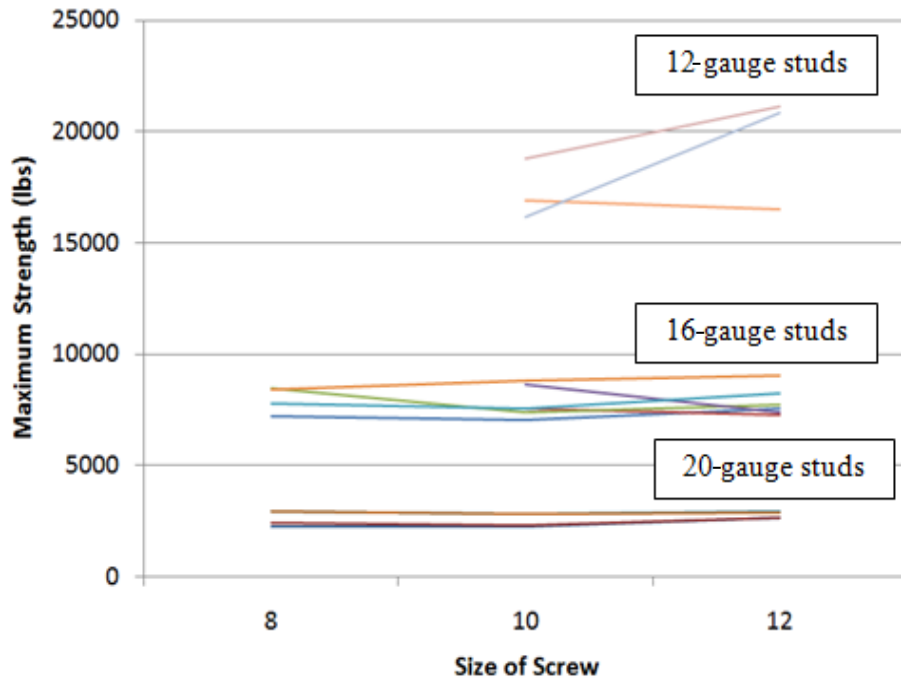


Figure 24. Maximum Strength vs. Size of Screw

of a screw is a much larger factor when you consider shearing or yielding a screw in tension compared to the area of the hole pulling over a screw.

5.3.2. Toughness

The toughness values are very dependent on the maximum deflection in the tests and because the samples consist of two studs some samples failed one stud much earlier than the other. This results in a large reduction in observed toughness for such samples and makes the trend graphs less predictable but still valuable. For example **Error! Reference source not found.** shows a general trend with a few samples being outliers.

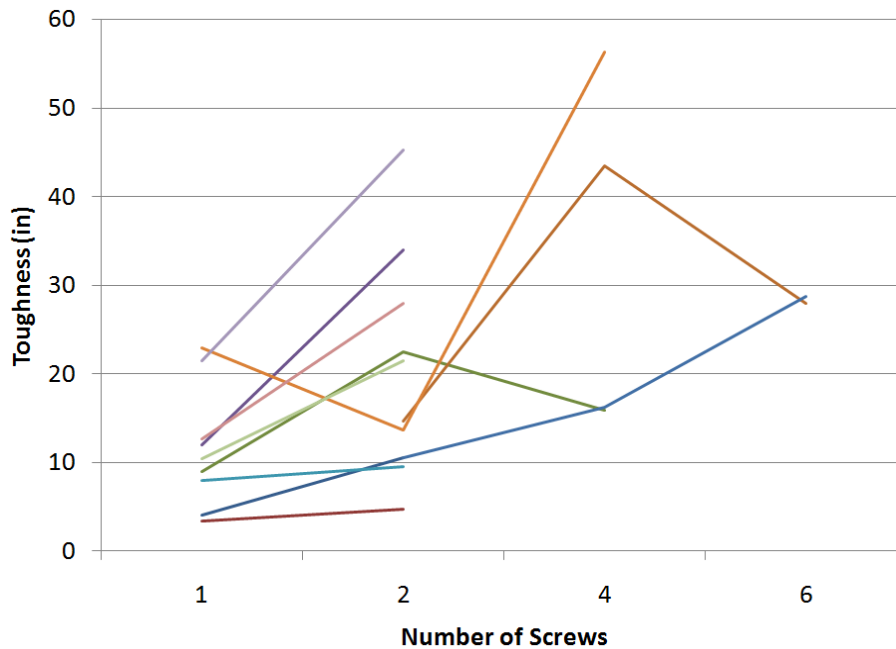


Figure 25. Toughness vs. Number of Screws

Error! Reference source not found. shows a significant increase in toughness by adding extra screws. The area under the load–displacement curve grows with the number of screws because the failure modes mostly depend on a shear or pullout of the screws at some point in the behavior. This upward trend is among the largest of any of the variables including stud gauge. Similar to the trend in the number of screws is the trend in size of the screws. A net increase of toughness by increasing the size of the screw, shown in **Error! Reference source not found.**, occurs for the same reasons as the number of screws. The stud gauge effect is shown in Figure 27 and, like the number of screws, is a very strong indicator of the overall toughness. This trend is most likely due to the bearing of the stud on the track flange, which reduces the force in the screws slightly. Increasing the thickness of the track resulted in a decrease in toughness (Fig. 28), which is counterintuitive. This is most likely due to the rotation restriction of the track flange. As the connection becomes stiffer, more of the rotational force is carried by the bottom screws and therefore the screw fails sooner. This effect also depends on the length of the track flange in some samples as shown in Figure 28. Some groups show a sharp decline in toughness and others show a large increase, which signifies that the effect is failure mode dependent.

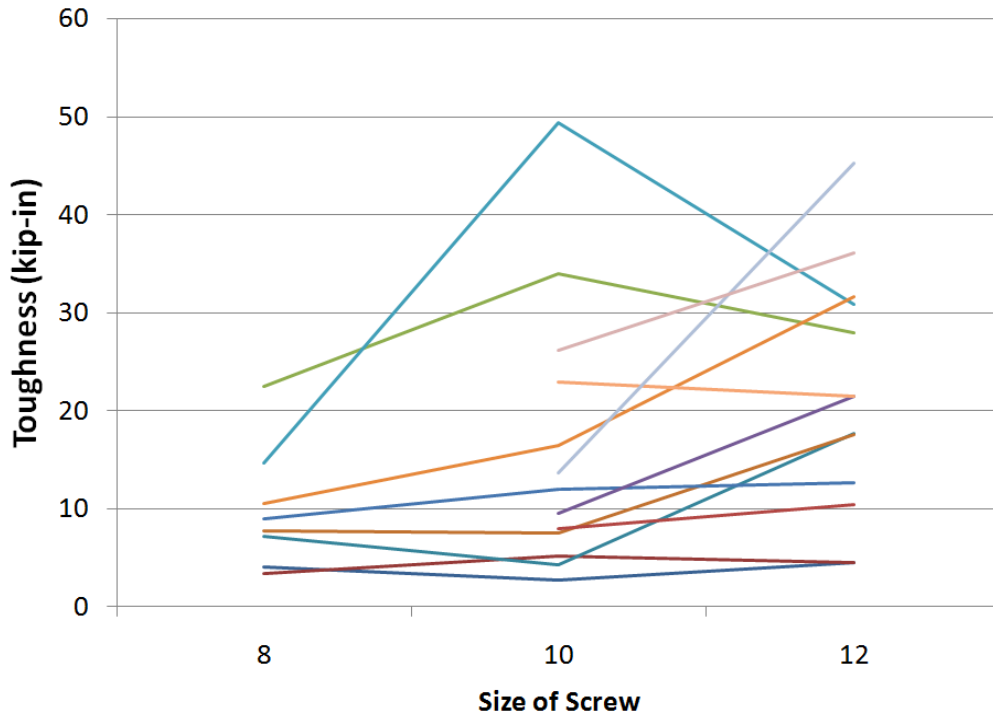


Figure 26. Toughness vs. Size of Screw

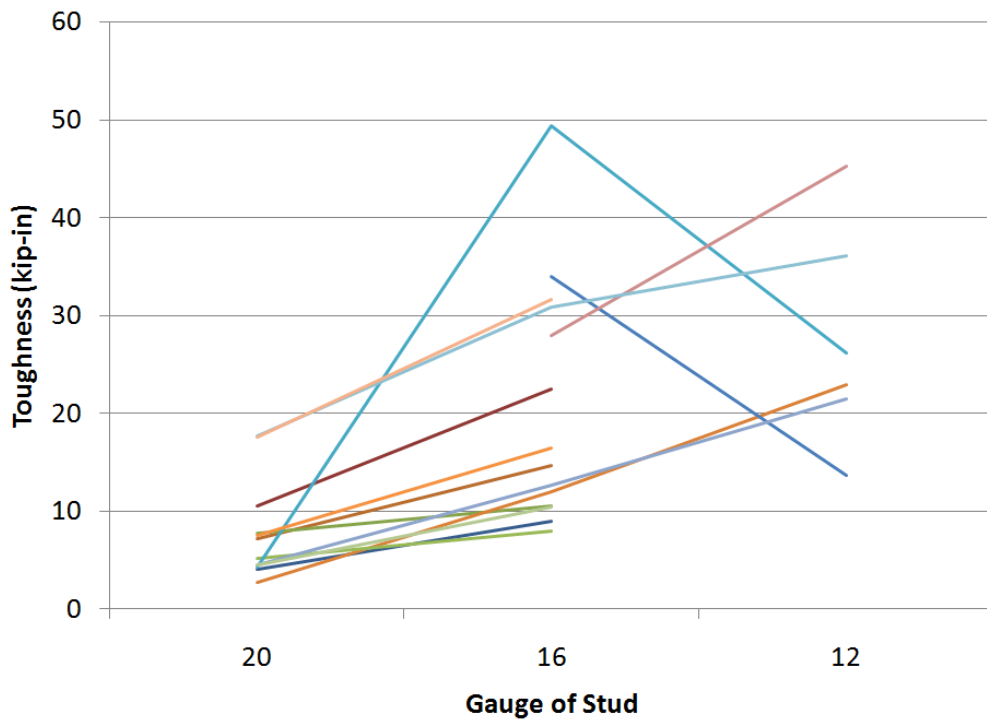


Figure 27. Toughness vs. Stud Gauge

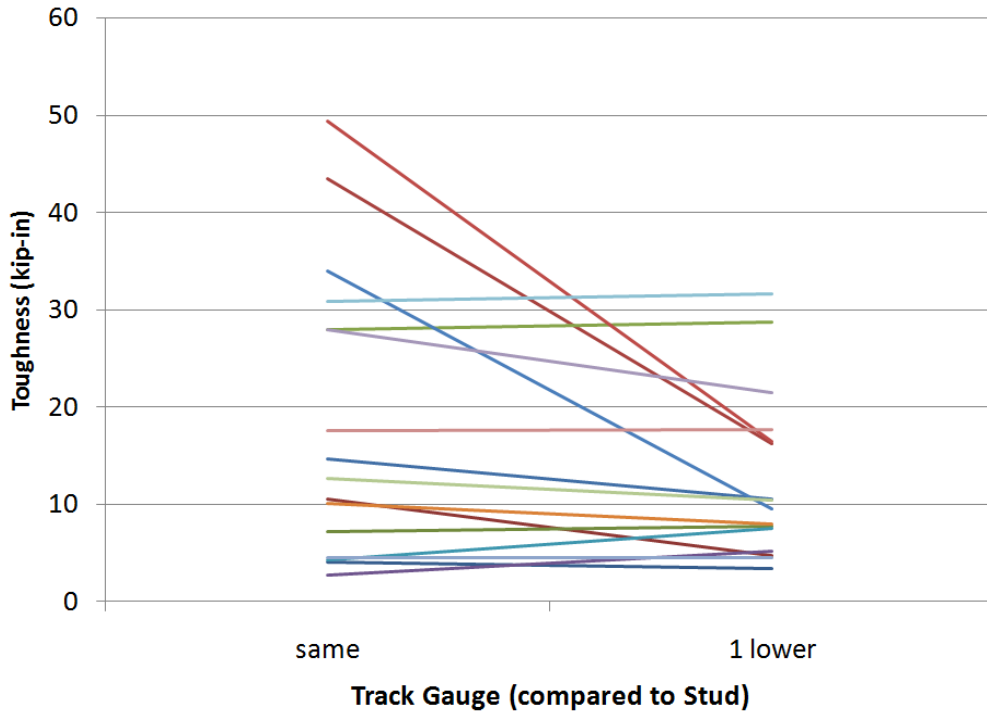


Figure 28. Toughness vs. Track Gauge

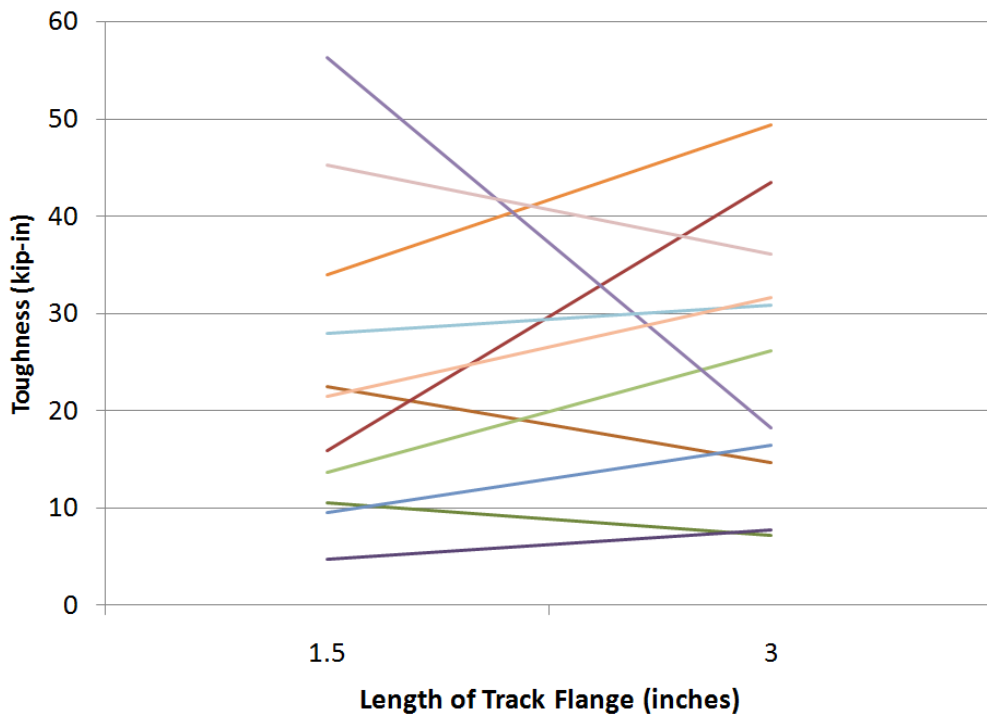


Figure 29. Toughness vs. Length of Track Flange

5.4. Short-Beam Failure Modes

As described in Section **Error! Reference source not found.**, the sample failures can be grouped into four general behaviors. This section places each sample into one of these groups and shows how the load–deflection curve fits into that failure mode.

5.4.1. Failure Mode 1

Behavior one consisted of the stud's web crippling then the screws on the bottom of the studs failing in a pull out manner as shown in **Error! Reference source not found.**–Figure 32. Notice that the stud fails and then after some large deflection, the web of the stud begins to bear on the track flange. This action results in a high-energy load–deflection curve, but would not necessarily correspond to good blast resistance in a real wall because the longer spans will allow the stud to deflect farther before any significant load would be carried by the track. The shortening of the stud in the long direction due to the angles being formed would pull the end of the stud away from the track and quickly remove any bearing capacity.



Figure 30. Crippling of Stud



Figure 31. Screw Pulling Out

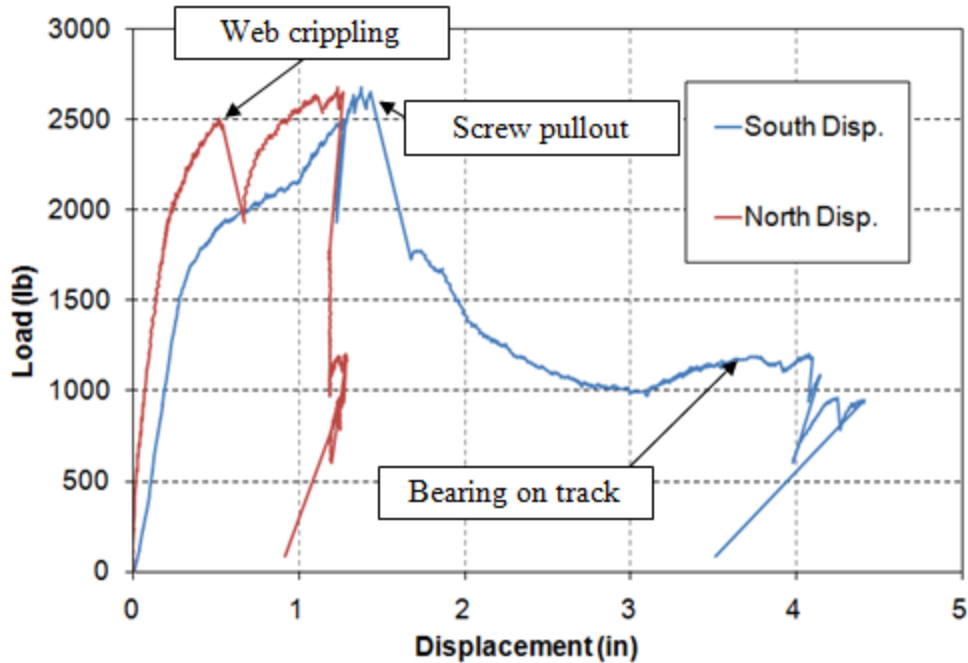


Figure 32. Typical Load-Displacement Plot of Failure Mode One

5.4.2. Failure Mode 2

The second failure behavior was when the stud crippld in the middle of the span and the screws on the bottom of the stud sheared off due to the lateral torsional load as shown in Figure 33– Figure 35. There is minimal capacity after the yielding of the first stud but these details can be easily improved by adding some other lateral support.



Figure 33. Stud Crippling at Mid-Span



Figure 34. Screws after Shearing Due to Torsional Load

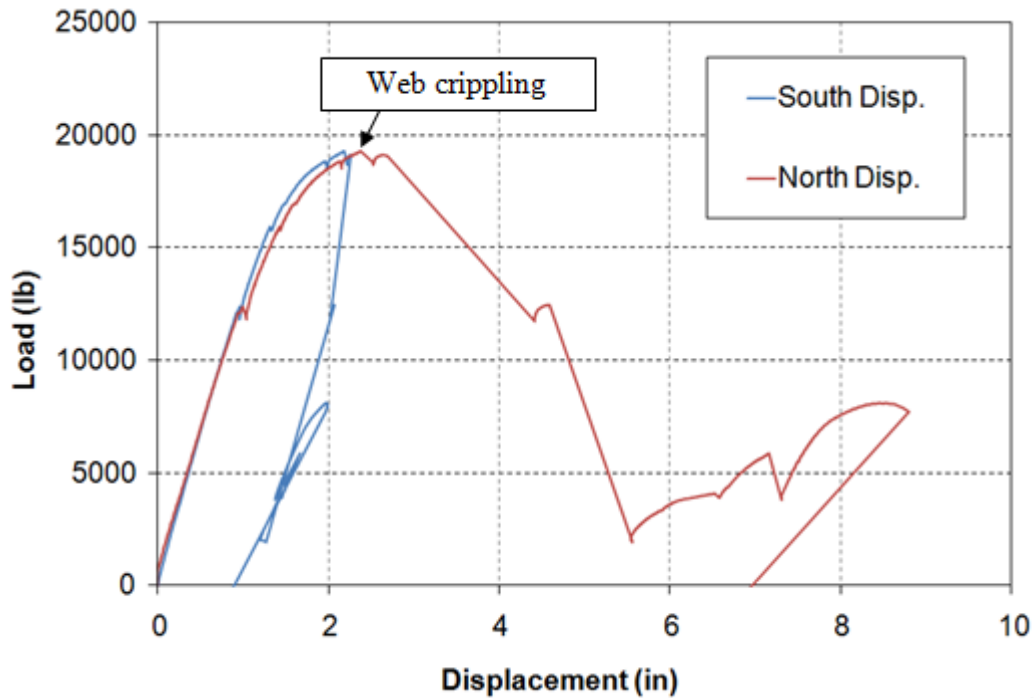


Figure 35. Typical Load–Displacement Plot of Failure Mode Two

5.4.3. Failure Mode 3

The third failure behavior occurred when the track could not support enough load to cripple the stud but allowed the stud to break through the track flange as shown in Figure 36 and Figure 37. This failure mode has no ductility and immediately releases the load. This would lead to a catastrophic failure inside the structure. This is the failure mode this research is trying to prevent

because the capacity of the stud is being severely restricted by the capacity of the connection. Upgrading the track size or length should be done even farther so that the stud can deflect more and resist more energy before failing.



Figure 36. Failure of Track Flange

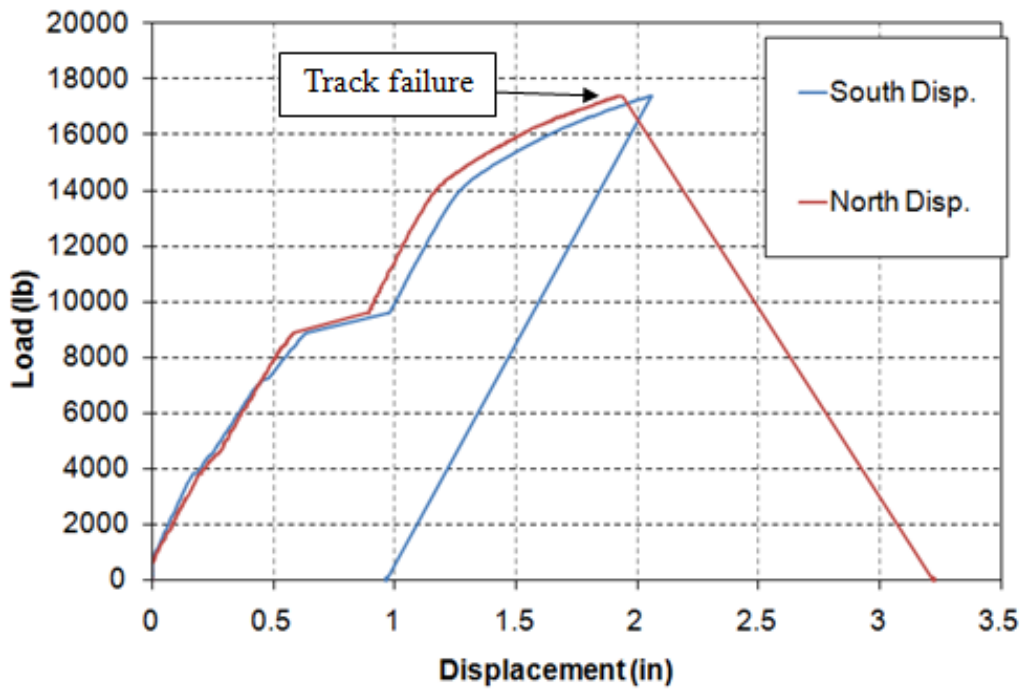


Figure 37. Typical Load–Displacement Plot of Failure Mode Three

5.4.4. Failure Mode 4

The fourth failure behavior occurred when the stud hinged in the middle and developed axial tension. This tension is a beginning to rupturing the stud in a tension failure which would be the maximum capacity available in the stud. This failure mode results in a screw pullout or pullover failure as shown in Figure 38 and allows the capacity to rise considerably once the stud carries tension, as shown in Figure 39.



Figure 38. Tension Development

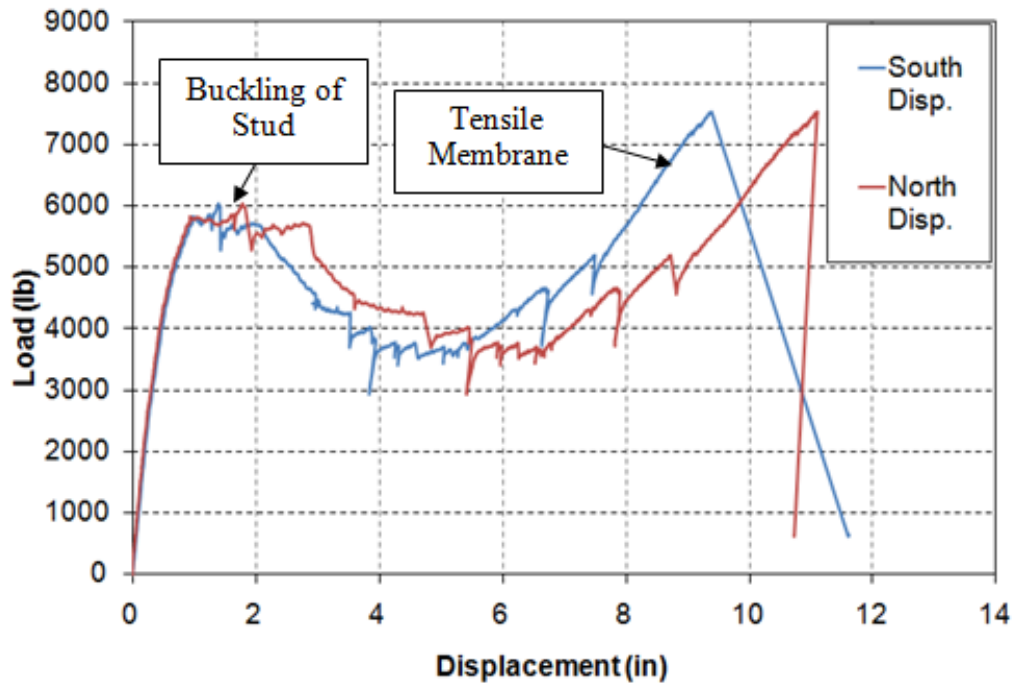


Figure 39. Typical Load-Displacement Plot of Failure Mode Four

5.5. Discussion

Several observations can be made from the data in this phase of testing. Figure 27 shows that both the peak load and energy dissipated increase dramatically with an increase in the number of screws. The energy increase is much higher because the tensile membrane behavior has more of an effect on the area of the curve rather than the peak. Figure 40. shows this by comparing the load–displacement plots. The energy dissipated is very clearly shown as the difference in both peak load and peak deflection. Figure 41 shows a comparison between samples with two, four and six screws and how some samples depend on the number of screws for tension only. This keeps the peak load relatively constant but allows the deflections to reach higher values as the number of screws increase. Figure 42 shows similar results for 1.5-in to 3-in track. The added length of the track allows it to deform and helps the stud to develop more of the tension behavior as opposed to the shorter track, which relies more on the screws. On the other side of that argument is the stiffness of the track. The stiffer track caused by a thicker gauge prevents the tensile membrane from developing but increases bearing strength as shown in Figure 43. This extra stiffness allowed more shear behavior but lost its benefit because it prevents rotation and tension development.

Table 8. Strength Increase Comparison

Compared to	Screws	Track	Peak load	Energy increase
1 screw	2	1.5 in	14%	89%
1 screw	4	1.5 in	15%	111%
2 screws	4	3 in	108%	173%
2 screws	6	3 in	111%	185%

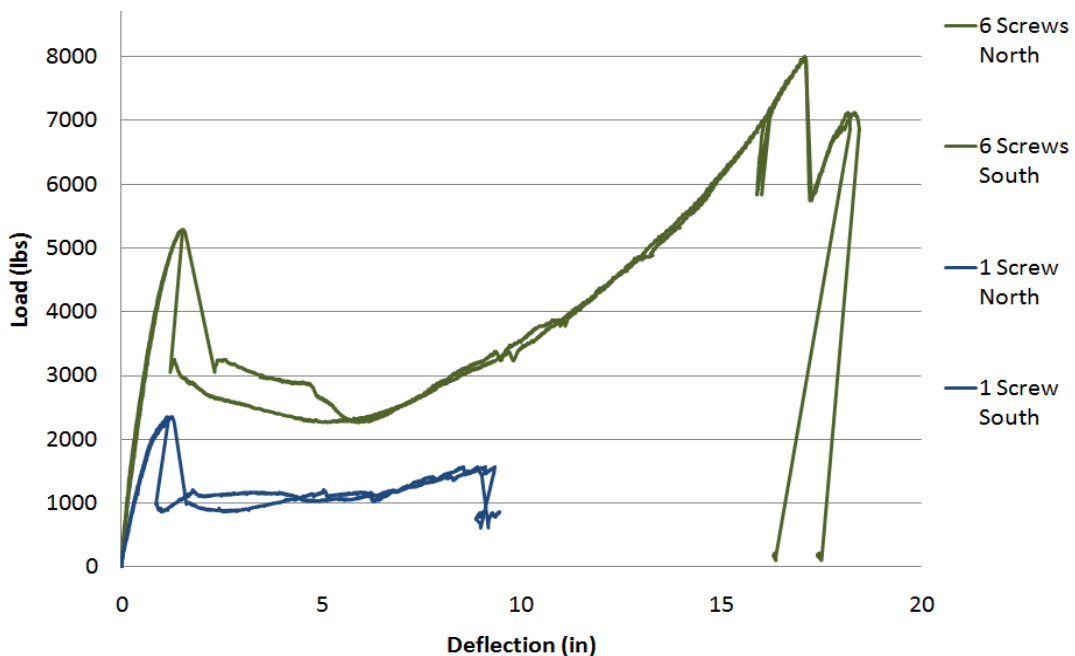


Figure 40. Load–Deflection Plots for One and Six Screws

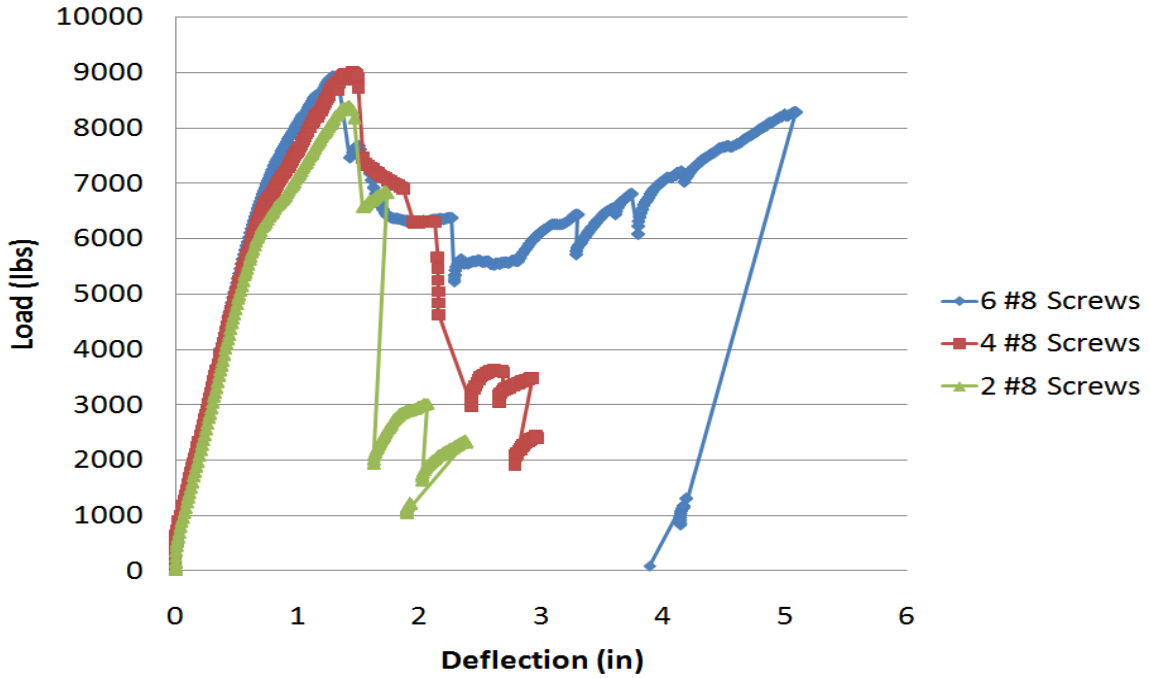


Figure 41. Load-Deflection Plots for Two, Four and Six Screws

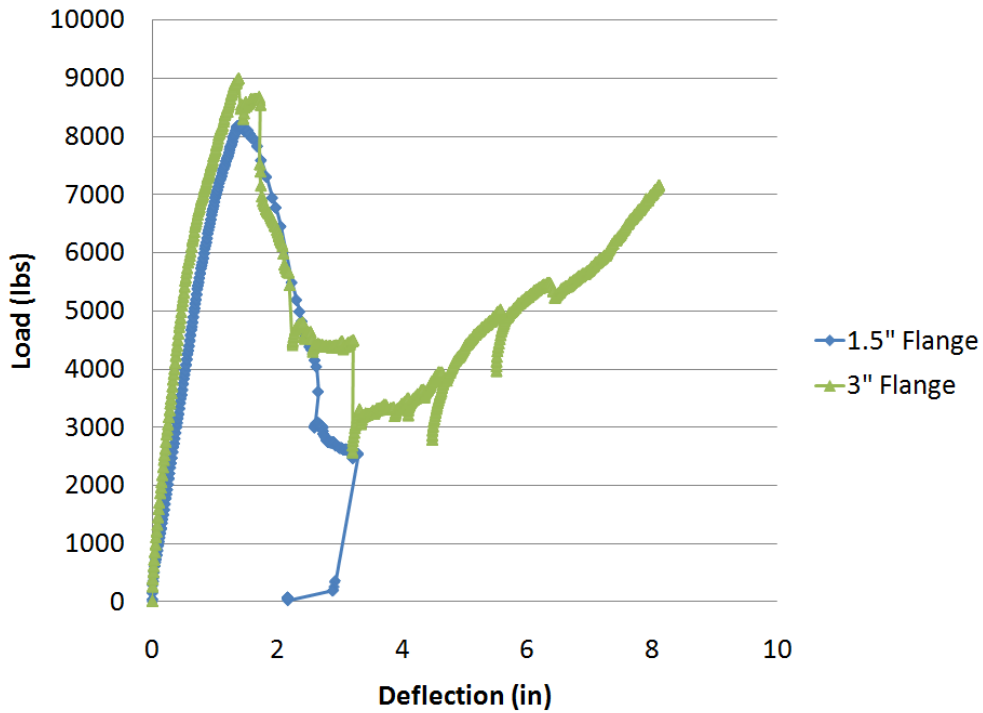


Figure 42. Load-Deflection Plots for 1.5-in and 3-in Flanges

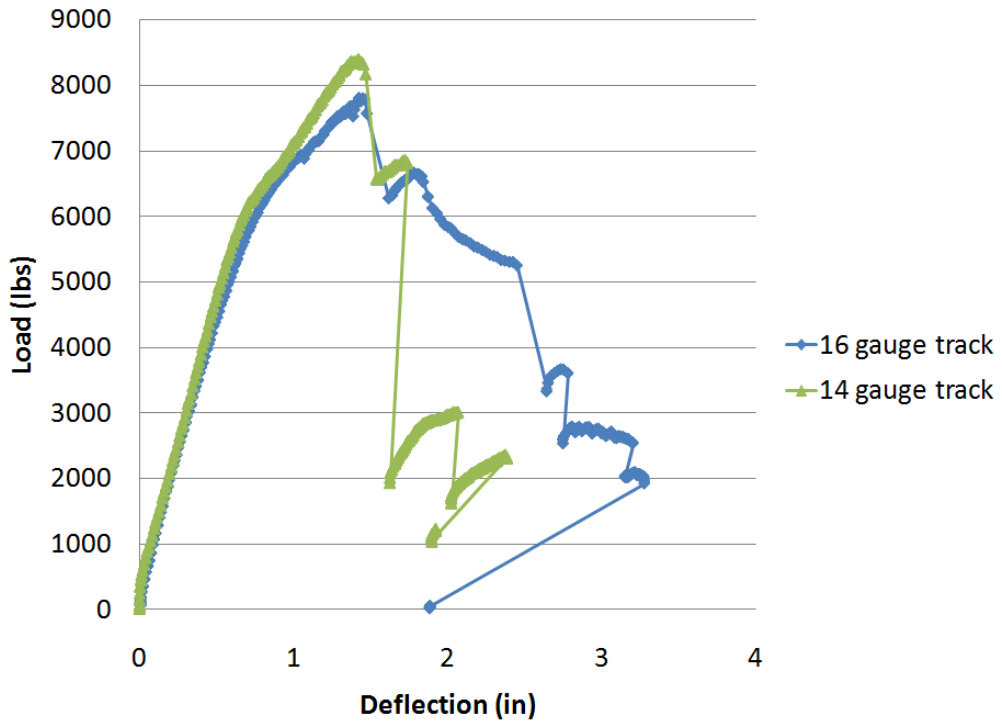


Figure 43. Load–Displacement Plots for 14- and 16-gauge Track

6. FULL-LENGTH BEAM SAMPLES

6.1. Objective

As the span length increases to a full-length of 10 ft, several other limit states become relevant. Tension membrane, torsional buckling, and hinge development are all possible with the presence of shear and moment interactions. Due to this, several 10-ft samples were tested to help model the applicability of the short-span tests. The matrix was selected based on the trends observed in the short-beam tests described in Sections 4 and 5. The sample numbers for the full-length beams correspond to the same number for the short-beam samples with the same connection details.

6.2. Experimental Set-Up

The 10-ft samples were secured in a similar way to the short-beam samples by using tracks bolted to a rigid frame and loaded with a 16-point loading tree as shown in Figure 44. The selected test matrix is shown in **Error! Reference source not found.** The samples were loaded statically until failure, and the load was recorded using a data acquisition system. Deflection measurements were recorded at the midpoint of each stud and the quarter point of one stud as shown in Figure 45.

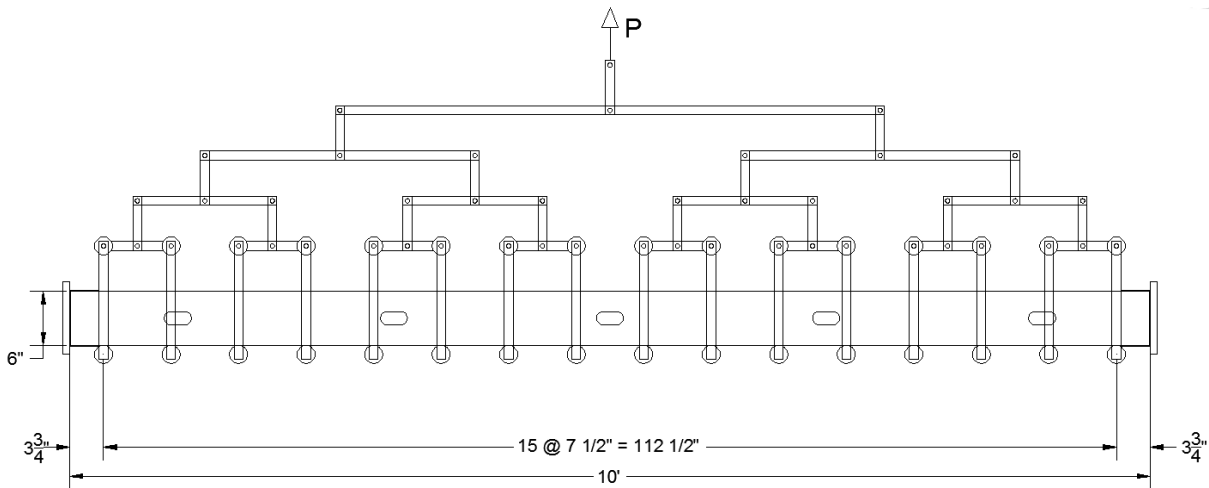


Figure 44. Ten-foot 16-point Loading Tree Diagram

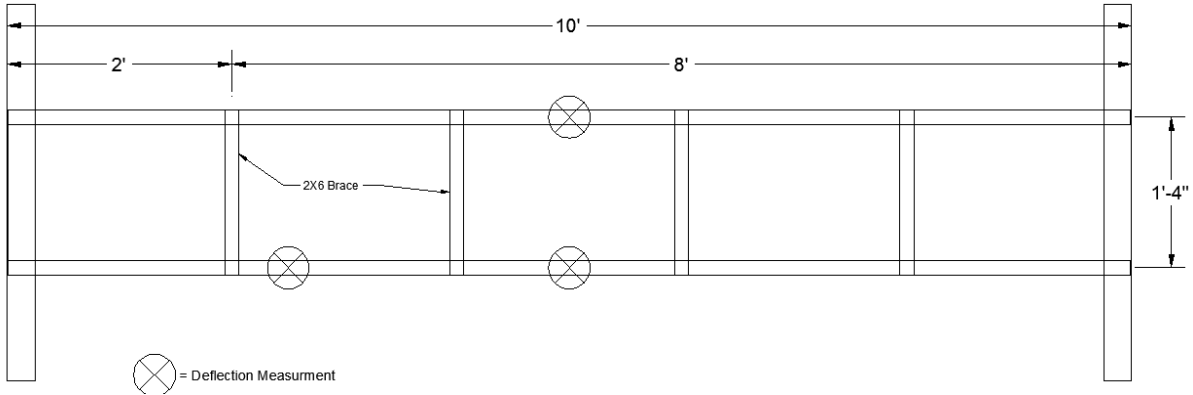


Figure 45. Ten-foot Sample Deflection Measurement Locations

Table 9. Ten-foot Sample Matrix

Sample #	Stud	6-in Track gauge	Flanges in	Size of Screws	Number of Screws
8	600S137-33 (20 ga)	20	1.5	#8	1
9				#10	1
10				#12	1
15	600S162-54 (16 ga)	16	3	#8	6
20		14			6
22					2
23		16	#10	2	
24			#12	2	
26		1.5	16	#8	2
28				#10	2
29	#12			1	
30	#12			2	
32	14	#10	2		
40	12		4		
41			2		
42		1			

Figures 46–48 are photographs of the installed test configuration.

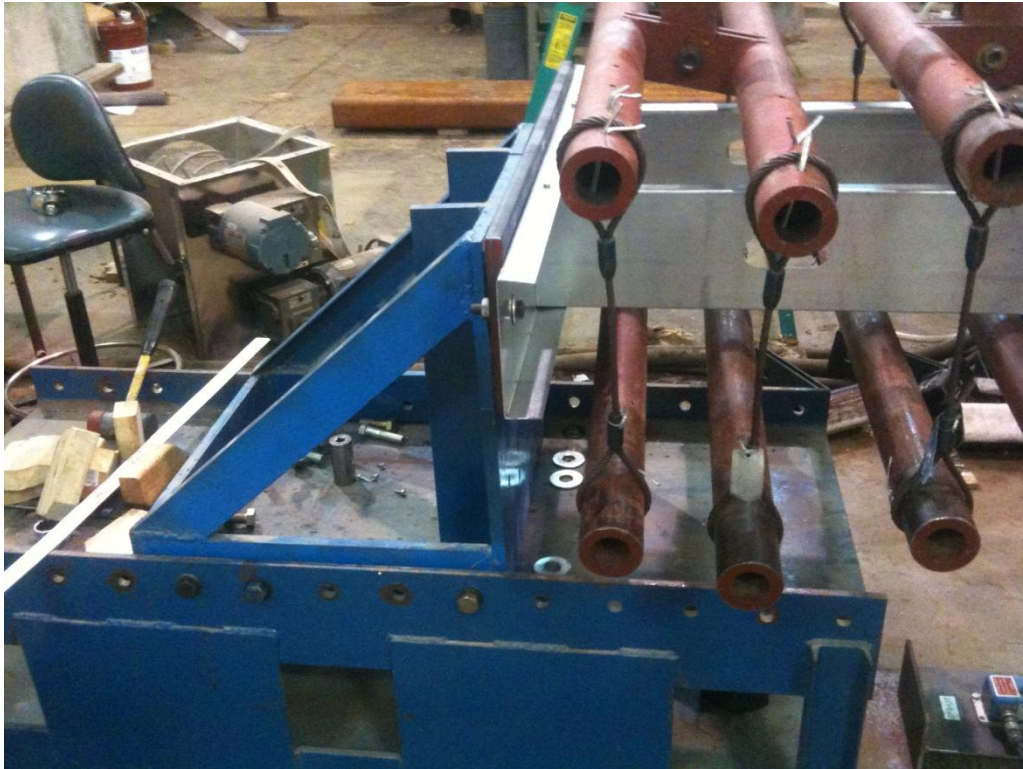


Figure 46. Ten-foot Sample Support



Figure 47. Ten-foot Sample Prior to Testing



Figure 48. Ten-foot Sample Deflection Gauge Locations

6.3. Results

The load capacity results of each of the full-length tree samples are shown in

Table 10.. In addition, the maximum deflection is also given in the Table. The load capacities of the full-length samples compared to the short-span samples are also given in Table 10. Load-deflection plots of each sample as well as post-failure pictures are given in Appendix B. The general response includes a sharp rise in load until the studs buckle and then tensile membrane behavior was observed. Depending on the strength of the connection the screws either failed in shear or the track-to-floor connection pulled over the bolt as shown in Figure B-. It is important to notice that when the stud develops tensile membrane action the energy increases dramatically.

Table 10. Ten-foot Samples Results

Sample #	Experimental Peak Load (kips)		Experimental Peak Energy (kip-in)		Maximum Deflection (in) (Full Span)	Rotation Angle θ (Full Span)
	Short Beam	Full Span	Short Beam	Full Span		
8	2229	2356	4.1	11.4	9.47	9.0
9	2252	2314	2.7	13.0	9.9	9.4
10	2677	2210	4.5	10.8	9.7	9.2
15	9194	8009	28.0	66.4	18.4	17.0
20	8953	10153	28.7	20.7	18.2	16.9
22	8404	5184	10.5	29.0	12.14	11.4

Sample #	Experimental Peak Load (kips)		Experimental Peak Energy (kip-in)		Maximum Deflection (in) (Full Span)	Rotation Angle θ (Full Span)
	Short Beam	Full Span	Short Beam	Full Span		
23	8834	7790	16.5	28.9	12.71	12.0
24	9050	7868	31.7	20.5	16.6	15.5
26	8460	4742	22.5	17.5	13.1	12.3
28	7404	4890	34.0	17.2	15	14.0
29	7059	4533	12.0	11.8	8	7.6
30	7712	6576	28.0	26.6	16.1	15.0
32	2252	2533	9.5	11.1	15.4	14.4
40	19271	13675	56.3	39.9	9.6	9.1
41	16197	12666	13.7	31.1	7.8	7.4
42	16914	12640	22.9	14.1	3.4	3.2

6.4. Discussion

The full-length samples showed many of the same trends as seen in the short-beam tests with a few differences. The size of the screw made a large difference when there was a shear failure of the screw but a negligible difference otherwise. **Error! Reference source not found.** shows that the size of the screw made almost no difference in the weaker samples. Increasing the number of screws did not affect the initial stiffness or crippling load in any of the samples but helped the sample by allowing more tension development and higher deflections. **Error! Reference source not found.** shows how adding an extra screw lets the curve continue up into almost 10 in of deflection. Similar to the short-beam tests, the length



Figure 49. Failure of Track-to-Floor Connection

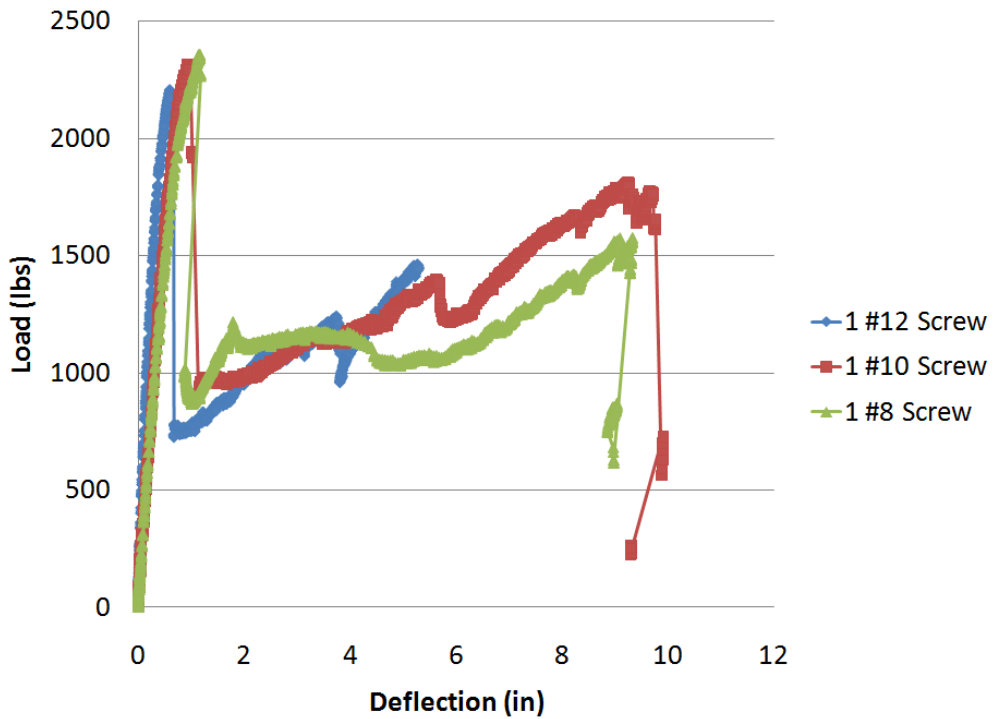


Figure 50. Load–Displacement Plots for #8, #10, and #12 Screws

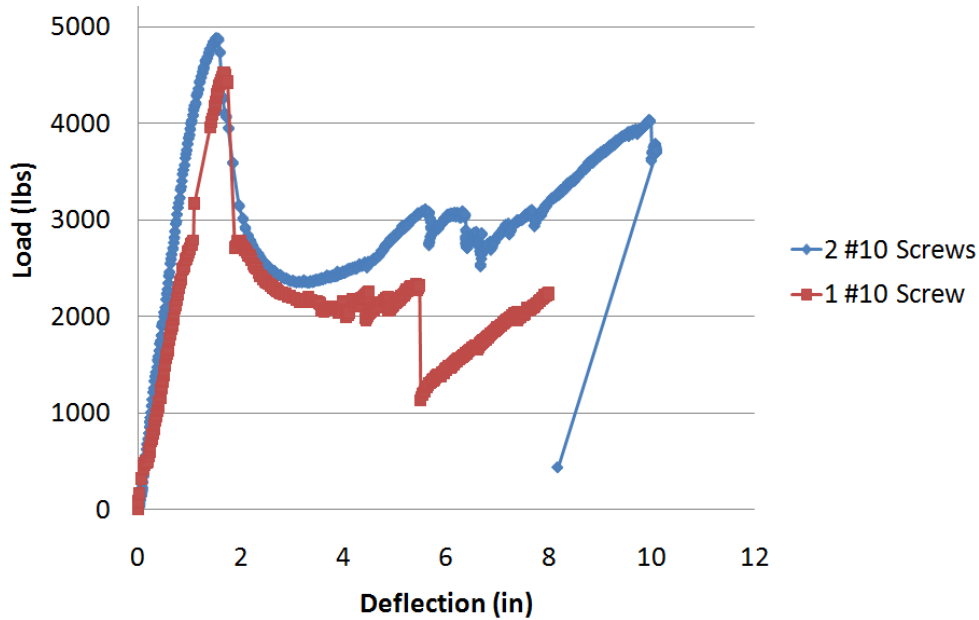


Figure 51. Load vs. Displacement for 1 and 2 #10 Screws

of the flange allowed for more ductility and rotation in the connection without overloading the screws in shear resulting in larger peak and energy values as shown in Figure 52. However, this impact was much larger in the full-length samples because the rotation value had a larger effect once the span increased. Figure 53 and Figure 54 show a general upward trend in the amount of energy dissipated, or toughness, as the number of screws increase. Figure 54 shows only the values representing samples which are identical except for the number of screws used. Figure 55 shows the identical samples with the general trend of the size of the screw not having an effect on the toughness.

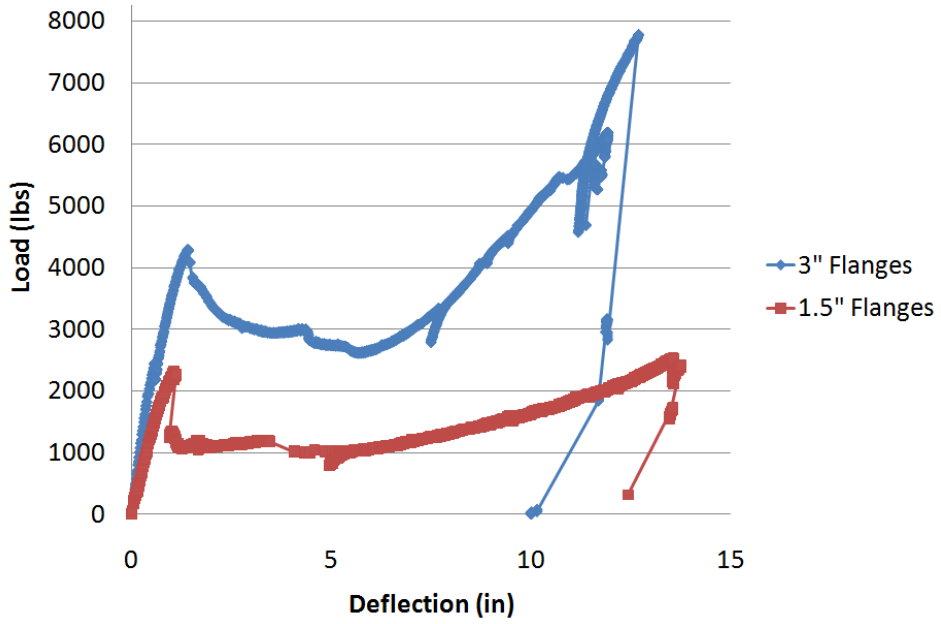


Figure 52. Load–Displacement Plot for 1.5-in and 3-in Flanges

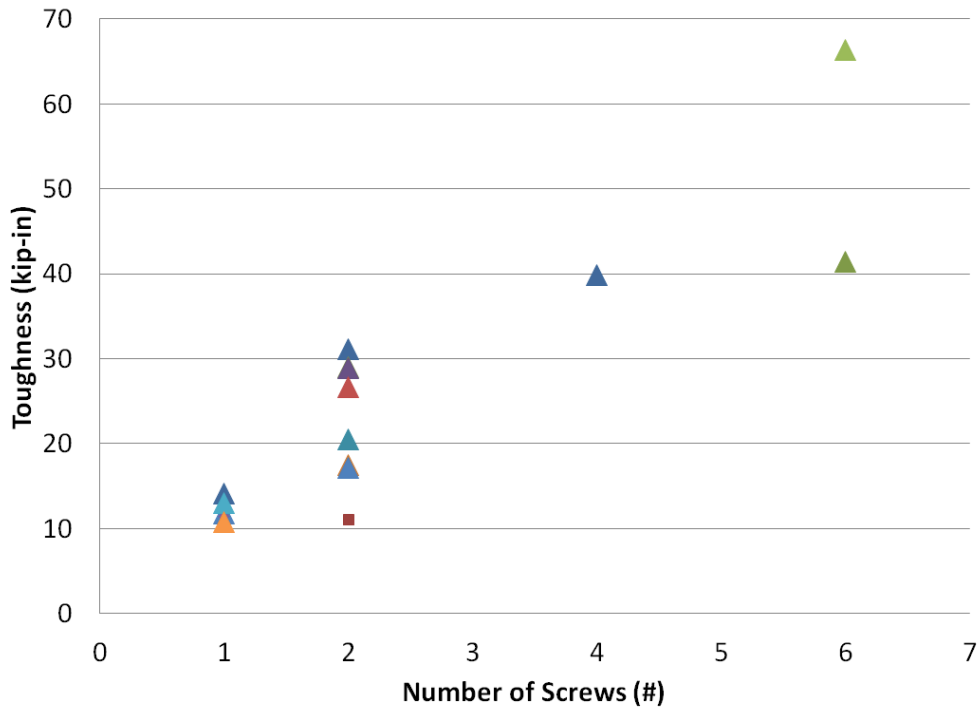


Figure 53. Toughness vs. Number of Screws Comparison (All Samples)

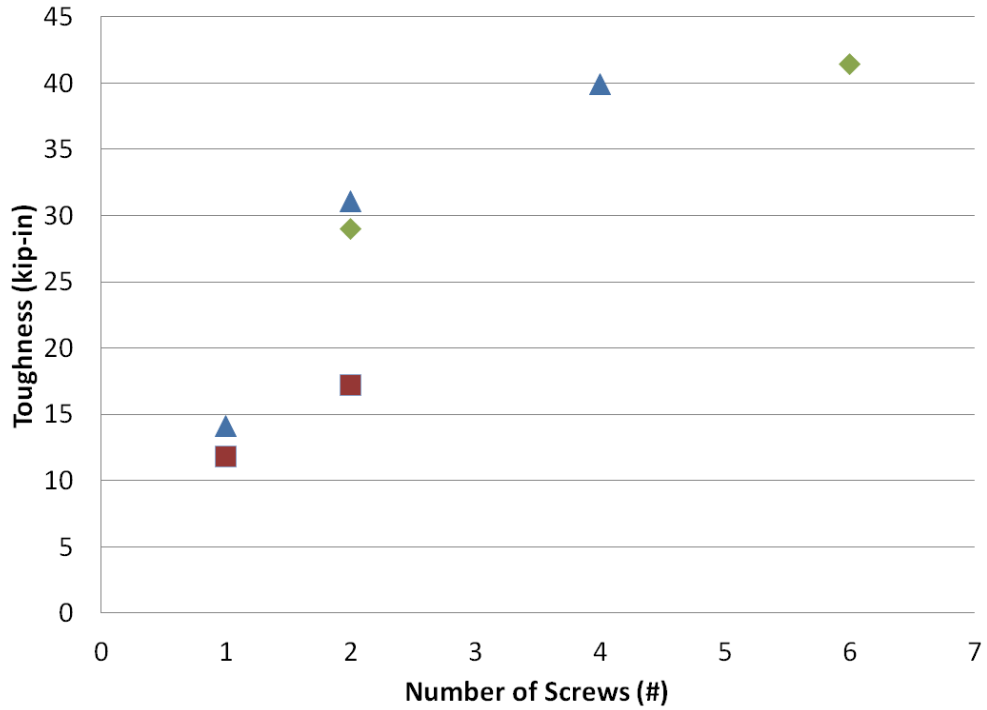


Figure 54. Toughness vs. Number of Screws Comparison (Similar Samples)

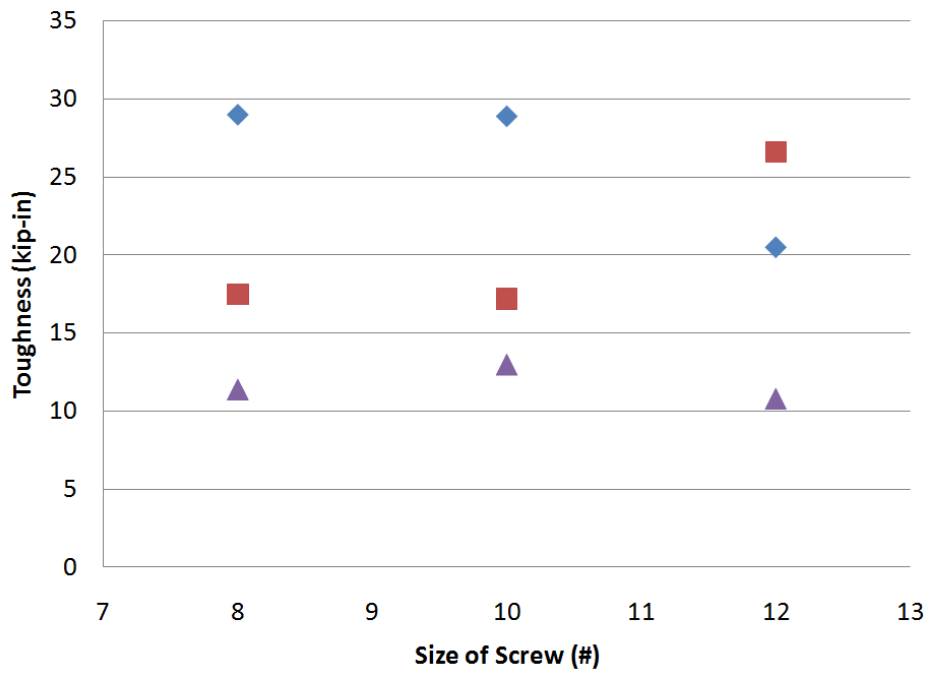


Figure 55. Toughness vs. Size of Screw Comparison

7. CONCLUSIONS AND RECOMMENDATIONS

7.1. Conclusions

All of the proposed modifications were selected to be a moderate change to traditional details so that any strength increase would be practically implemented. The addition of extra screws made a significant increase to strength and could easily be added to conventional practice for any structure facing a moderate threat. This detail could prevent the owner from facing the difficult decision between providing too much protection and risking running out of funds or foregoing any protection at all and risking the lives of the inhabitants.

One of the objectives of this research is to allow tensile membrane action to develop in the stud-track system to resist larger amount of energy. By adding extra screws on the lighter-gauge samples the shear capacity of the screws began to govern as the stud held a high axial tension. These extra screws help not only by adding extra shear area but also reducing the amount of tilting and bearing of the screws that occur. This is very beneficial because in a blast, a properly anchored stud will behave more like a “rope” and the buckling, which is hard to prevent, will be irrelevant.

The heavier-gauge systems still have problems developing tensile membrane action because the stud is very rigid and tends to rotate before it yields. This is a problem for blast design because as the stud rotates and shears the screws on the blast-side of the wall, the shear capacity of the connection drops and the stud easily slips through the opening. Although the lighter-gauge studs are performing closer to ideal for lower threat levels, the heavier sections have a large amount of untapped strength and with more robust connections are the most realistic options for higher threat levels.

7.2. Recommendations

The lighter-gauge samples show that tensile membrane action is fairly easily obtained and can be very useful in blast design. Engineers working with moderate blast threat levels should look into light-gauge steel stud systems and evaluate their effectiveness in their individual applications. By utilizing the extra capacity obtained by additional screws, the lighter-gauge material can be more efficiently used and will result in less-costly construction for a level of threat protection.

Heavier-gauge stud wall systems still have untapped strength that would drastically raise the practicality of using steel stud wall systems for blast design. Other connection methods that carry a large amount of shear without investing a large amount of time or resources to install could begin to develop more capacity in these samples quickly and should be pursued. An idea to accomplish this is to use welded connections so that as the stud rotates the track will be fixed flat to the stud and will allow a very high shear load so that more tension can be developed in the stud. Another idea is to use off-the-shelf clips that properly anchor the studs to the floors.

This project focused on the connection of the stud to the track and neglected the connection of the track to the floor and beams. Some samples in the full-length span test developed enough tension in the stud to pull the track web over the bolt and washer attaching it to the support as shown in **Error! Reference source not found.** As the tensile force grows in the stud it will

need to be carried by the surrounding structure as well. Some ideas to reduce failure modes include staggering the bolts going to the floor to keep the track from rotating as much, increasing the size of the washers against the web of the track, and possibly using square washers or plates so that the track could approach a fixed-type connection to the floor.

The large number of structures that fit into the current research gap show that the inclusion of some of these connection details in the blast analysis and design process may provide the engineering community a tool to protect more buildings that are currently un-protected. Also the results in this report and others similar reports should be incorporated into existing blast design software currently used by blast design engineers and government agencies.

Earlier in this thesis, the UFC criteria were discussed and the limits were later compared to observed rotations. The large discrepancy between these values shows the need for a change to the way the UFC criteria are written. Most of the control samples were around 4° – 8° of rotation while the samples with modified connection details attained rotations of up to 19° . Perhaps the UFC limits can be re-evaluated based on the results of this project and the desired levels of protection. A design guide needs to be developed to predict the response based on the connection design.

8. REFERENCES

1. Older, S., Evaluation of Hybrid Anchor System for Blast-resistant Steel Stud Wall Design, in *Civil Engineering*. 2009, University of Missouri-Columbia: Columbia, Missouri.
2. Bewick, B., E.W. *Enhancement of Steel Stud Walls Subjected to Blast Loads Using Conventional Construction Methods*. in *Shock and Vibration Symposium*. 2010. Orlando, FL.
3. *Cold-Formed Steel Building Systems*. [cited 2010 December 9]; Available from: <http://www.dolphinsteel.com/buildingsystems/systems.htm>.
4. Biggs, J.M., *Introduction to Structural Dynamics*. 1964, New York: McGraw-Hill, Inc.
5. Longinow, A.A., F, *Blast Resistant Design with Structural Steel*. *Journal of Modern Steel Construction*, 2003(Oct. 2003): pp. 61–66.
6. Jobe, J., *Blast Resistant Forced Entry Steel Stud Wall Design*, in *Civil and Environmental Engineering*. 2005, University of Missouri-Columbia: Columbia, Missouri.
7. Departments of the Army, N., and Air Force, *Structures to Resist the Effects of Accidental Explosions*. 1990: Washington, D.C.
8. Yu, W.-W., *Cold-Formed Steel Design*. 2000, New York: John Wiley and Sons, Inc.
9. Brown, J.A., *Experimental Evaluation of Infill CMU and Steel Stud Wall Systems Under Uniform Lateral Pressure*, in *Civil and Environmental Engineering*. 2004, University of Missouri-Columbia: Columbia, Missouri.
10. Dinan, R., *Blast Resistant Steel Stud Wall Design*, in *Department of Civil Engineering*. 2005, University of Missouri-Columbia: Columbia, Missouri.
11. Shull, J., *Steel Stud Retrofit Connection Development and Design*, in *Civil and Environmental Engineering*. 2002, University of Missouri-Columbia: Columbia, Missouri.
12. LaBoube, R.A., *Crippling Capacity of Web Elements with Openings*. *Journal of Structural Engineering*, 1999. **125**(2): pp. 137–141.
13. *Cold-Formed Steel Design Manual*. 2008 ed, ed. AISI. 2008.
14. Holesapple, M.W., *Web crippling of cold-formed steel beams at end supports*. *Engineering Structures*, 2003. **25**(9): pp. 1211–1216.
15. Salim, S.K.a.H., *Use and Misuse of Structural Damping in Blast Response Calculations*. *Concrete and Blast Effects*, 1998. ACI Special Publications SP-175: pp. 121–130.
16. Johnson, R.M., *Engineering Analysis And Design Of Polypropylene Composite Sheets For Blast Retrofit*, in *Civil Engineering*. 2007, University of Missouri-Columbia: Columbia, MO.
17. *Structures to Resist the Effects of Accidental Explosions*, D.o. Defense, Editor.
18. *Cold-Formed Steel Design Manual*. 2008 Edition, Washington DC; American Iron and Steel Institute, 2009.
19. Commentary on North American Specification for the Design of Cold-Formed Steel Structural Members. AISI S100-2007-C, 2007 Edition, Washington DC; American Iron and Steel Institute, 2007.
20. ASTM, *Standard Test Methods and Definitions for Mechanical Testing of Steel Products*, in *ASTM A370-10*. 2010, ASTM International.

Appendix A: Short-Beam Data

LIST OF FIGURES: APPENDIX A

Figure	Page
A-1. Sample 1 after Failure.....	55
A-2. Sample 1 Load–Displacement Plot.....	55
A-3. Sample 2 after Failure.....	56
A-4. Sample 2 Load–Displacement Plot.....	56
A-5. Sample 3 after Failure.....	57
A-6. Sample 3 Load–Displacement Plot.....	57
A-7. Sample 4 after Failure.....	58
A-8. Sample 4 Load–Displacement Plot.....	58
A-9. Sample 5 after Failure.....	59
A-10. Sample 5 Load–Displacement Plot.....	59
A-11. Sample 6 after Failure.....	60
A-12. Sample 6 Load–Displacement Plot.....	60
A-13. Sample 7 after Failure.....	61
A-14. Sample 7 Load–Displacement Plot.....	61
A-15. Sample 8 after Failure.....	62
A-16. Sample 8 Load–Displacement Plot.....	62
A-17. Sample 9 after Failure.....	63
A-18. Sample 9 Load–Displacement Plot.....	63
A-19. Sample 10 after Failure.....	64
A-20. Sample 10 Load–Displacement Plot.....	64
A-21. Sample 11 after Failure.....	65
A-22. Sample 11 Load–Displacement Plot.....	65
A-23. Sample 12 after Failure.....	66
A-24. Sample 12 Load–Displacement Plot.....	66
A-25. Sample 13 after Failure.....	67
A-26. Sample 13 Load–Displacement Plot.....	67
A-27. Sample 14 after Failure.....	68
A-28. Sample 14 Load–Displacement Plot.....	68
A-29. Sample 15 after Failure.....	69
A-30. Sample 15 Load–Displacement Plot.....	69
A-31. Sample 16 after Failure.....	70
A-32. Sample 16 Load–Displacement Plot.....	70
A-33. Sample 17 after Failure.....	71
A-34. Sample 17 Load–Displacement Plot.....	71
A-35. Sample 18 after Failure.....	72
A-36. Sample 18 Load–Displacement Plot.....	72
A-37. Sample 19 after Failure.....	73
A-38. Sample 19 Load–Displacement Plot.....	73
A-39. Sample 20 after Failure.....	74
A-40. Sample 20 Load–Displacement Plot.....	74
A-41. Sample 21 after Failure.....	75
A-42. Sample 21 Load–Displacement Plot.....	75

A-43. Sample 22 after Failure	76
A-44. Sample 22 Load–Displacement Plot	76
A-45. Sample 23 after Failure	77
A-46. Sample 23 Load–Displacement Plot	77
A-47. Sample 24 after Failure	78
A-48. Sample 24 Load–Displacement Plot	78
A-49. Sample 25 after Failure	79
A-50. Sample 25 Load–Displacement Plot	79
A-51. Sample 26 after Failure	80
A-52. Sample 26 Load–Displacement Plot	80
A-53. Sample 27 after Failure	81
A-54. Sample 27 Load–Displacement Plot	81
A-55. Sample 28 after Failure	82
A-56. Sample 28 Load–Displacement Plot	82
A-57. Sample 29 after Failure	83
A-58. Sample 29 Load–Displacement Plot	83
A-59. Sample 30 after Failure	84
A-60. Sample 30 Load–Displacement Plot	84
A-61. Sample 31 after Failure	85
A-62. Sample 31 Load–Displacement Plot	85
A-63. Sample 32 after Failure	86
A-64. Sample 32 Load–Displacement Plot	86
A-65. Sample 33 after Failure	87
A-66. Sample 33 Load–Displacement Plot	87
A-67. Sample 34 after Failure	88
A-68. Sample 34 Load–Displacement Plot	88
A-69. Sample 35 after Failure	89
A-70. Sample 35 Load–Displacement Plot	89
A-71. Sample 36 after Failure	90
A-72. Sample 36 Load–Displacement Plot	90
A-73. Sample 37 after Failure	91
A-74. Sample 37 Load–Displacement Plot	91
A-75. Sample 38 after Failure	92
A-76. Sample 38 Load–Displacement Plot	92
A-77. Sample 39 after Failure	93
A-78. Sample 39 Load–Displacement Plot	93
A-79. Sample 40 after Failure	94
A-80. Sample 40 Load–Displacement Plot	94
A-81. Sample 41 after Failure	95
A-82. Sample 41 Load–Displacement Plot	95
A-83. Sample 42 after Failure	96
A-84. Sample 42 Load–Displacement Plot	96
A-85. Sample 43 after Failure	97
A-86. Sample 43 Load–Displacement Plot	97
A-87. Sample 44 after Failure	98
A-88. Sample 44 Load–Displacement Plot	98

A-89. Sample 45 after Failure	99
A-90. Sample 45 Load–Displacement Plot.....	99
A-91. Sample 46 after Failure	100
A-92. Sample 46 Load–Displacement Plot.....	100
A-93. Sample 47 after Failure	101
A-94. Sample 47 Load–Displacement Plot.....	101
A-95. Sample 48 after Failure	102
A-96. Sample 48 Load–Displacement Plot.....	102



Figure A-1. Sample 1 after Failure

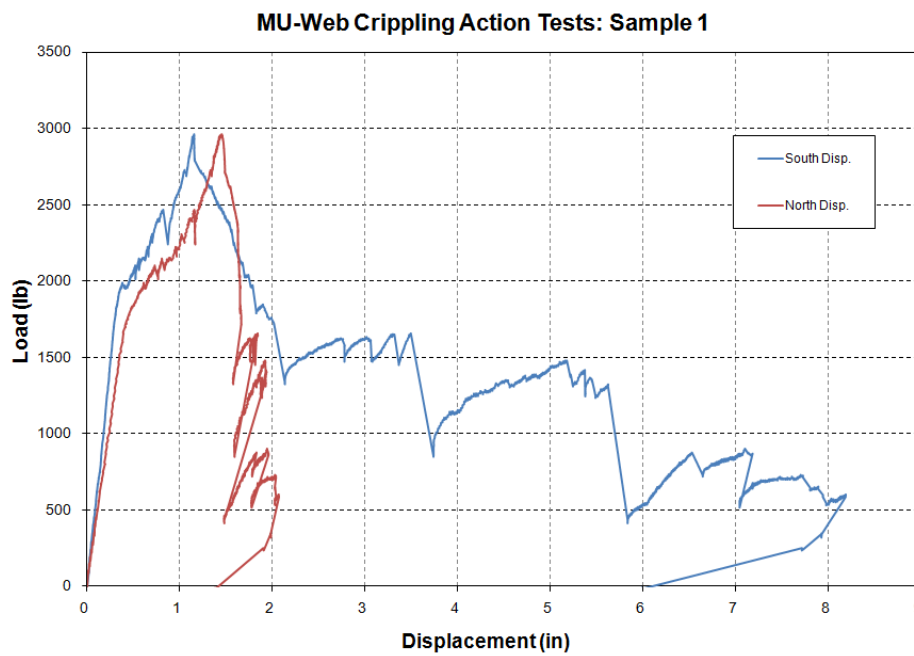


Figure A-2. Sample 1 Load–Displacement Plot



Figure A-3. Sample 2 after Failure

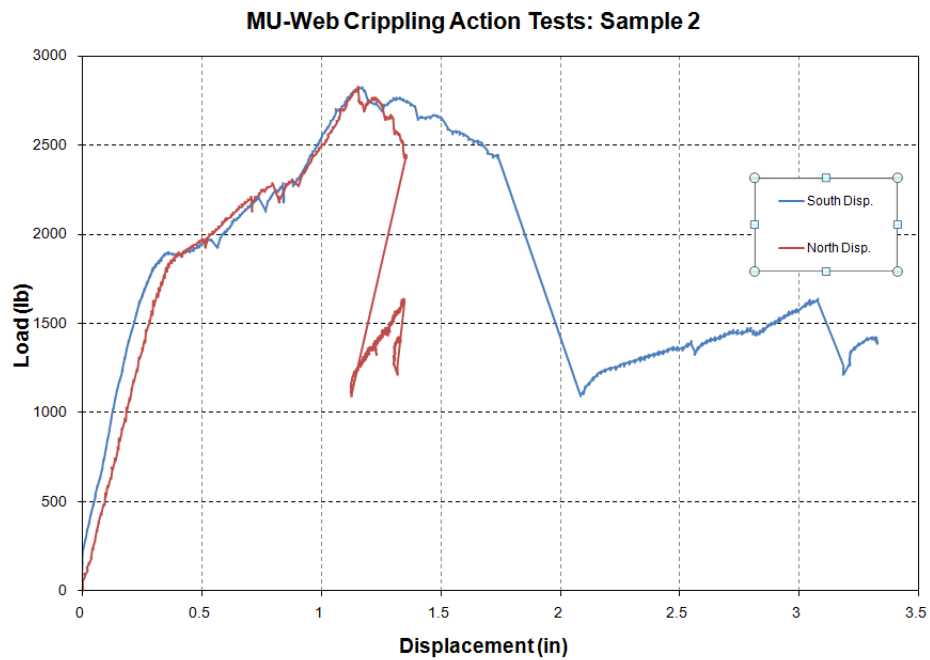


Figure A-4. Sample 2 Load-Displacement Plot



Figure A-5. Sample 3 after Failure

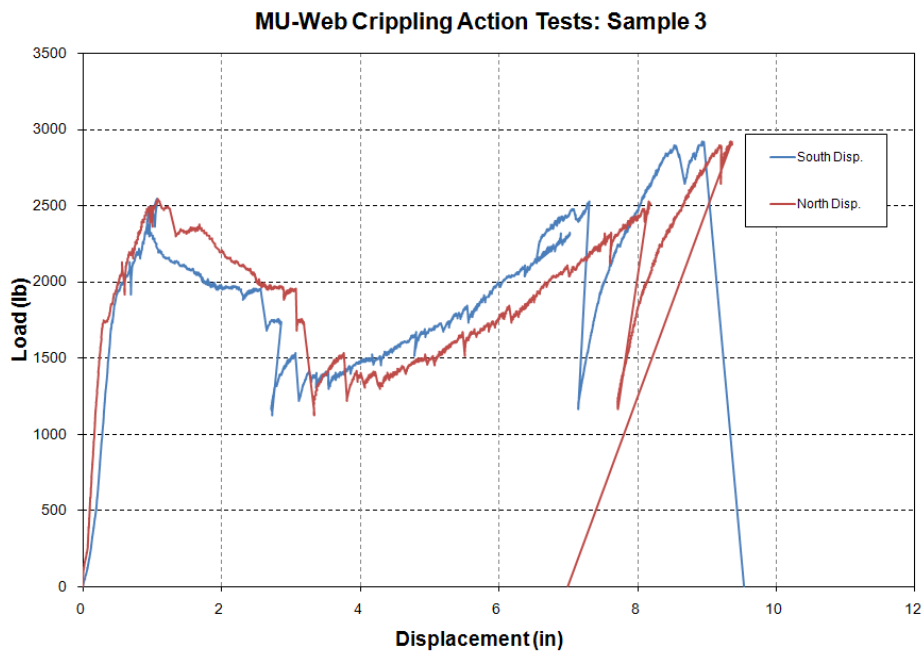


Figure A-6. Sample 3 Load–Displacement Plot



Figure A-7. Sample 4 after Failure

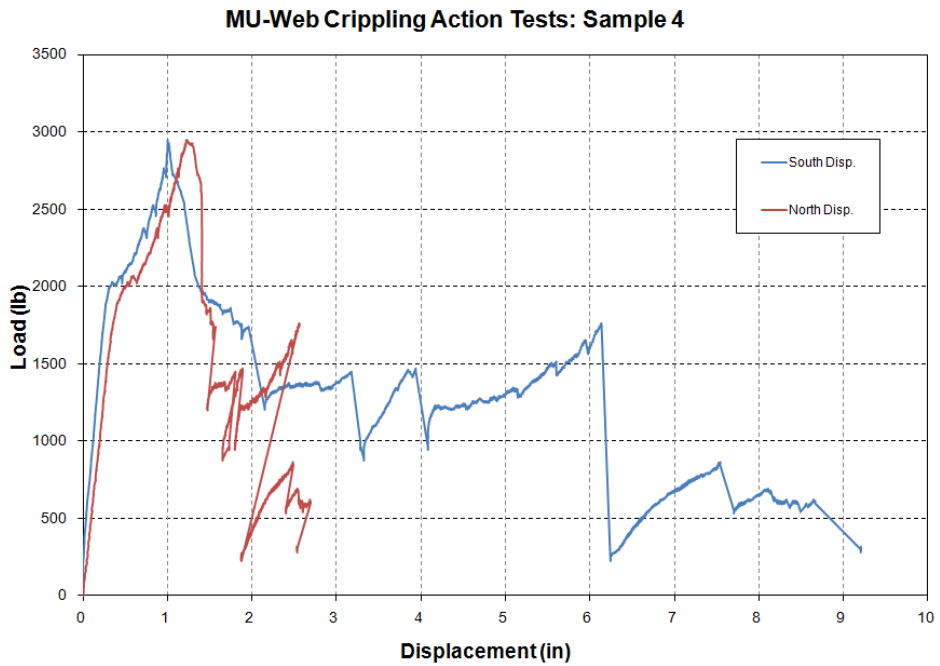


Figure A-8. Sample 4 Load-Displacement Plot



Figure A-9. Sample 5 after Failure

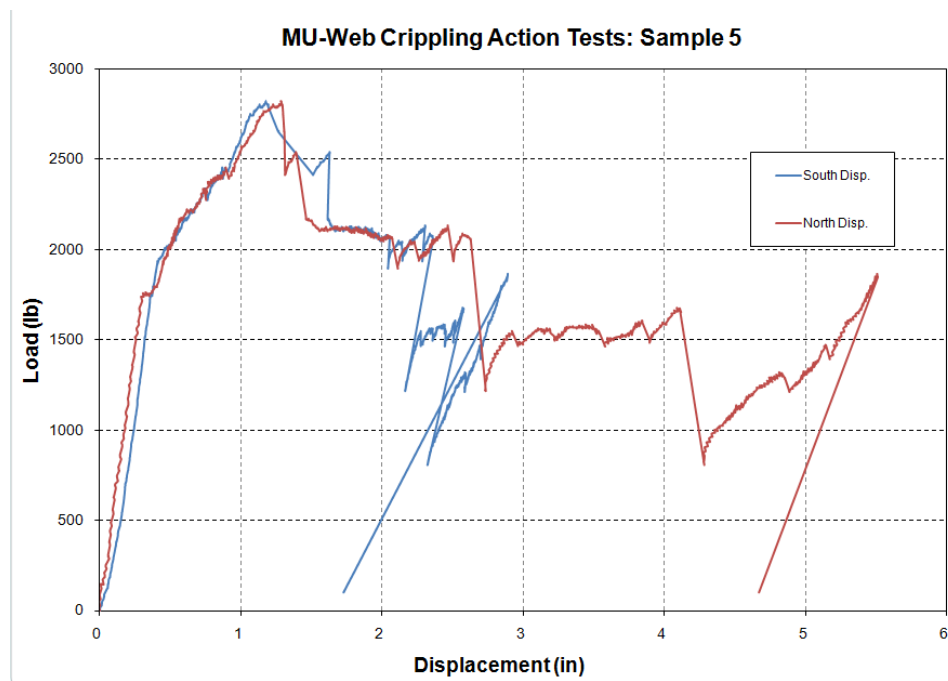


Figure A-10. Sample 5 Load-Displacement Plot



Figure A-11. Sample 6 after Failure

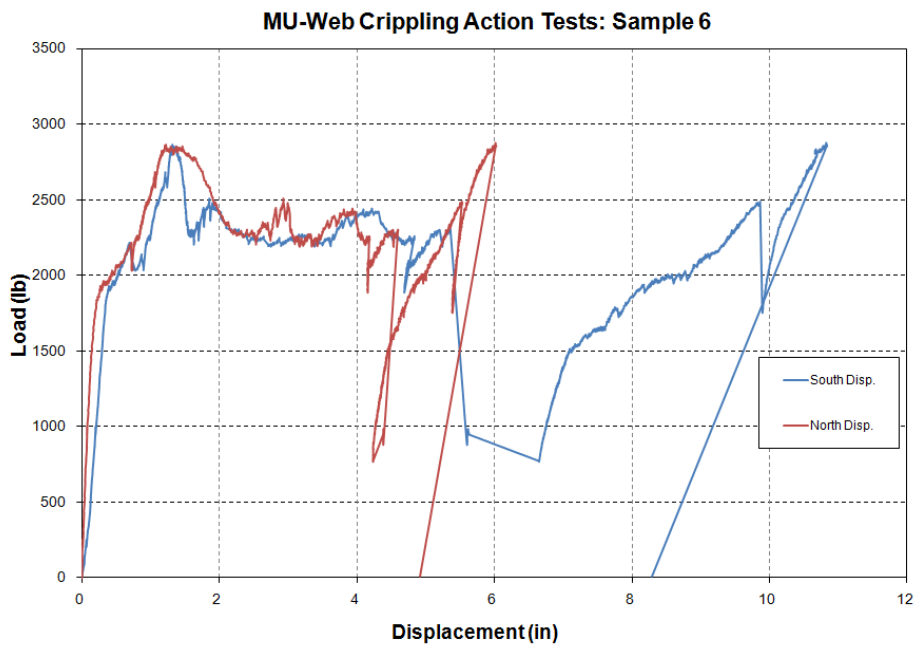


Figure A-12. Sample 6 Load-Displacement Plot



Figure A-13. Sample 7 after Failure

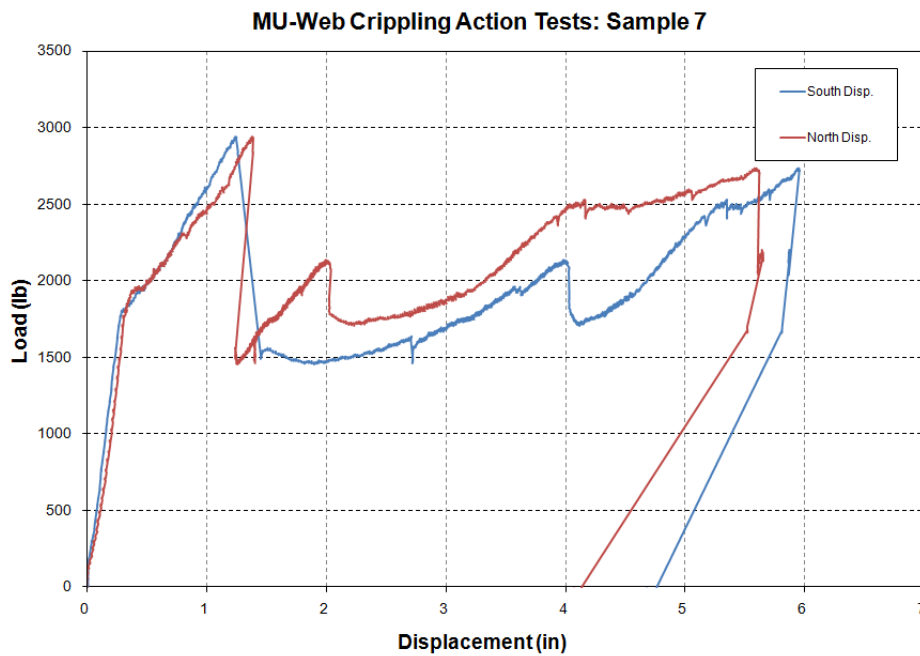


Figure A-14. Sample 7 Load-Displacement Plot



Figure A-15. Sample 8 after Failure

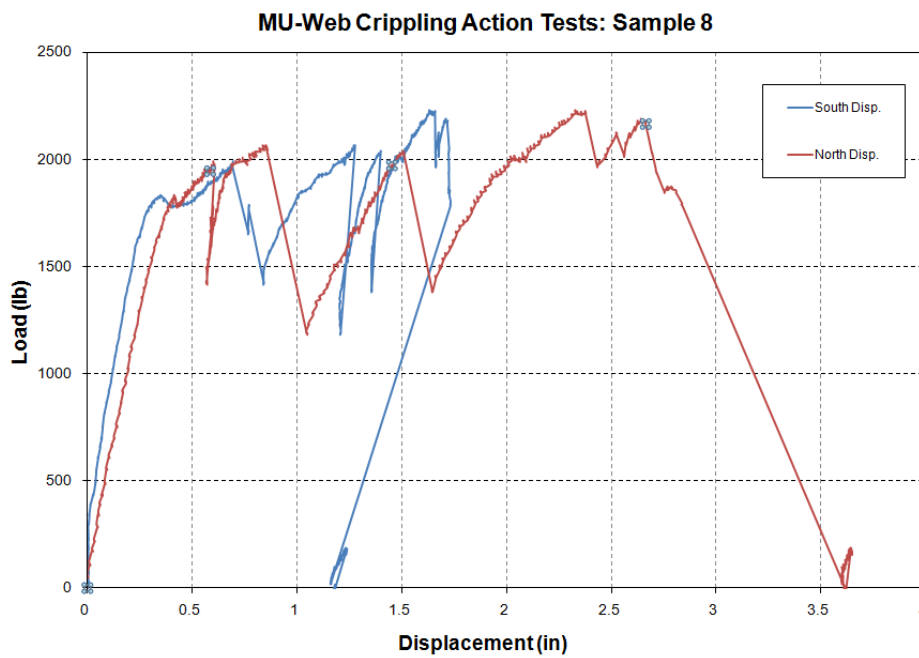


Figure A-16. Sample 8 Load-Displacement Plot



Figure A-17. Sample 9 after Failure

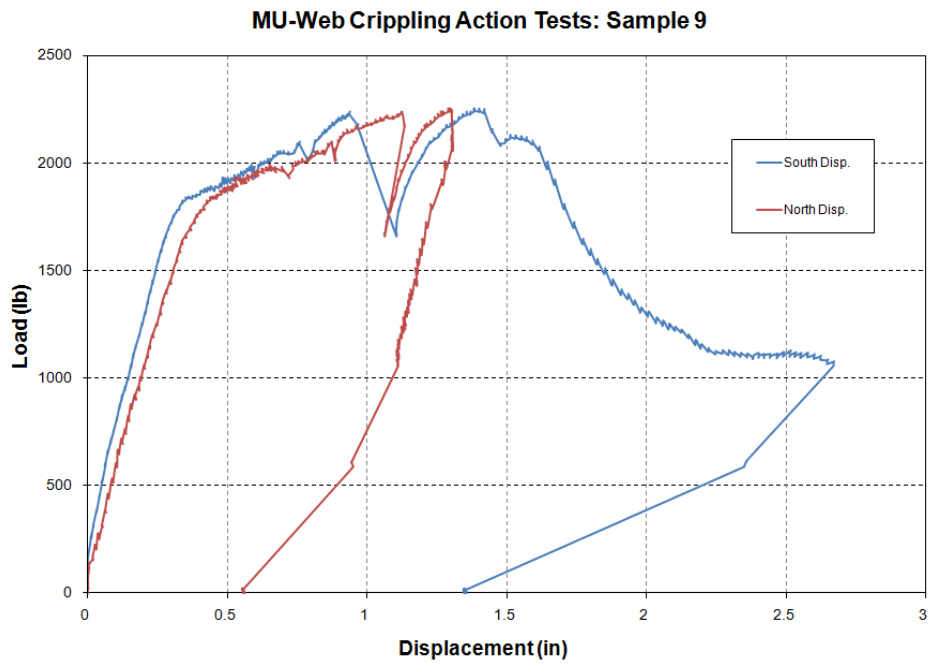


Figure A-18. Sample 9 Load-Displacement Plot



Figure A-19. Sample 10 after Failure

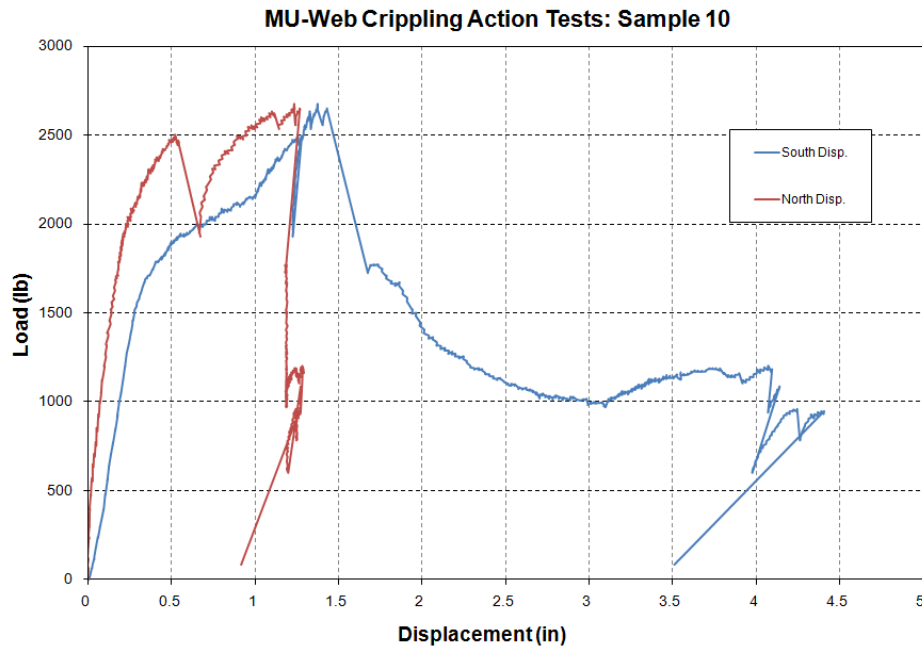


Figure A-20. Sample 10 Load-Displacement Plot



Figure A-21. Sample 11 after Failure

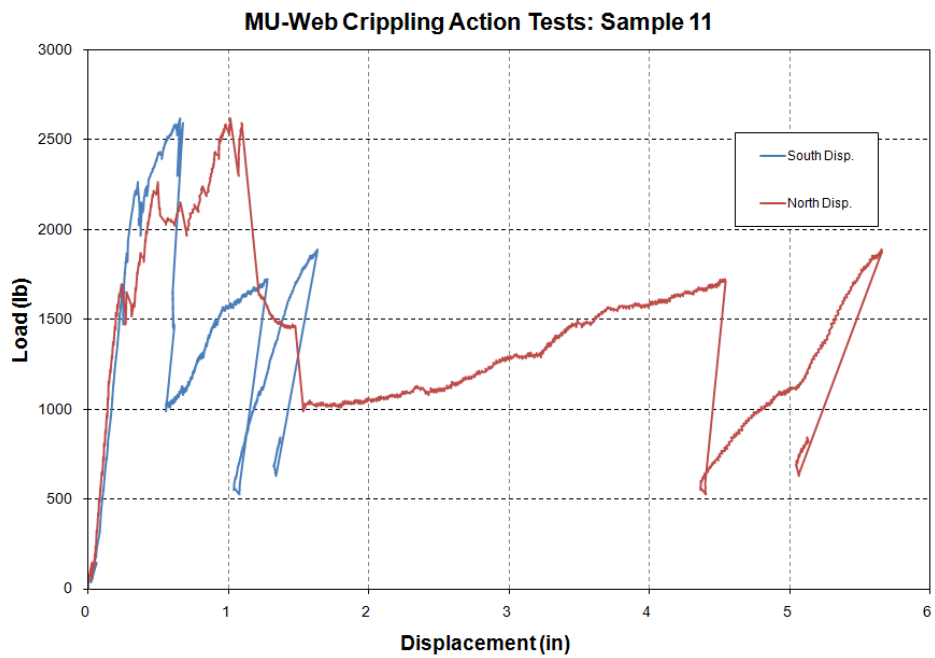


Figure A-22. Sample 11 Load-Displacement Plot



Figure A-23. Sample 12 after Failure

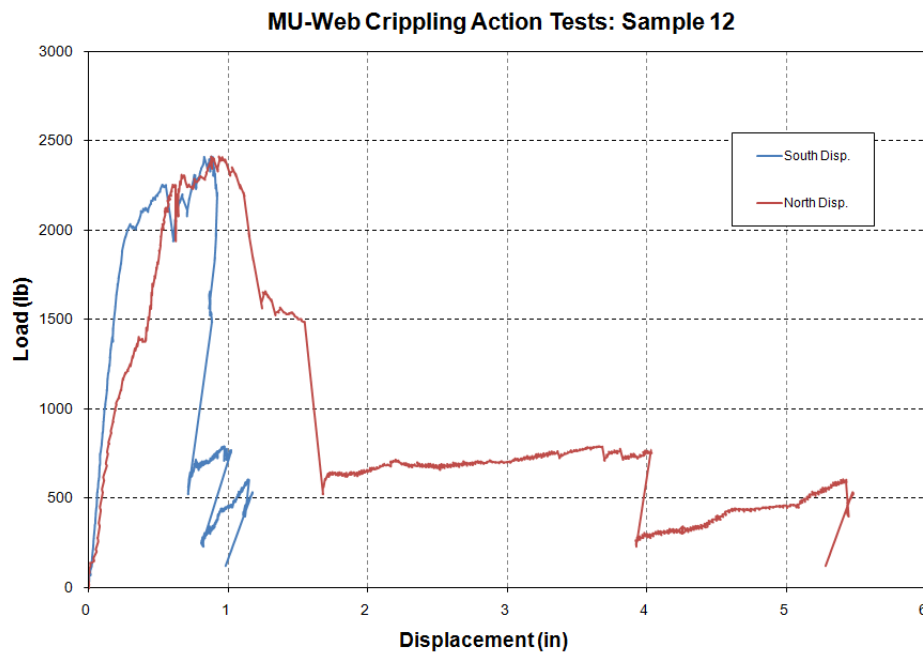


Figure A-24. Sample 12 Load–Displacement Plot



Figure A-25. Sample 13 after Failure

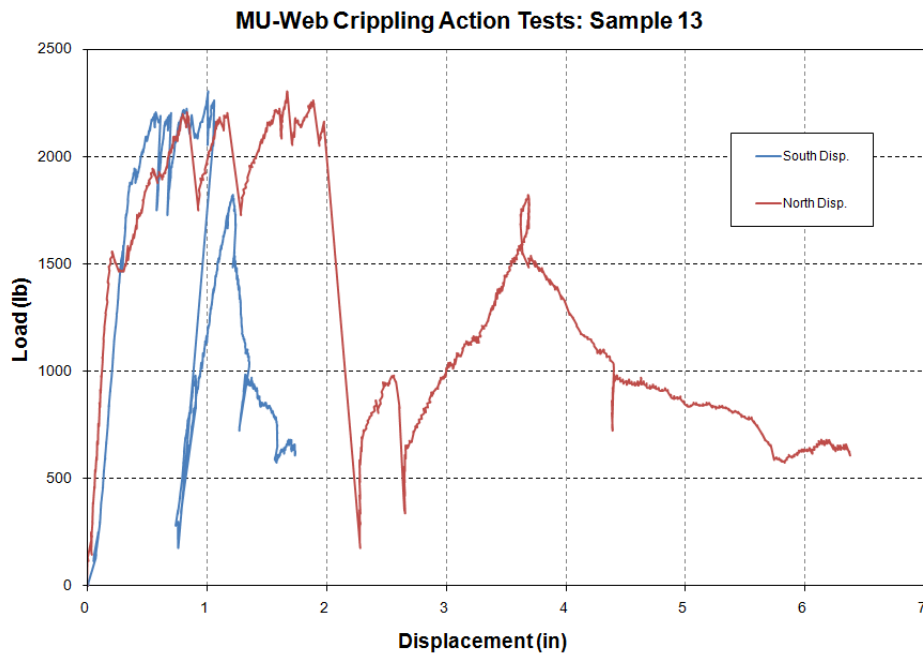


Figure A-26. Sample 13 Load–Displacement Plot



Figure A-27. Sample 14 after Failure

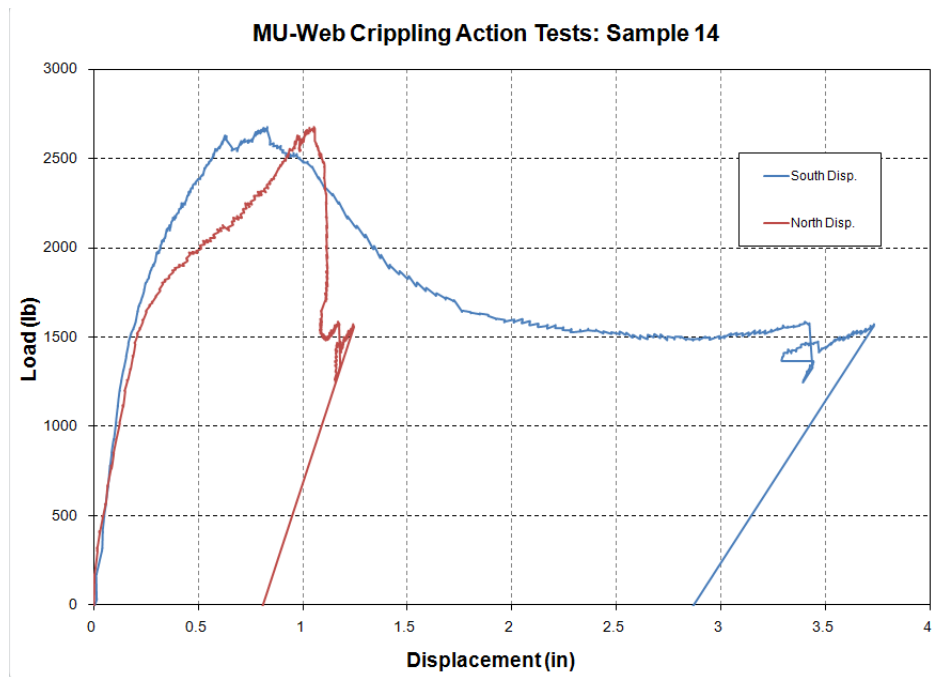


Figure A-28. Sample 14 Load-Displacement Plot



Figure A-29. Sample 15 after Failure

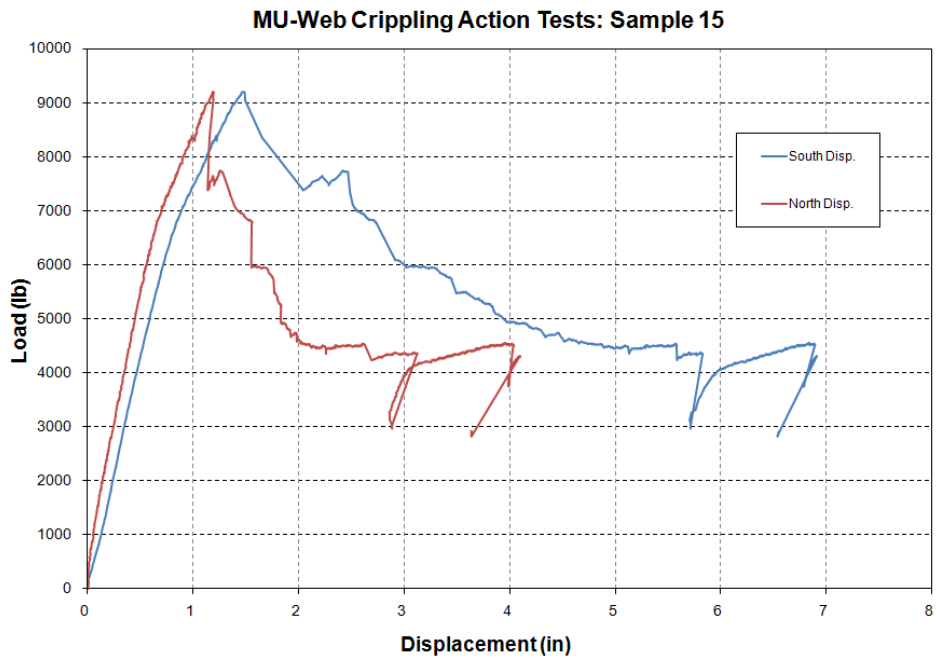


Figure A-30. Sample 15 Load-Displacement Plot



Figure A-31. Sample 16 after Failure

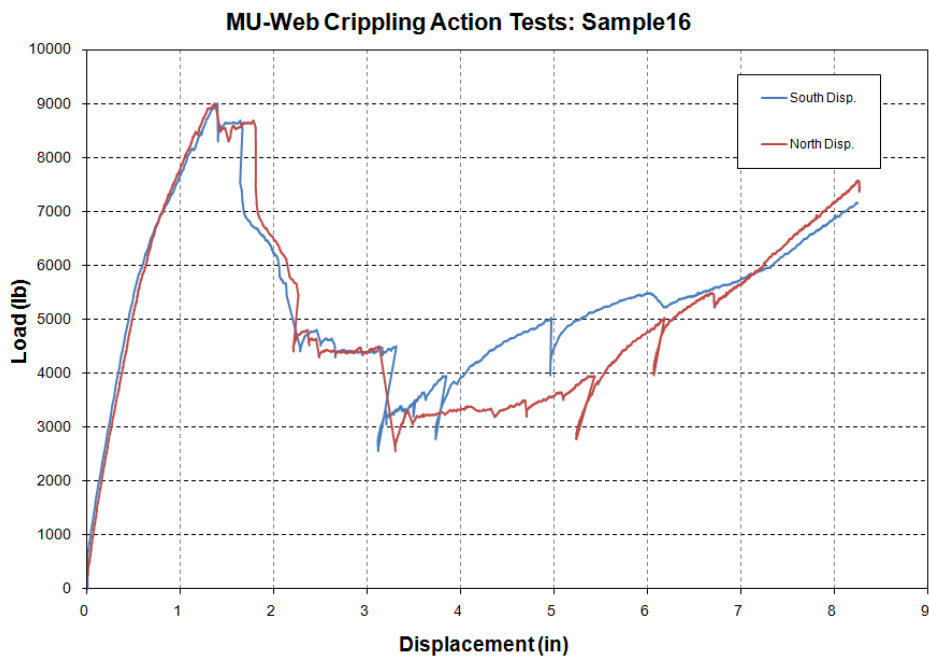


Figure A-32. Sample 16 Load-Displacement Plot



Figure A-33. Sample 17 after Failure

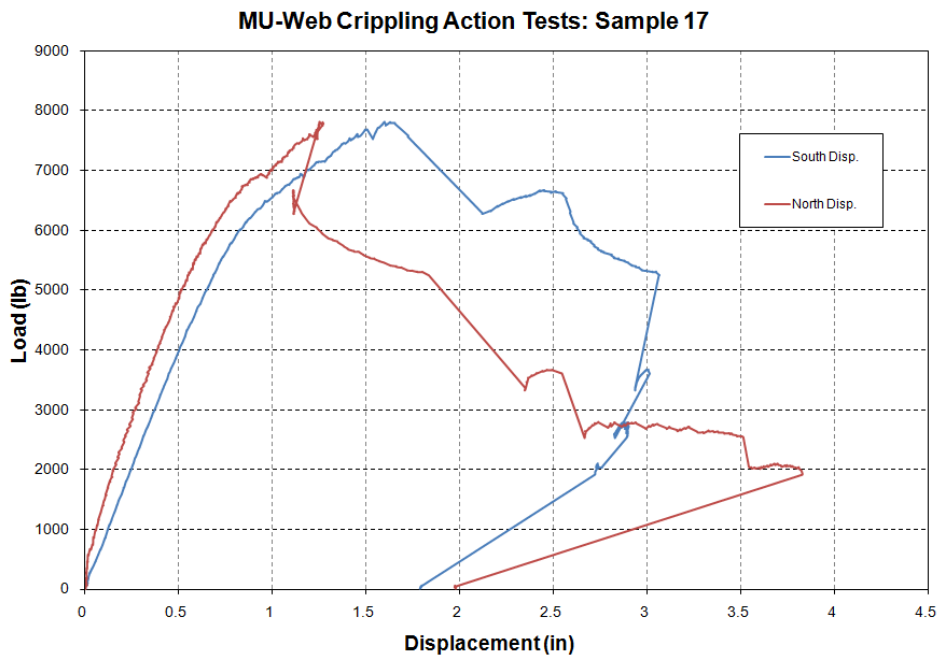


Figure A-34. Sample 17 Load-Displacement Plot



Figure A-35. Sample 18 after Failure

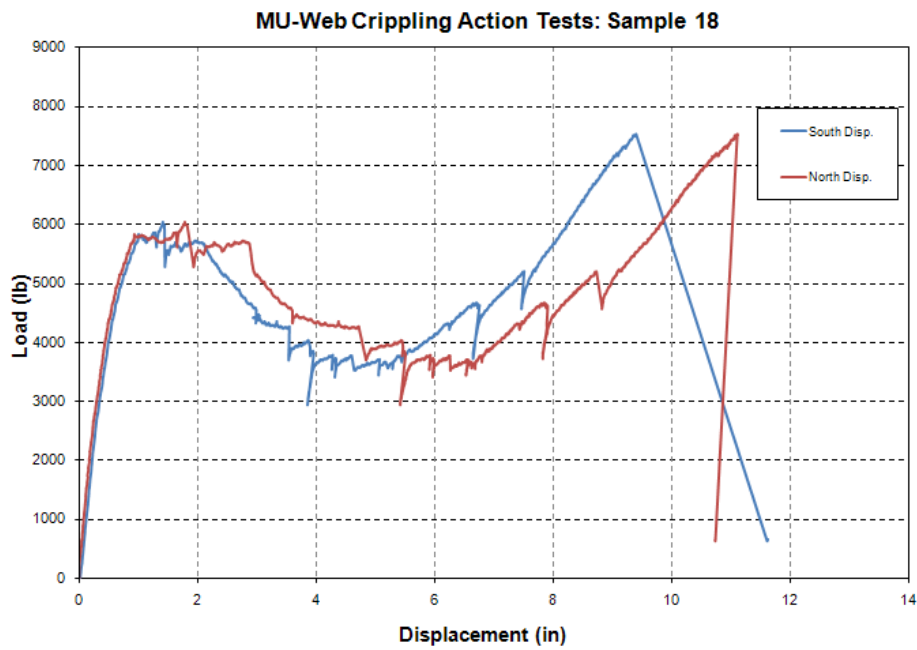


Figure A-36. Sample 18 Load–Displacement Plot



Figure A-37. Sample 19 after Failure

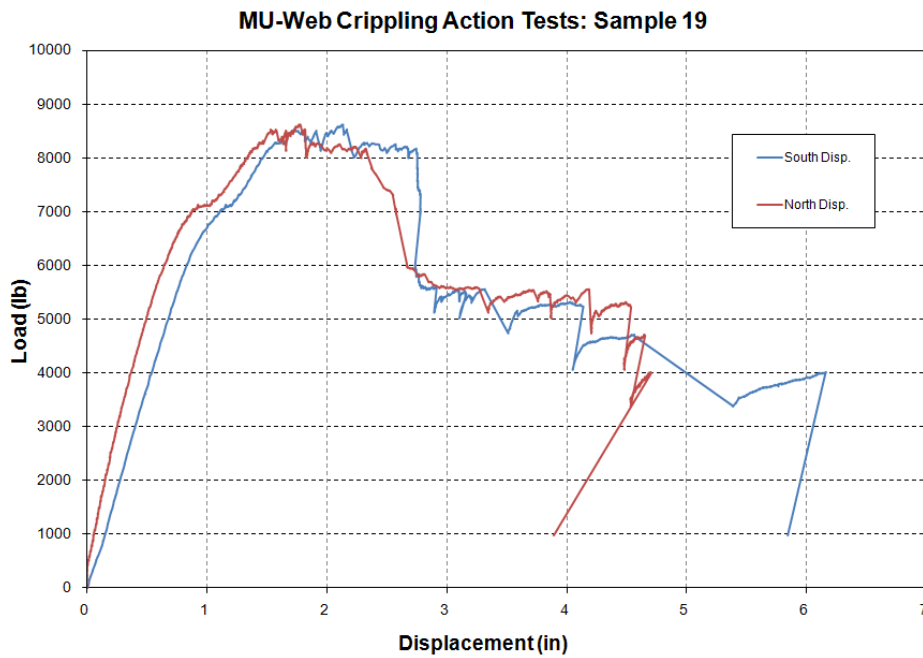


Figure A-38. Sample 19 Load-Displacement Plot



Figure A-39. Sample 20 after Failure

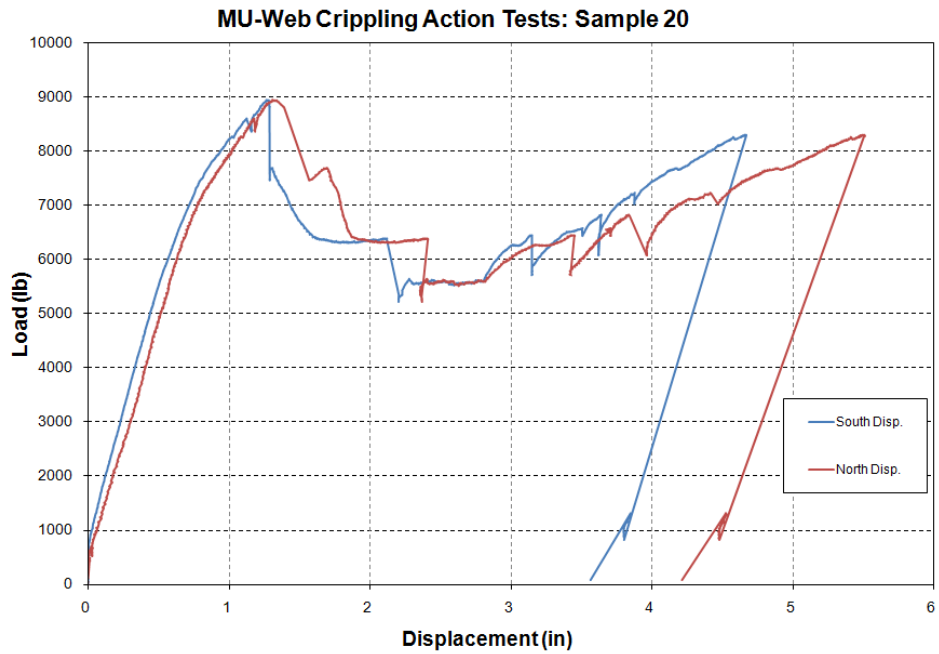


Figure A-40. Sample 20 Load-Displacement Plot



Figure A-41. Sample 21 after Failure

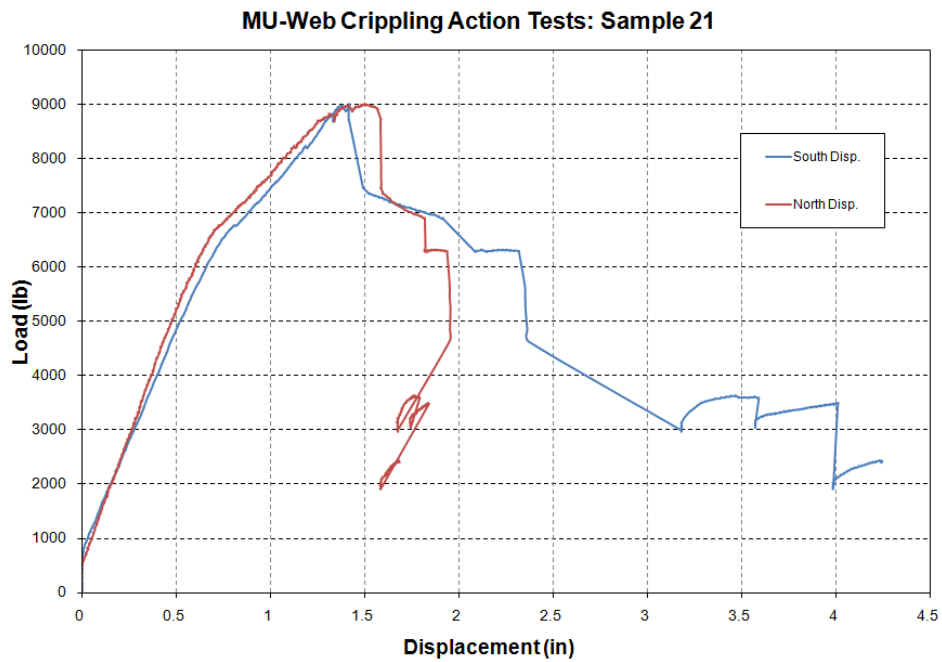


Figure A-42. Sample 21 Load-Displacement Plot



Figure A-43. Sample 22 after Failure

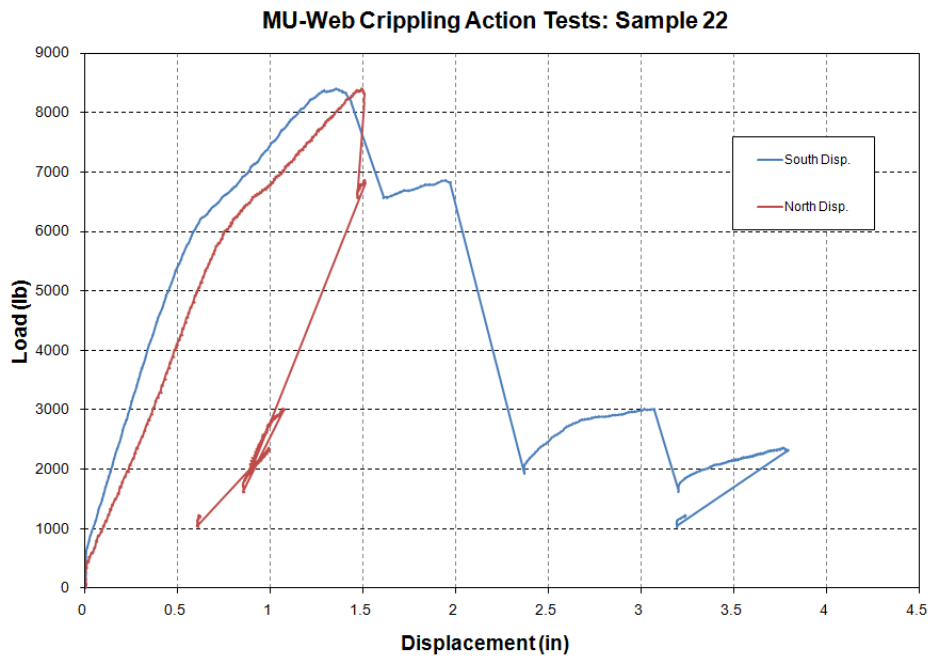


Figure A-44. Sample 22 Load–Displacement Plot



Figure A-45. Sample 23 after Failure

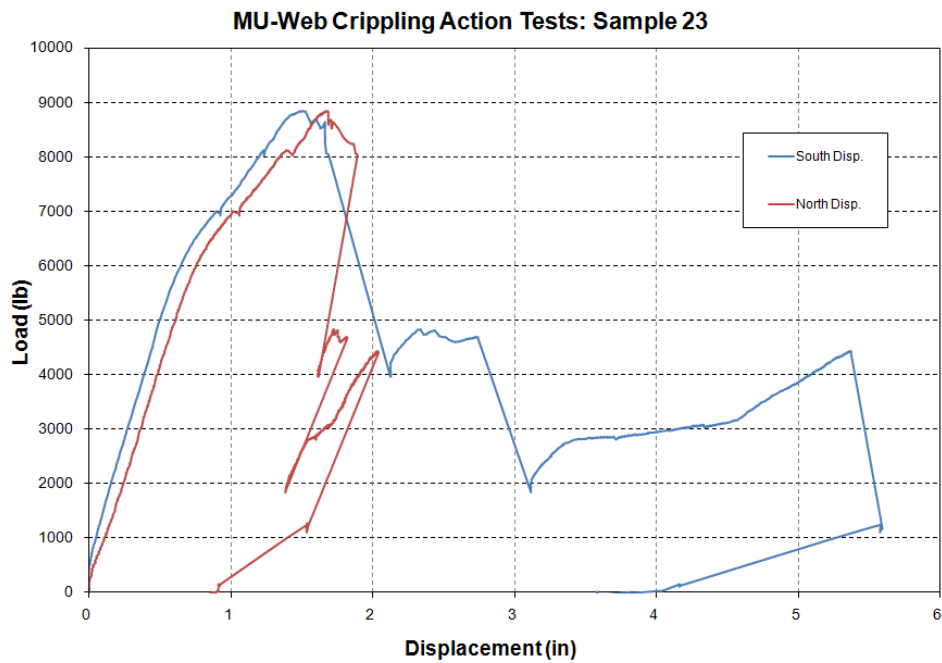


Figure A-46. Sample 23 Load-Displacement Plot



Figure A-47. Sample 24 after Failure

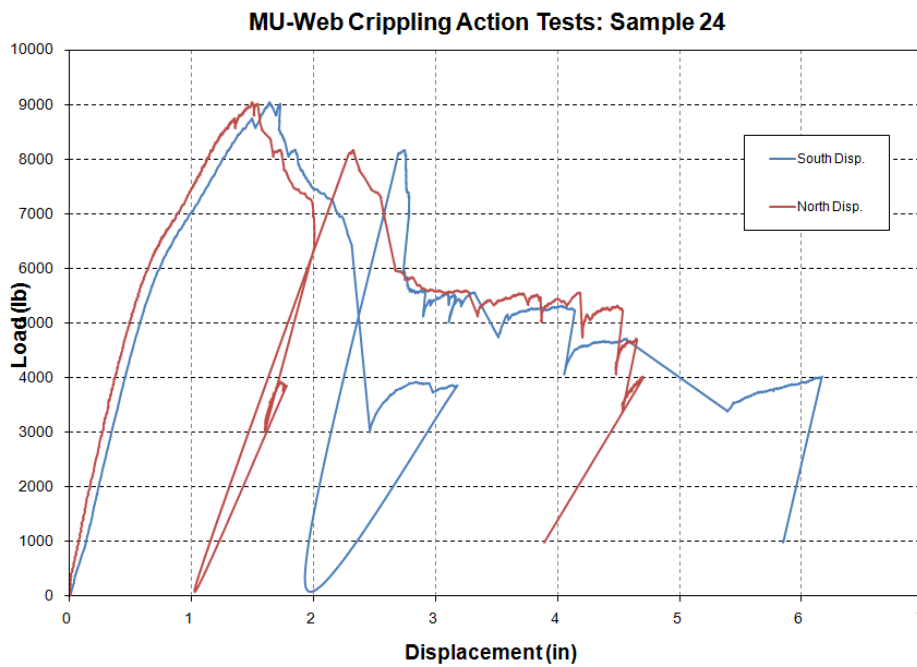


Figure A-48. Sample 24 Load-Displacement Plot



Figure A-49. Sample 25 after Failure

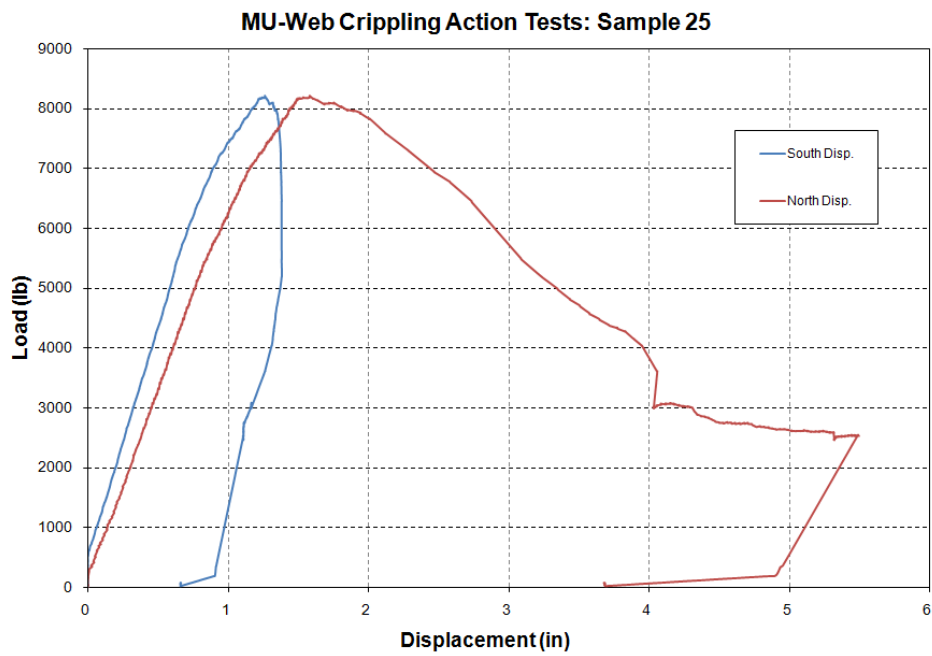


Figure A-50. Sample 25 Load-Displacement Plot



Figure A-51. Sample 26 after Failure

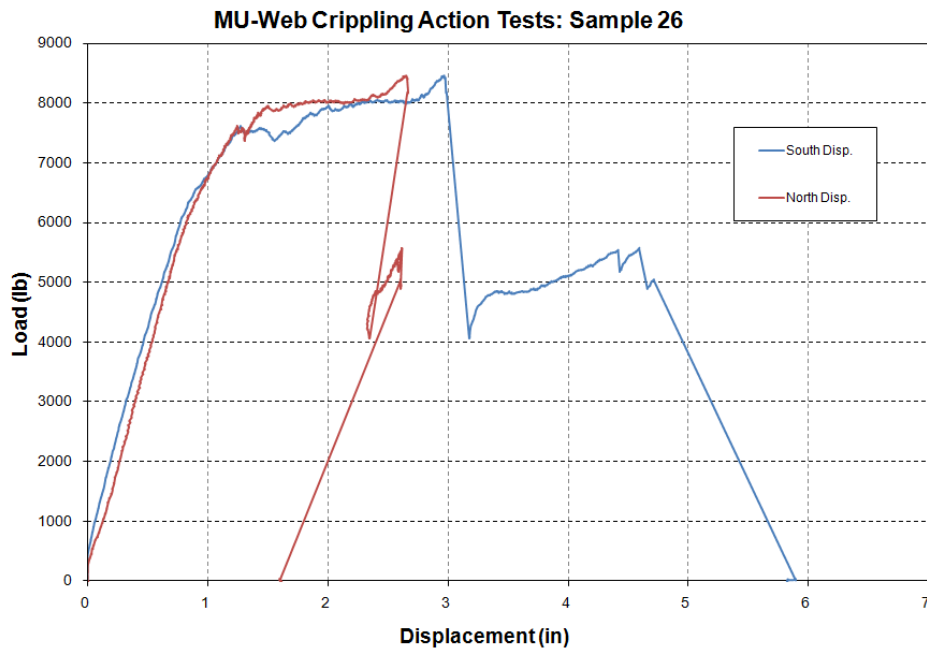


Figure A-52. Sample 26 Load-Displacement Plot



Figure A-53. Sample 27 after Failure

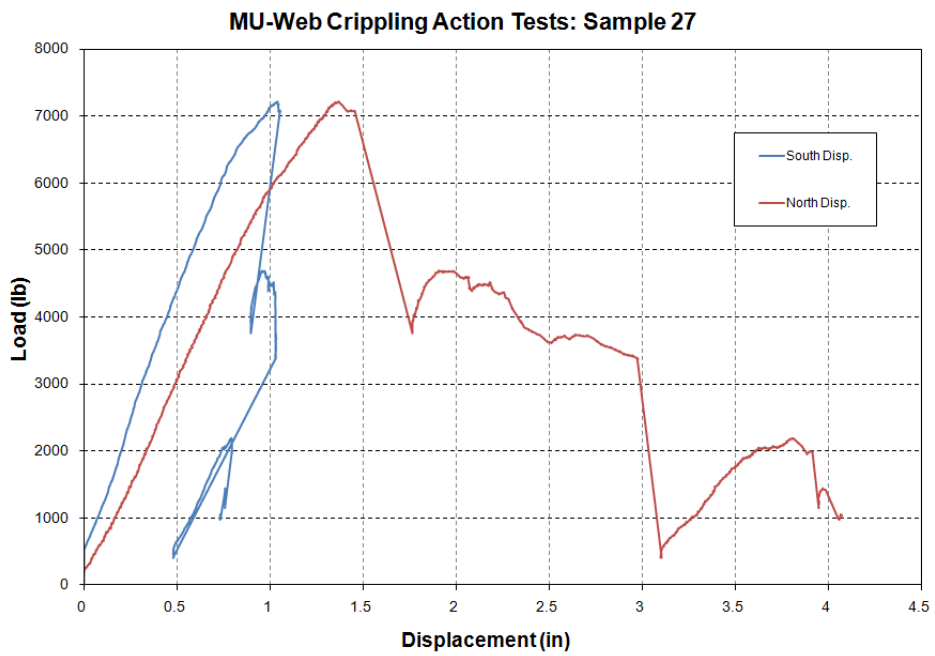


Figure A-54. Sample 27 Load–Displacement Plot



Figure A-55. Sample 28 after Failure

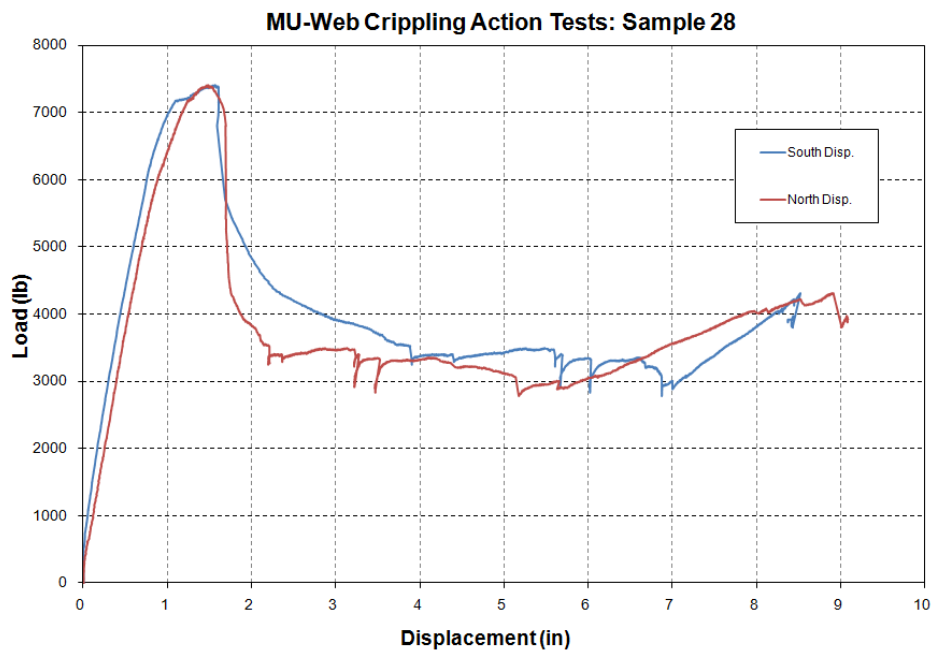


Figure A-56. Sample 28 Load-Displacement Plot



Figure A-57. Sample 29 after Failure

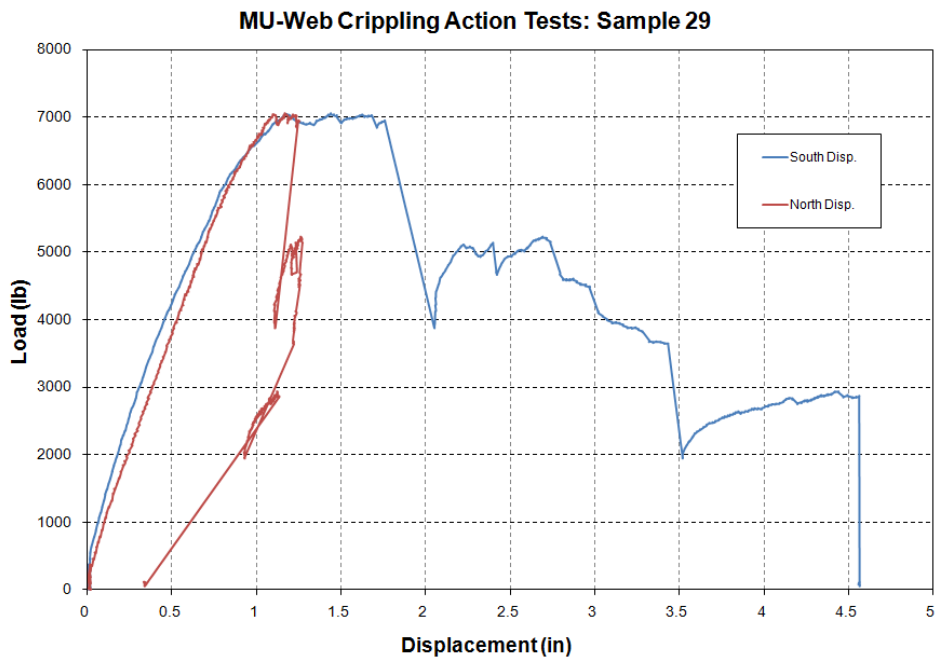


Figure A-58. Sample 29 Load-Displacement Plot



Figure A-59. Sample 30 after Failure

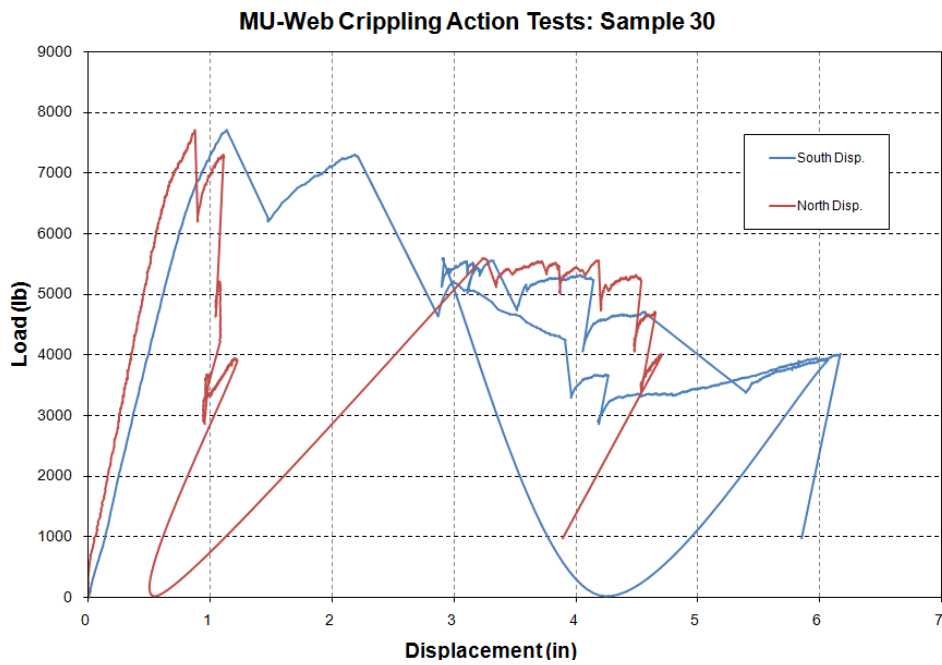


Figure A-60. Sample 30 Load-Displacement Plot



Figure A-61. Sample 31 after Failure

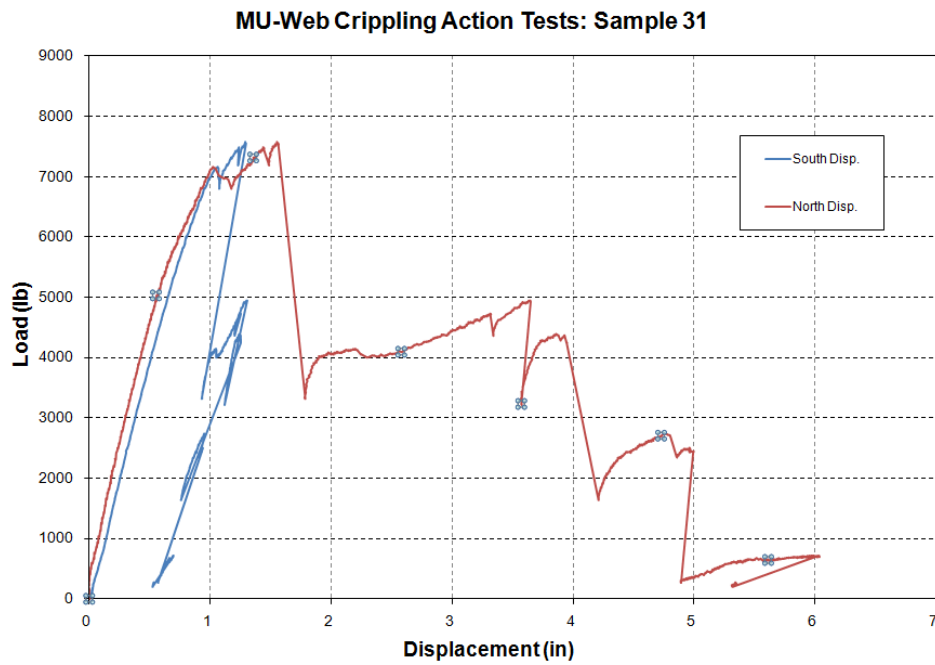


Figure A-62. Sample 31 Load-Displacement Plot



Figure A-63. Sample 32 after Failure

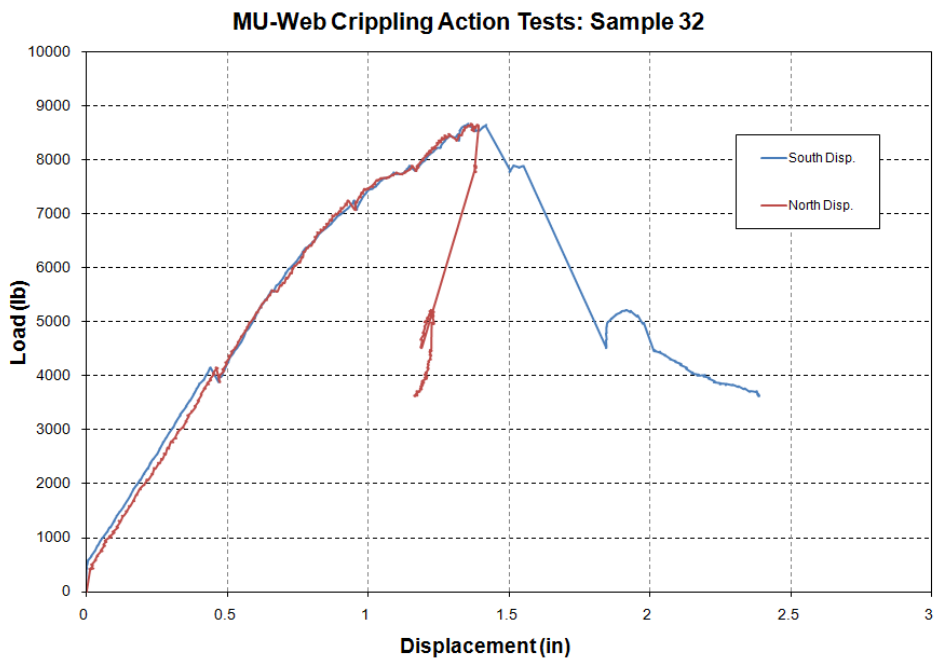


Figure A-64. Sample 32 Load–Displacement Plot



Figure A-65. Sample 33 after Failure

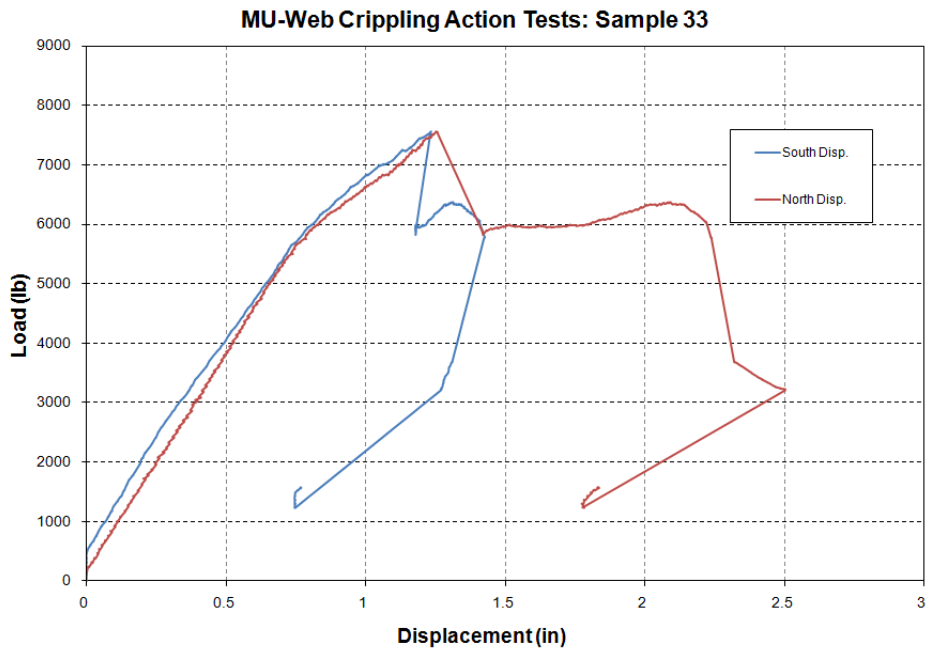


Figure A-66. Sample 33 Load-Displacement Plot



Figure A-67. Sample 34 after Failure

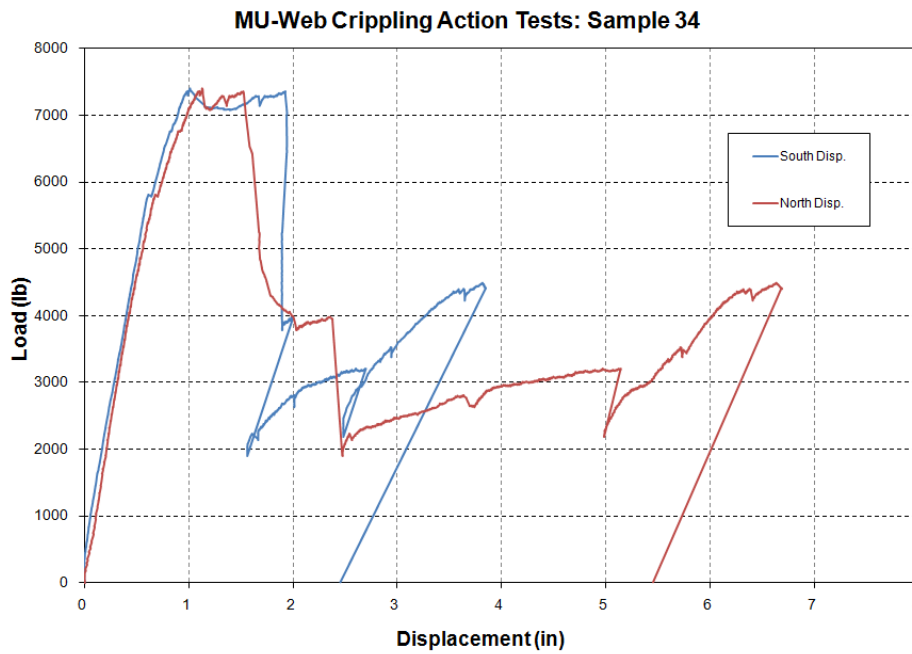


Figure A-68. Sample 34 Load-Displacement Plot



Figure A-69. Sample 35 after Failure

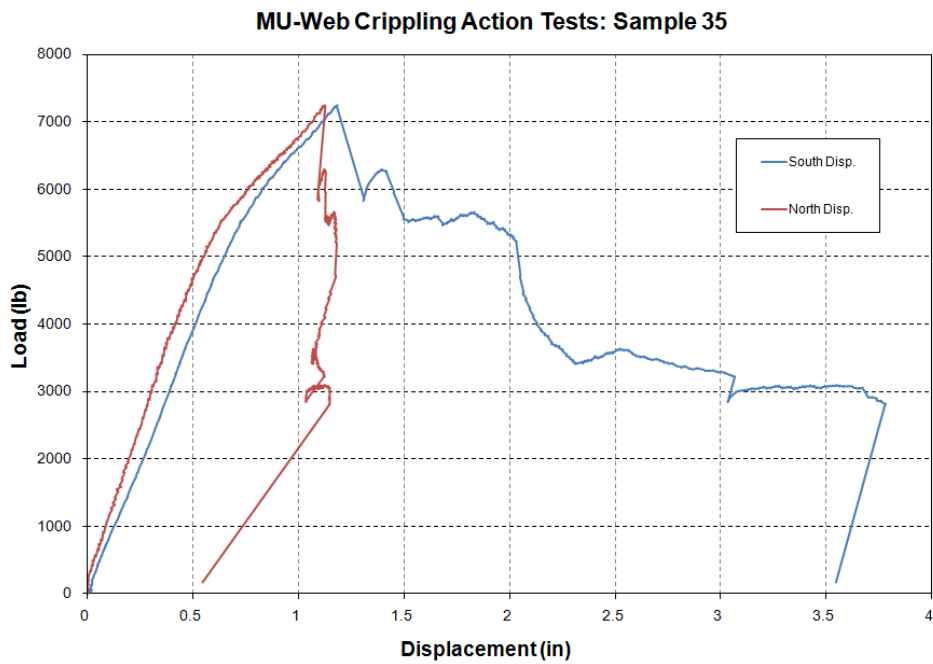


Figure A-70. Sample 35 Load-Displacement Plot



Figure A-71. Sample 36 after Failure

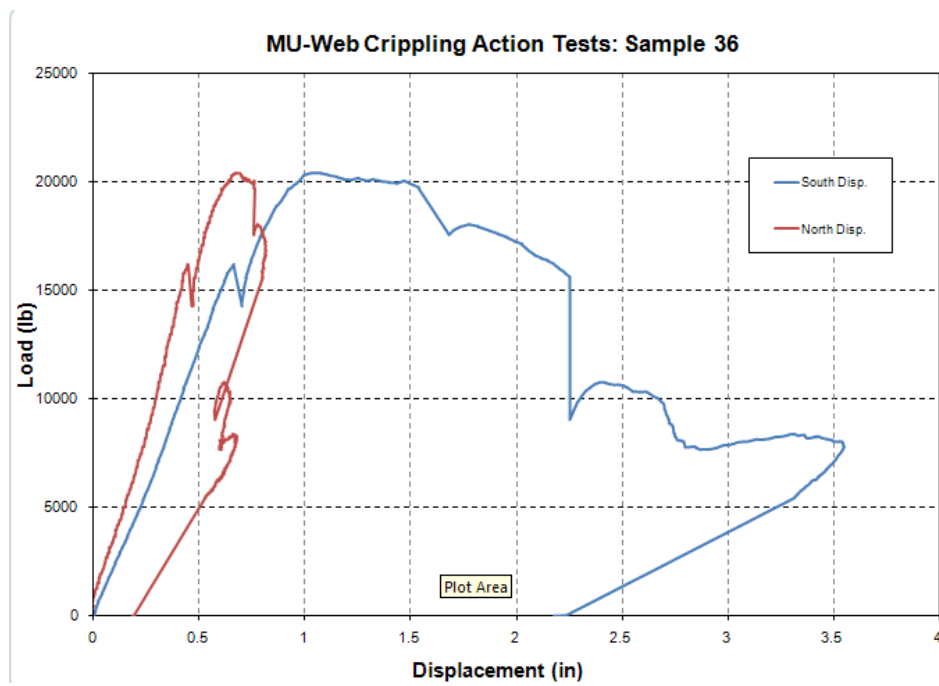


Figure A-72. Sample 36 Load–Displacement Plot



Figure A-73. Sample 37 after Failure

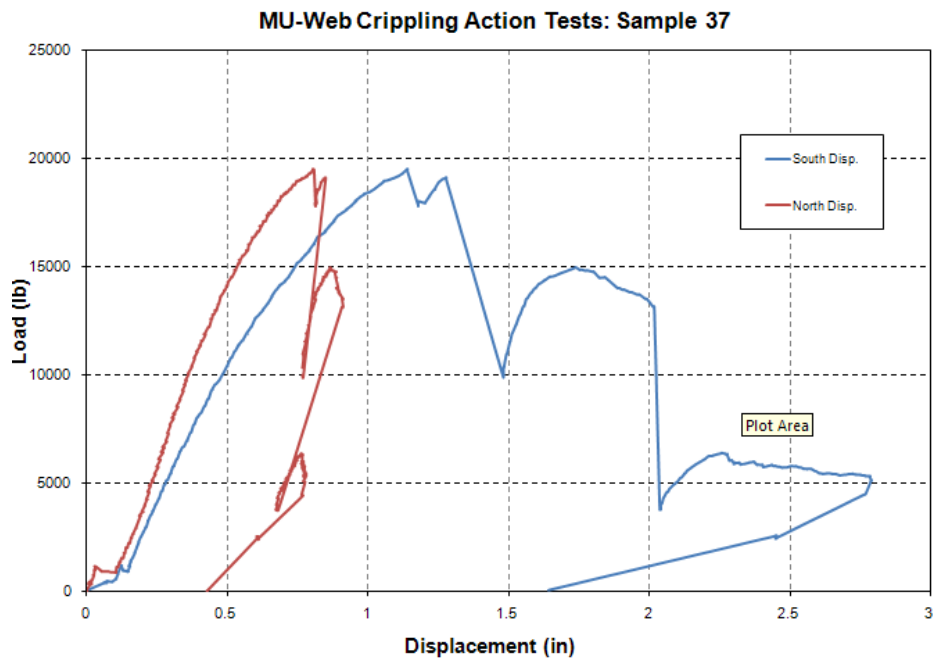


Figure A-74. Sample 37 Load-Displacement Plot



Figure A-75. Sample 38 after Failure

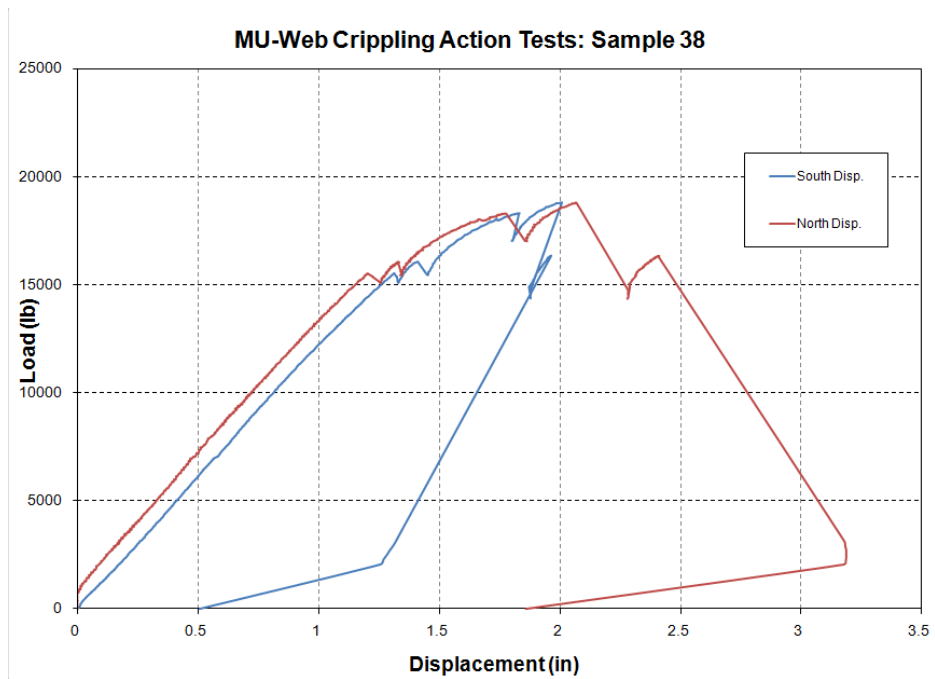


Figure A-76. Sample 38 Load-Displacement Plot



Figure A-77. Sample 39 after Failure

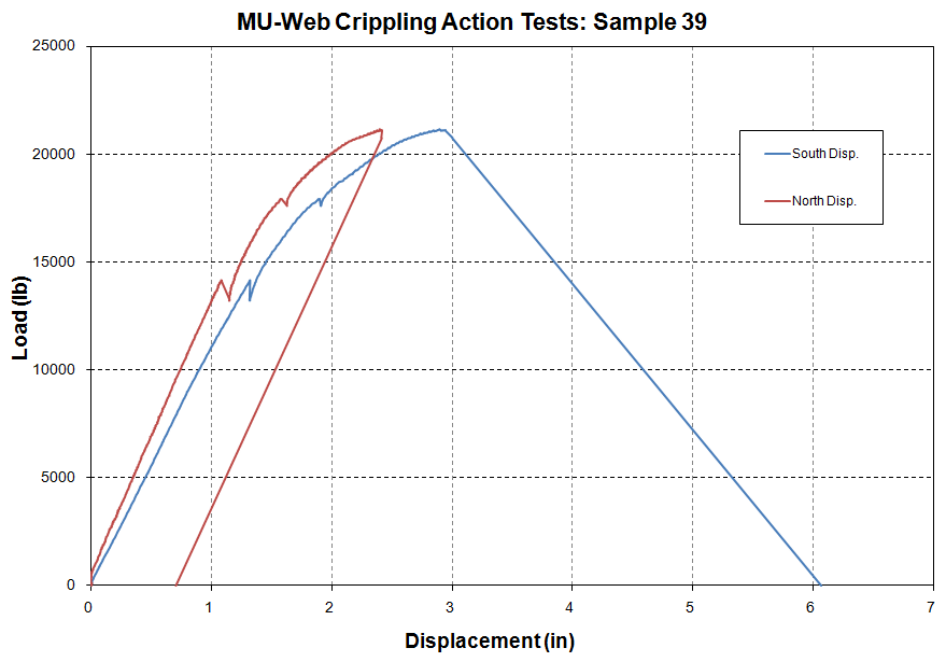


Figure A-78. Sample 39 Load-Displacement Plot



Figure A-79. Sample 40 after Failure

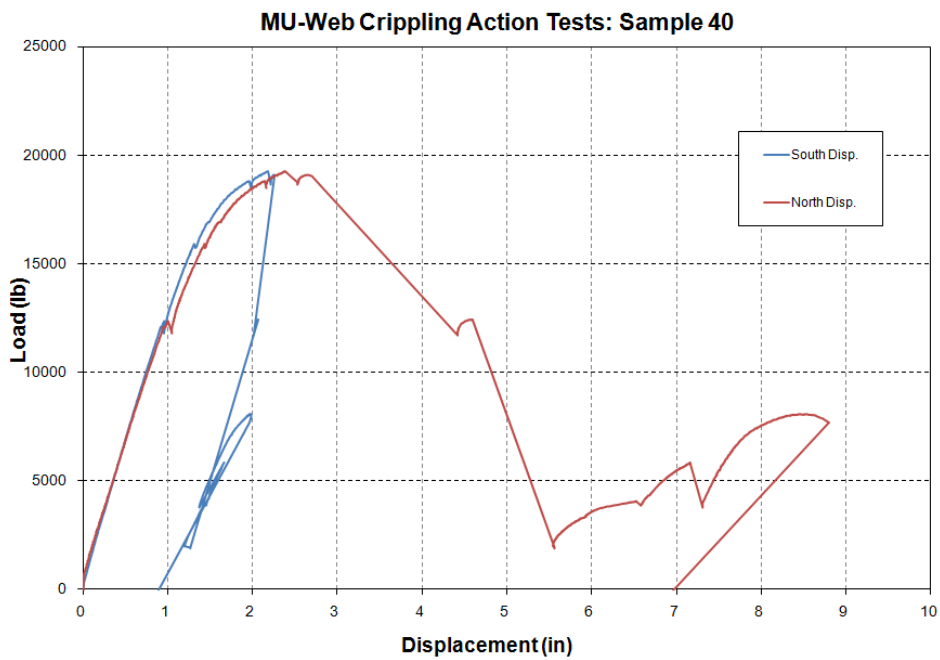


Figure A-80. Sample 40 Load-Displacement Plot



Figure A-81. Sample 41 after Failure

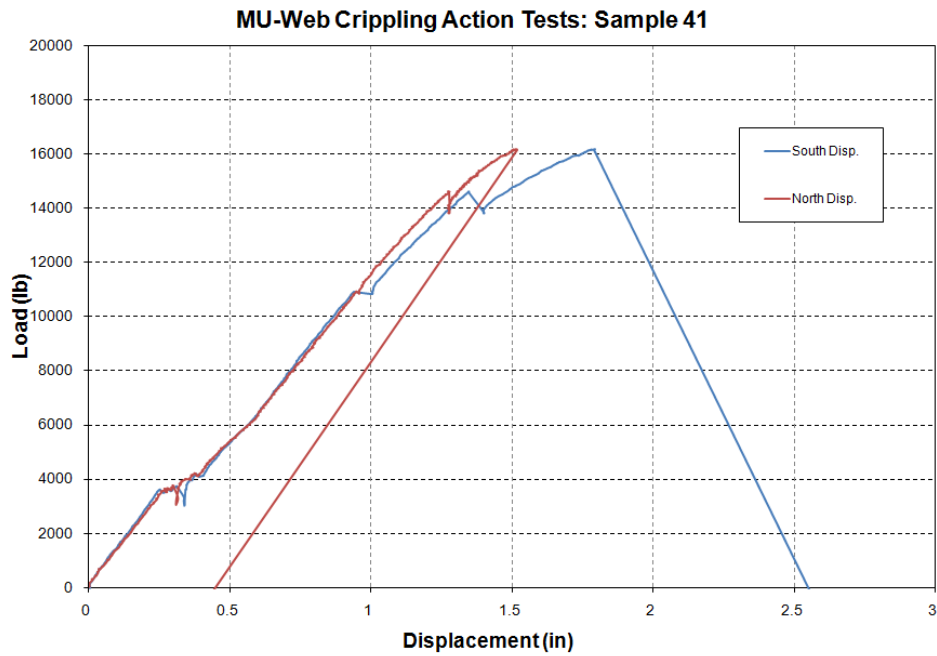


Figure A-82. Sample 41 Load–Displacement Plot



Figure A-83. Sample 42 after Failure

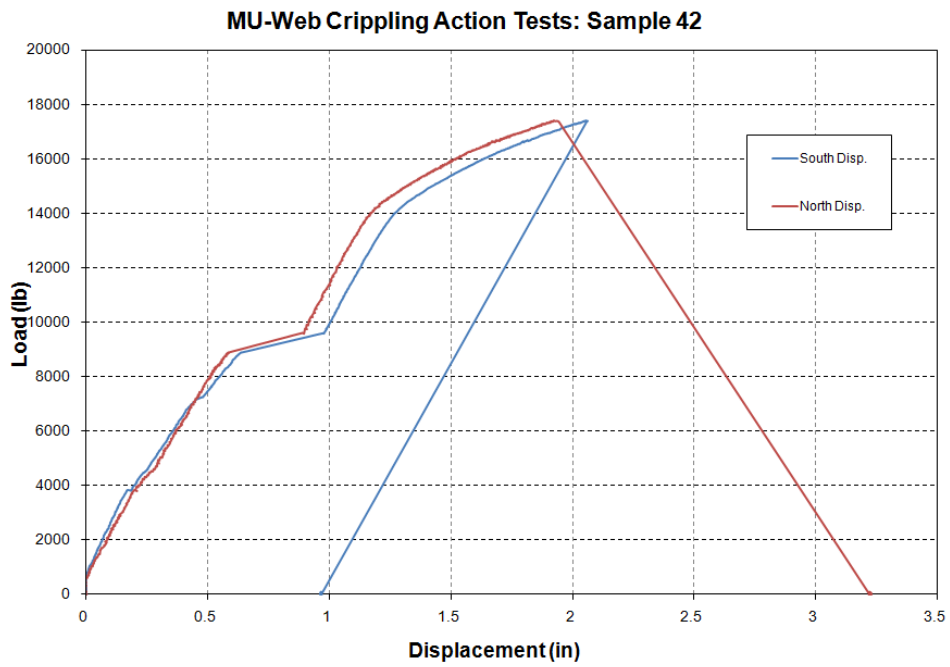


Figure A-84. Sample 42 Load-Displacement Plot



Figure A-85. Sample 43 after Failure

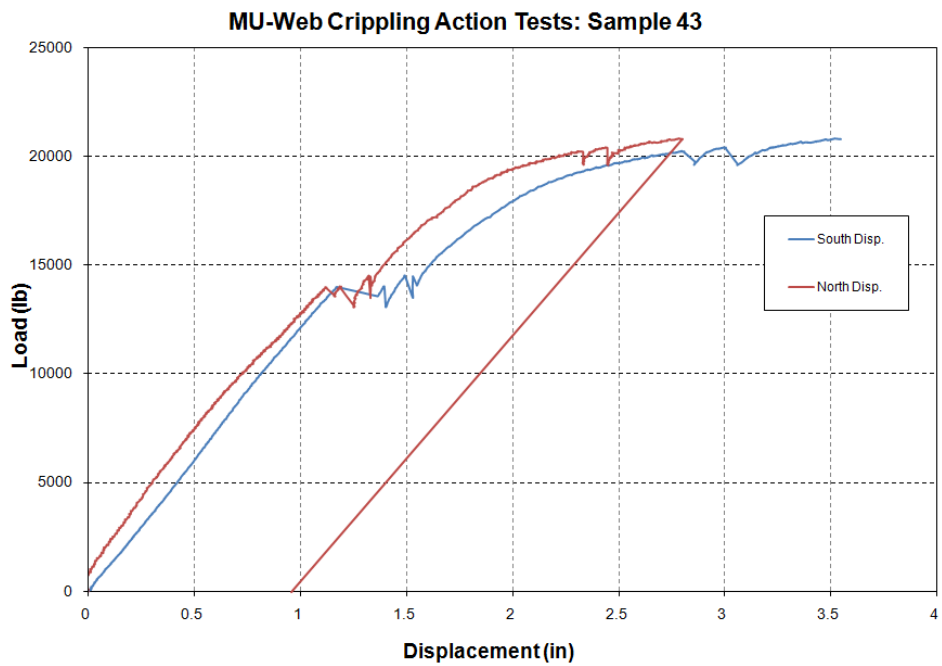


Figure A-86. Sample 43 Load-Displacement Plot



Figure A-87. Sample 44 after Failure

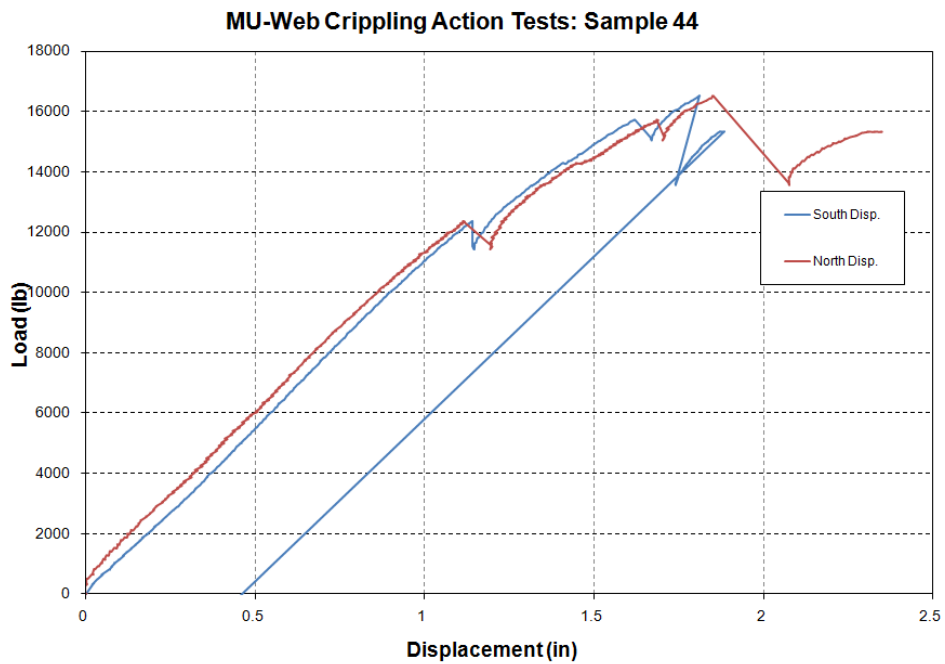


Figure A-88. Sample 44 Load-Displacement Plot



Figure A-89. Sample 45 after Failure

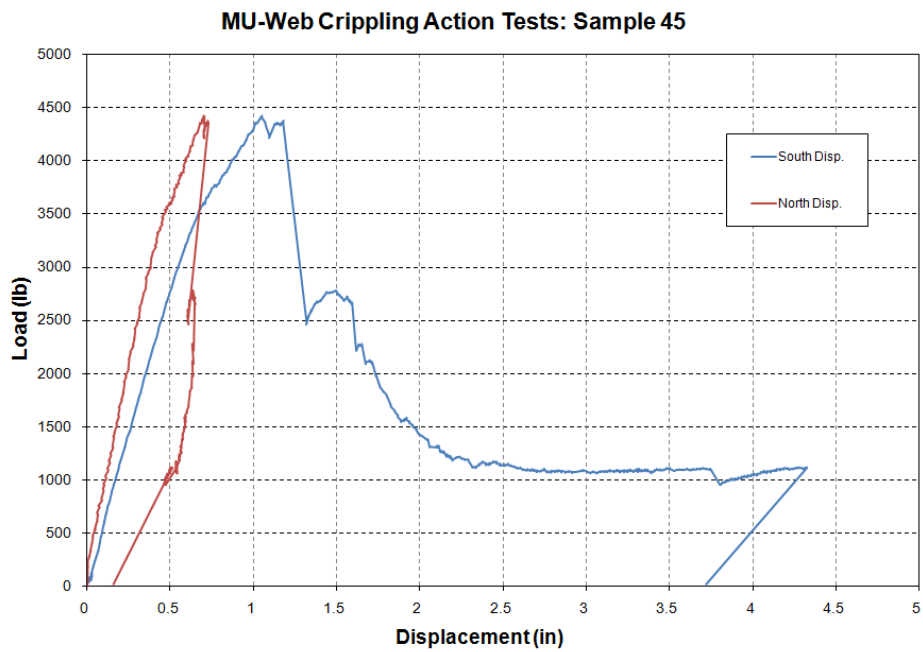


Figure A-90. Sample 45 Load-Displacement Plot



Figure A-91. Sample 46 after Failure

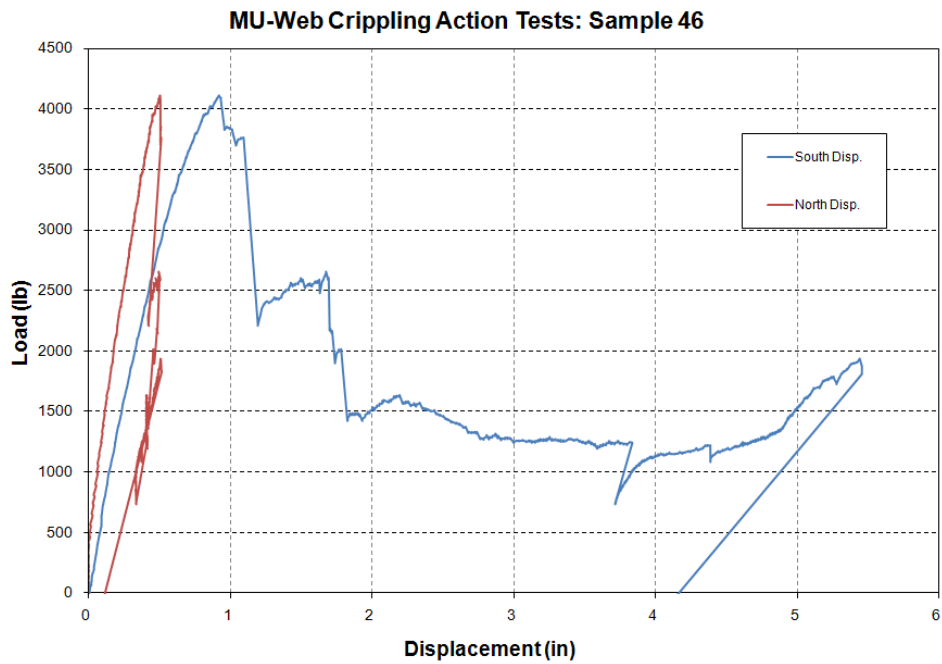


Figure A-92. Sample 46 Load-Displacement Plot



Figure A-93. Sample 47 after Failure

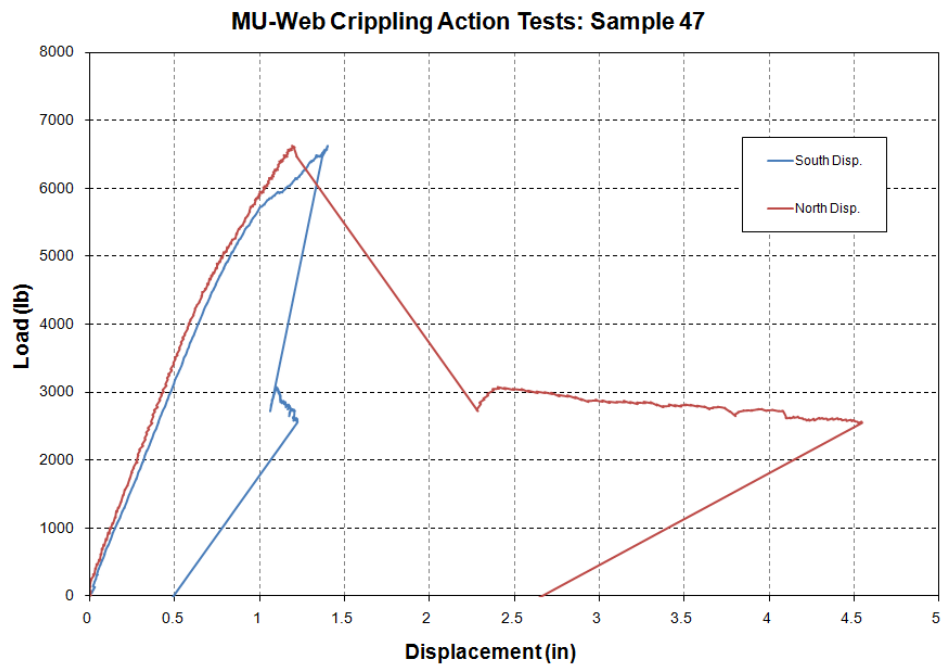


Figure A-94. Sample 47 Load-Displacement Plot



Figure A-95. Sample 48 after Failure

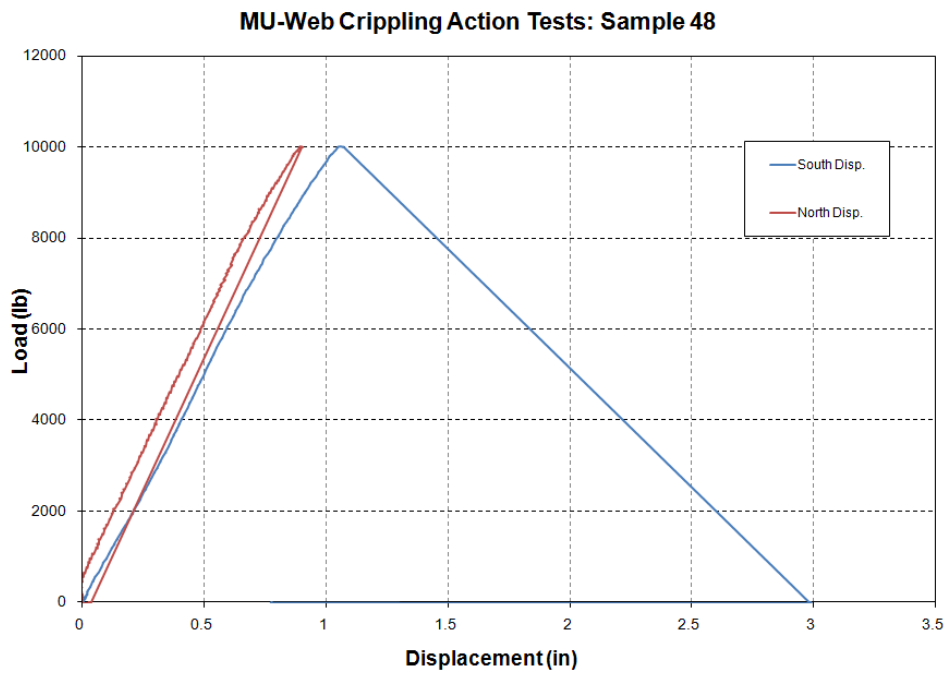


Figure A-96. Sample 48 Load-Displacement Plot

Appendix B: Full Length Beam Data

LIST OF FIGURES: APPENDIX B

Figure	Page
B-1. Full-Length Sample 18 after Failure.....	105
B-2. Full-Length Sample 18 after Failure.....	105
B-3. Full-Length Sample 18 after Failure.....	106
B-4. Full-Length Sample 18 Load–Displacement Plot.....	106
B-5. Full-Length Sample 19 after Failure.....	107
B-6. Full-Length Sample 19 after Failure.....	107
B-7. Full-Length Sample 19 Load–Displacement Plot.....	108
B-8. Full-Length Sample 20 after Failure.....	108
B-9. Full-Length Sample 20 after Failure.....	109
B-10. Full-Length Sample 20 Load–Displacement Plot.....	109
B-11. Full-Length Sample 25 after Failure.....	110
B-12. Full-Length Sample 25 after Failure.....	110
B-13. Full-Length Sample 25 after Failure.....	111
B-14. Full-Length Sample 25 Load–Displacement Plot.....	111
B-15. Full-Length Sample 36 after Failure.....	112
B-16. Full-Length Sample 36 after Failure.....	112
B-17. Full-Length Sample 36 Load–Displacement Plot.....	113
B-18. Full-Length Sample 40 after Failure.....	113
B-19. Full-Length Sample 40 after Failure.....	114
B-20. Full-Length Sample 40 Load–Displacement Plot.....	114
B-21. Full-Length Sample 43 after Failure.....	115
B-22. Full-Length Sample 43 after Failure.....	115
B-23. Full-Length Sample 43 Load–Displacement Plot.....	116
B-24. Full-Length Sample 45 after Failure.....	116
B-25. Full-Length Sample 45 Load–Displacement Plot.....	117
B-26. Full-Length Sample 48 after Failure.....	117
B-27. Full-Length Sample 48 after Failure.....	118
B-28. Full-Length Sample 48 Load–Displacement Plot.....	118
B-29. Full-Length Sample 50 after Failure.....	119
B-30. Full-Length Sample 50 after Failure.....	119
B-31. Full-Length Sample 50 Load–Displacement Plot.....	120
B-32. Full-Length Sample 51 after Failure.....	120
B-33. Full-Length Sample 51 after Failure.....	121
B-34. Full-Length Sample 51 Load–Displacement Plot.....	121
B-35. Full-Length Sample 52 after Failure.....	122
B-36. Full-Length Sample 52 after Failure.....	122
B-37. Full-Length Sample 52 Load–Displacement Plot.....	123
B-38. Full-Length Sample 54 after Failure.....	123
B-39. Full-Length Sample 54 after Failure.....	124
B-40. Full-Length Sample 54 Load–Displacement Plot.....	124
B-41. Full-Length Sample 67 after Failure.....	125
B-42. Full-Length Sample 67 after Failure.....	125

B-43. Full-Length Sample 67 Load–Displacement Plot.....	126
B-44. Full-Length Sample 68 after Failure.....	126
B-45. Full-Length Sample 68 Load–Displacement Plot.....	127
B-46. Full-Length Sample 69 after Failure.....	127
B-47. Full-Length Sample 69 Load–Displacement Plot.....	128



Figure B-1. Full-Length Sample 18 after Failure



Figure B-2. Full-Length Sample 18 after Failure



Figure B-3. Full-Length Sample 18 after Failure

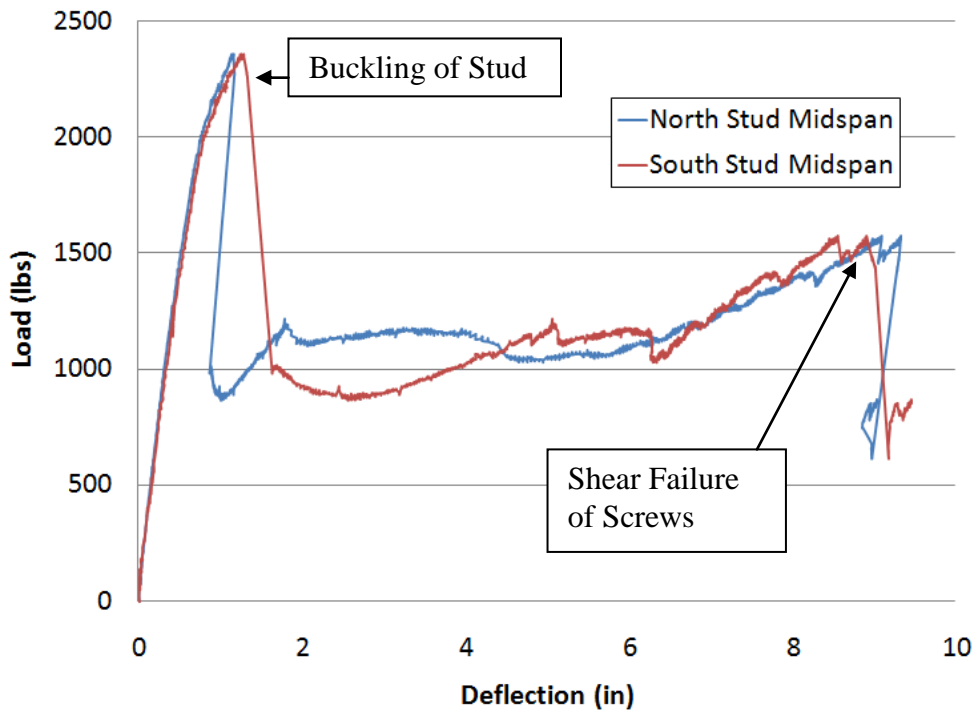


Figure B-4. Full-Length Sample 18 Load-Displacement Plot



Figure B-5. Full-Length Sample 19 after Failure



Figure B-6. Full-Length Sample 19 after Failure

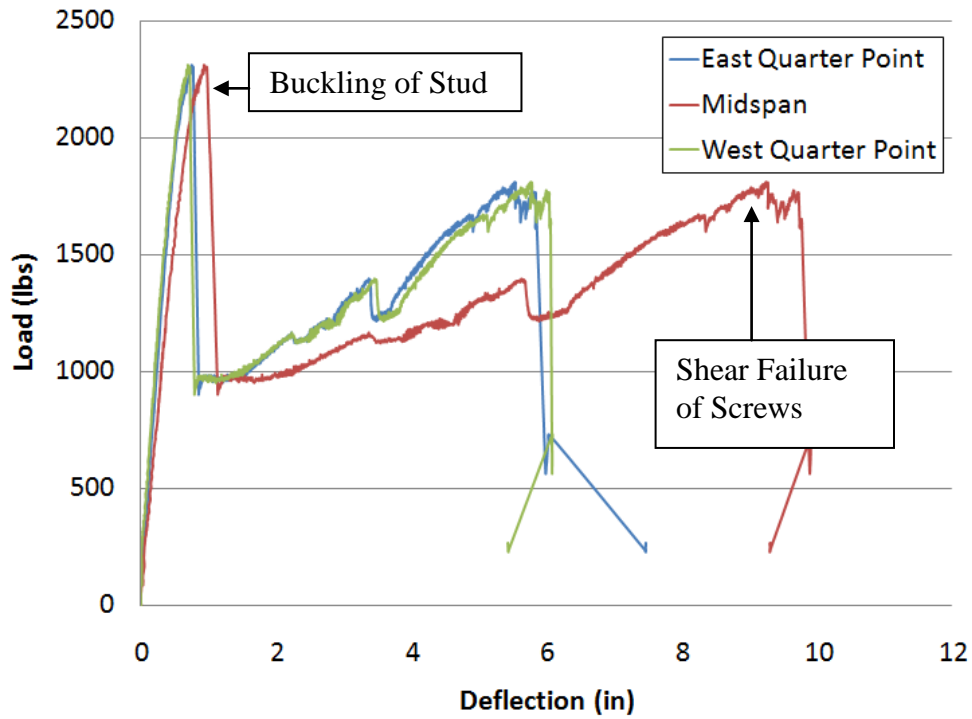


Figure B-7. Full-Length Sample 19 Load-Displacement Plot



Figure B-8. Full-Length Sample 20 after Failure



Figure B-9. Full-Length Sample 20 after Failure

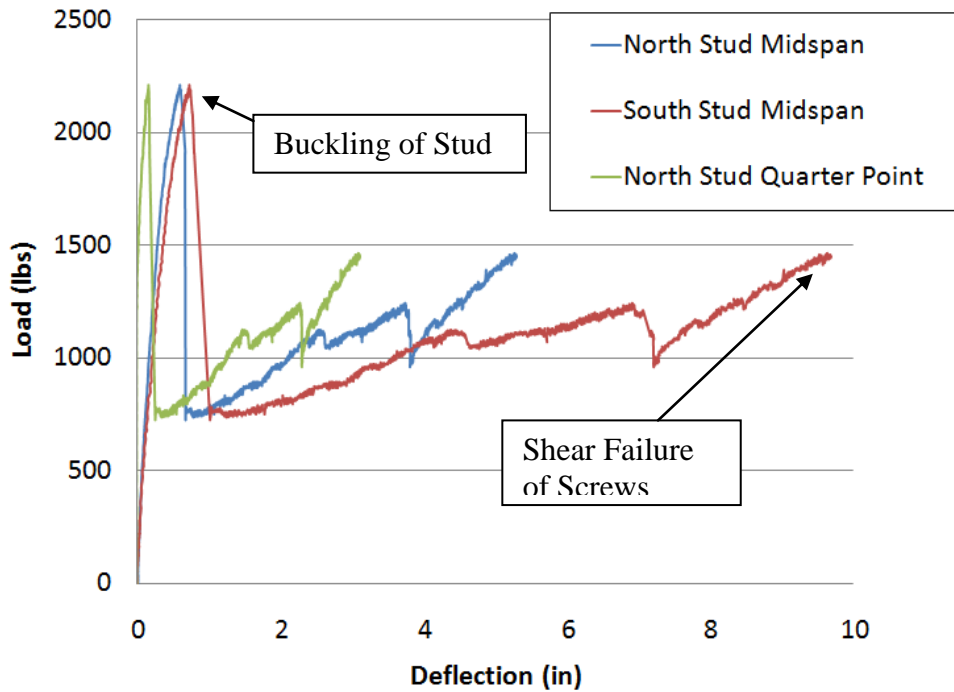


Figure B-10. Full-Length Sample 20 Load-Displacement Plot



Figure B-11. Full-Length Sample 25 after Failure



Figure B-12. Full-Length Sample 25 after Failure



Figure B-13. Full-Length Sample 25 after Failure

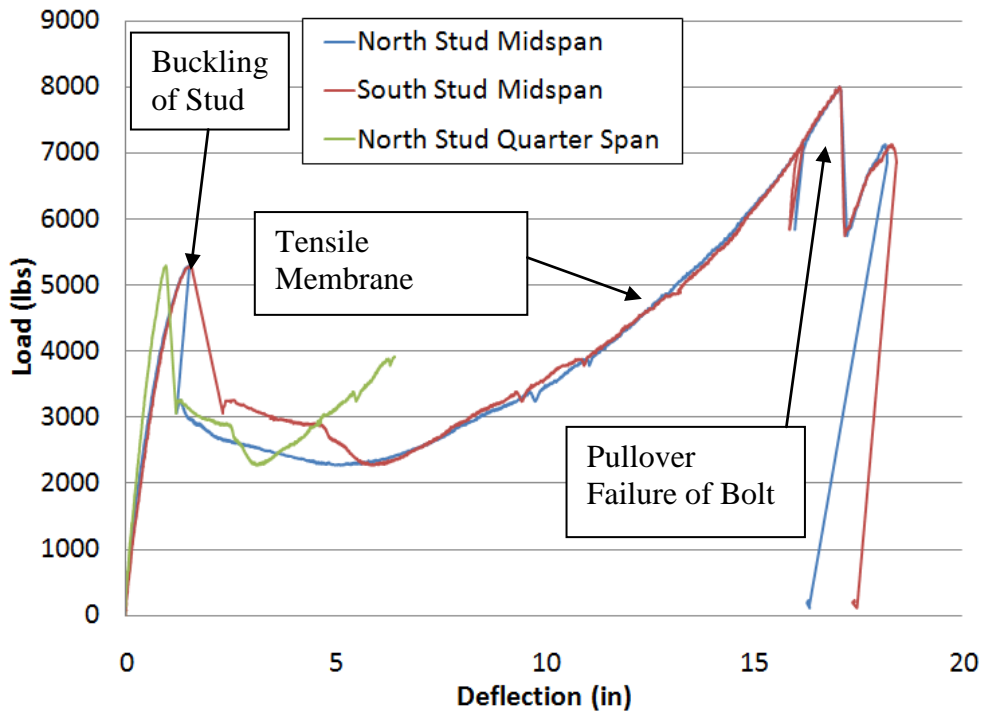


Figure B-14. Full-Length Sample 25 Load-Displacement Plot



Figure B-15. Full-Length Sample 36 after Failure



Figure B-16. Full-Length Sample 36 after Failure

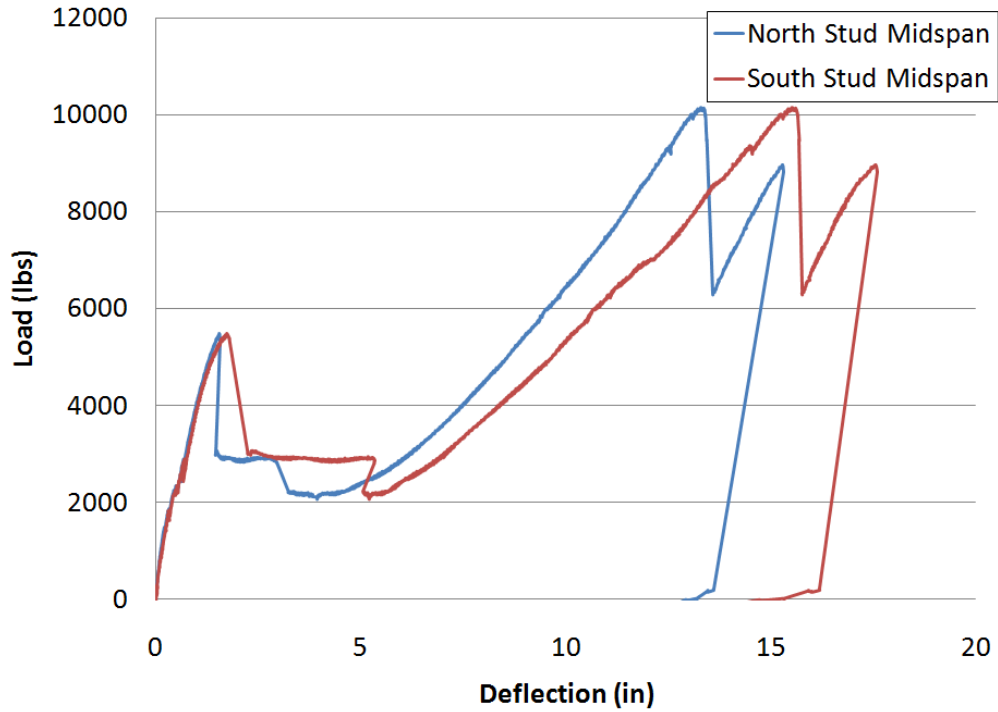


Figure B-17. Full-Length Sample 36 Load-Displacement Plot



Figure B-18. Full-Length Sample 40 after Failure

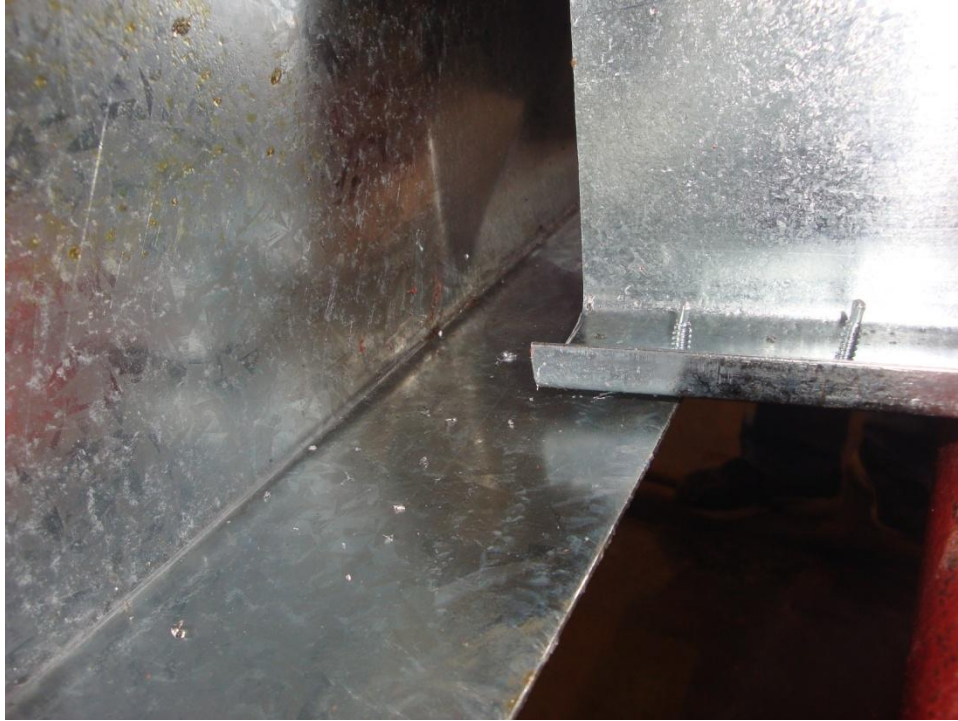


Figure B-19. Full-Length Sample 40 after Failure

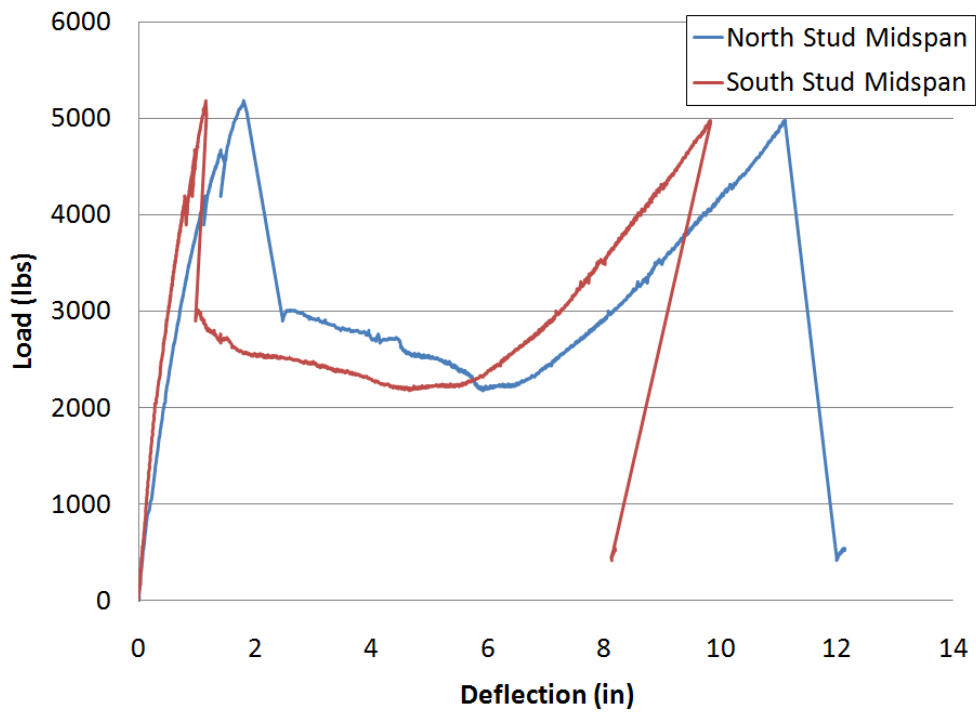


Figure B-20. Full-Length Sample 40 Load-Displacement Plot



Figure B-21. Full-Length Sample 43 after Failure



Figure B-22. Full-Length Sample 43 after Failure

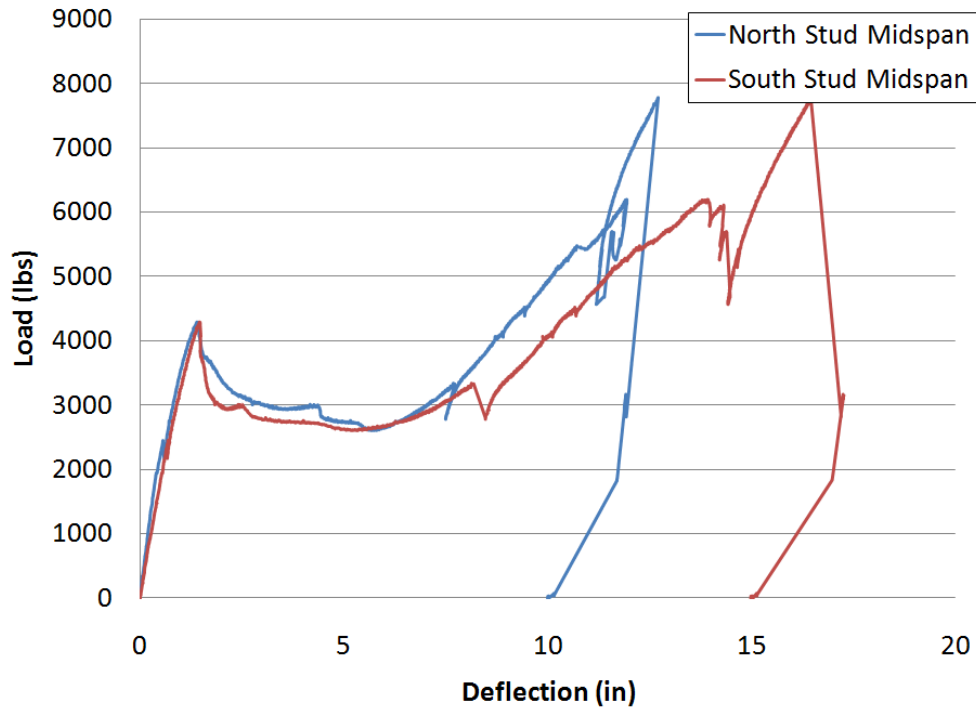


Figure B-23. Full-Length Sample 43 Load-Displacement Plot

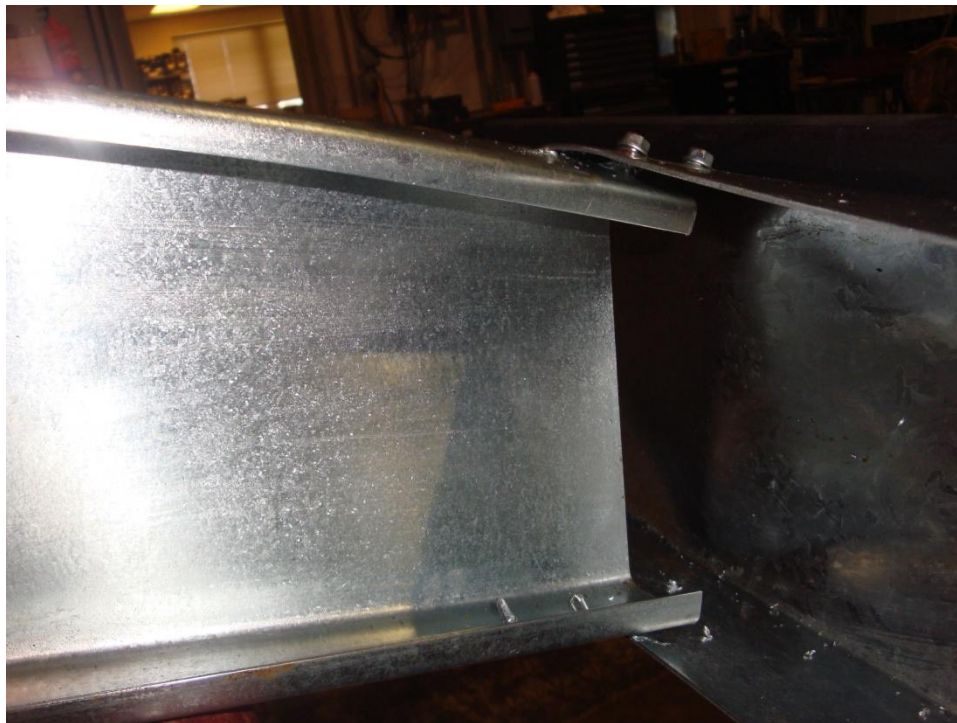


Figure B-24. Full-Length Sample 45 after Failure

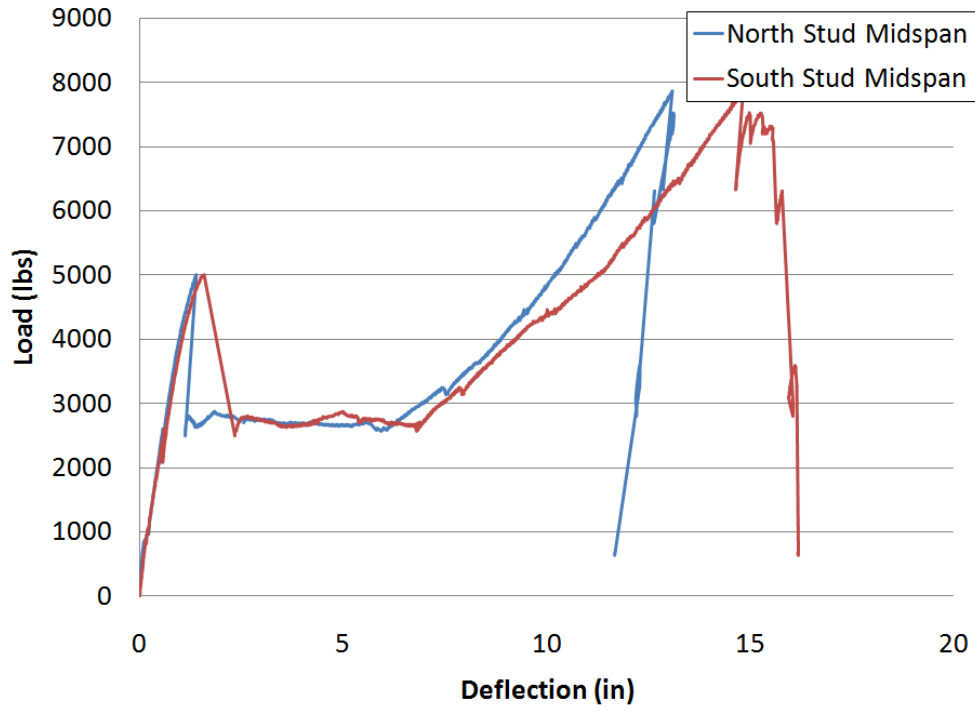


Figure B-25. Full-Length Sample 45 Load-Displacement Plot

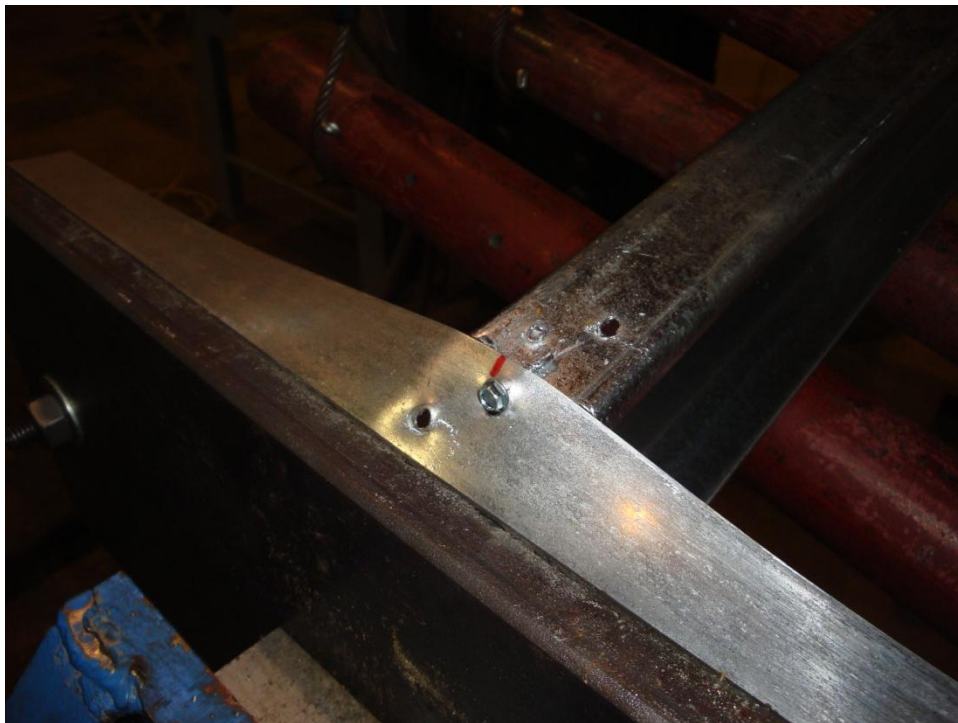


Figure B-26. Full-Length Sample 48 after Failure



Figure B-27. Full-Length Sample 48 after Failure

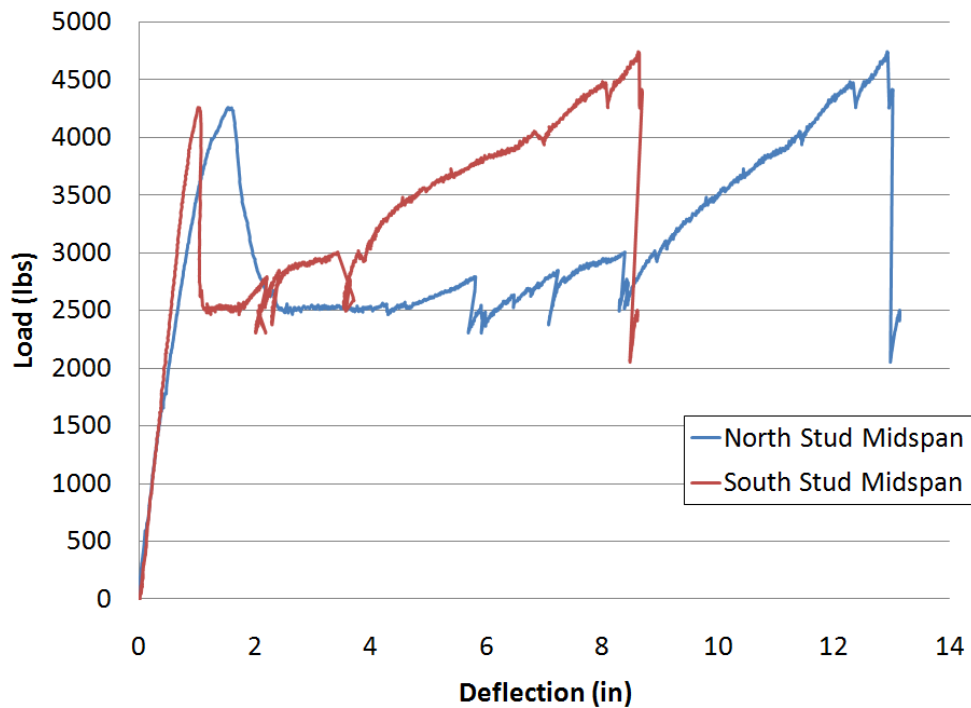


Figure B-28. Full-Length Sample 48 Load-Displacement Plot



Figure B-29. Full-Length Sample 50 after Failure

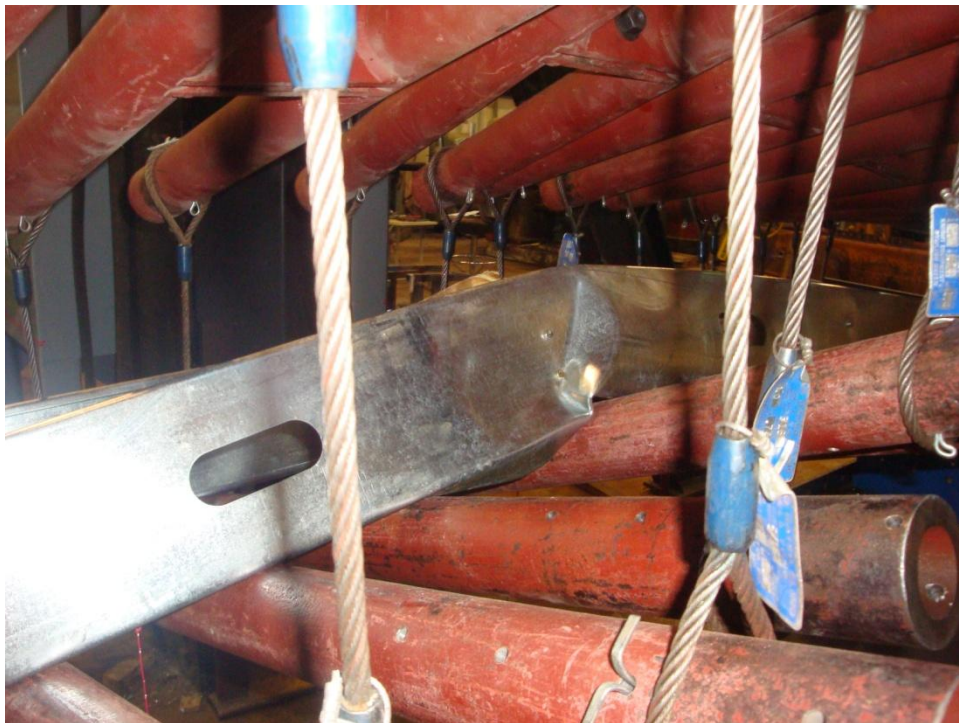


Figure B-30. Full-Length Sample 50 after Failure

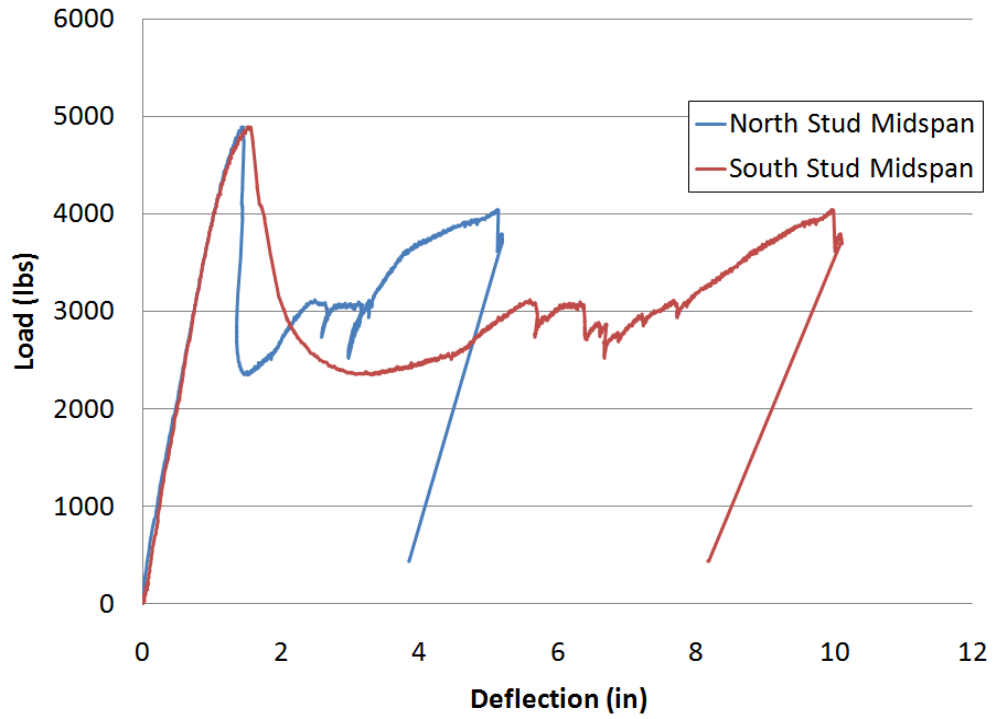


Figure B-31. Full-Length Sample 50 Load-Displacement Plot



Figure B-32. Full-Length Sample 51 after Failure



Figure B-33. Full-Length Sample 51 after Failure

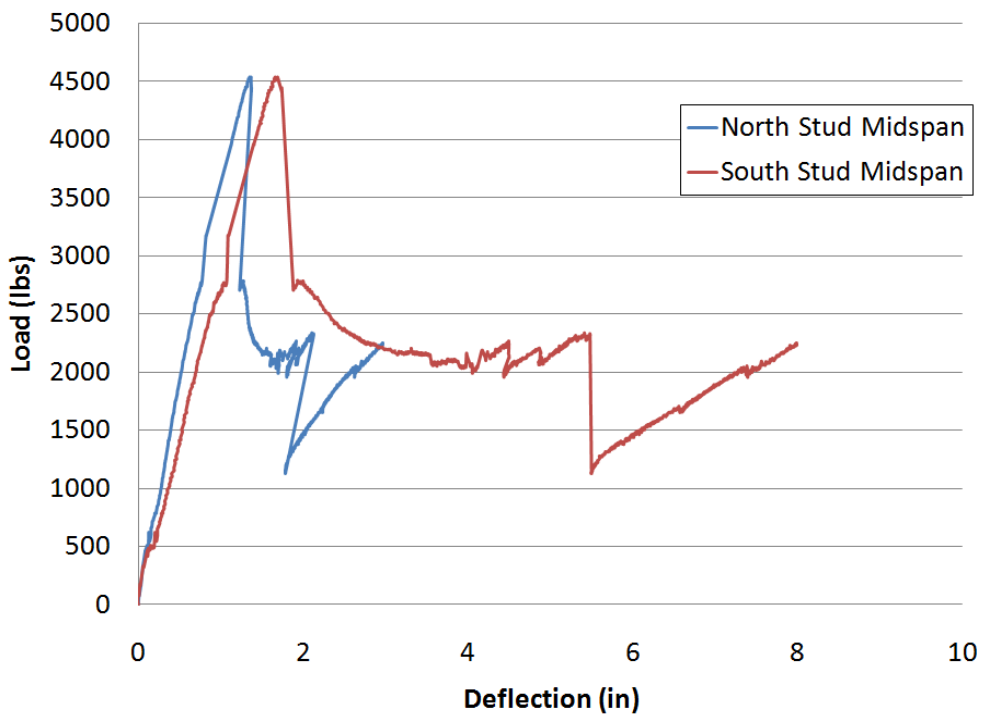


Figure B-34. Full-Length Sample 51 Load-Displacement Plot



Figure B-35. Full-Length Sample 52 after Failure



Figure B-36. Full-Length Sample 52 after Failure

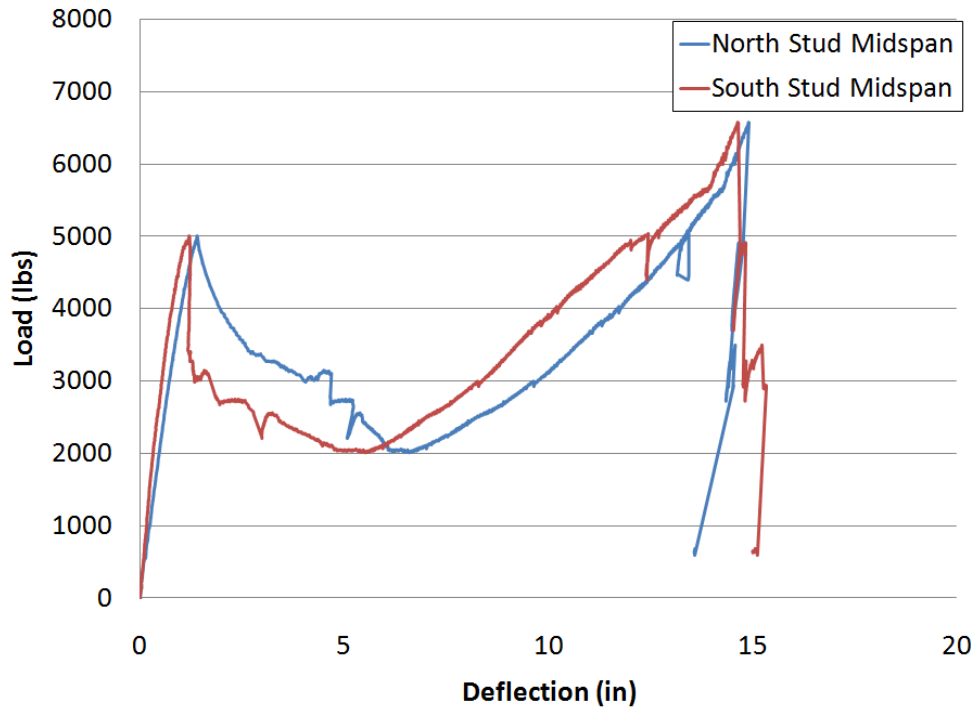


Figure B-37. Full-Length Sample 52 Load–Displacement Plot

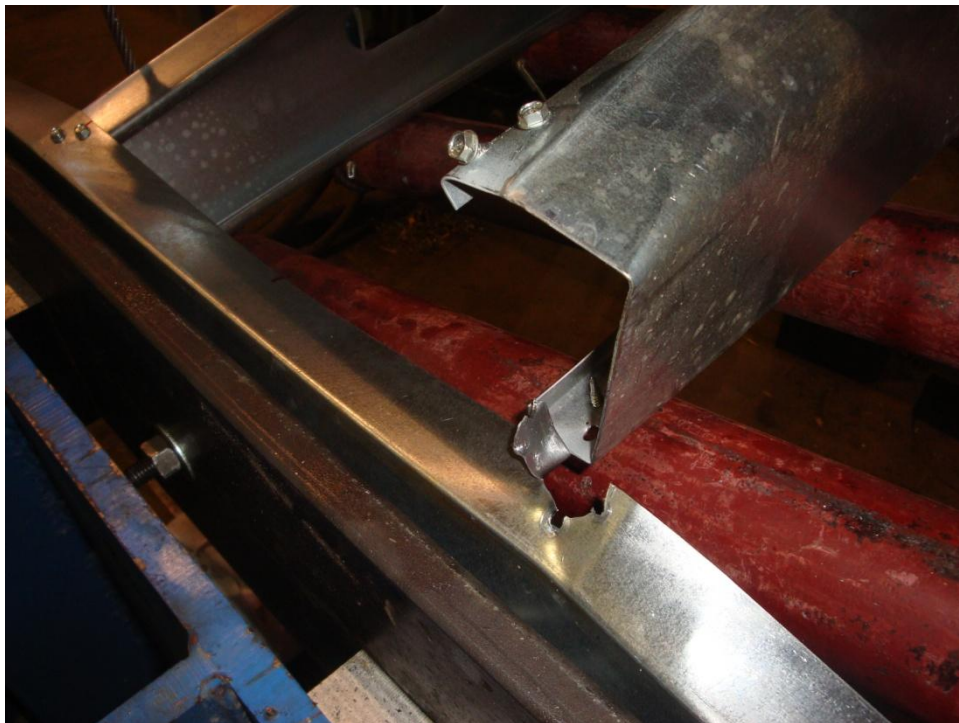


Figure B-38. Full-Length Sample 54 after Failure



Figure B-39. Full-Length Sample 54 after Failure

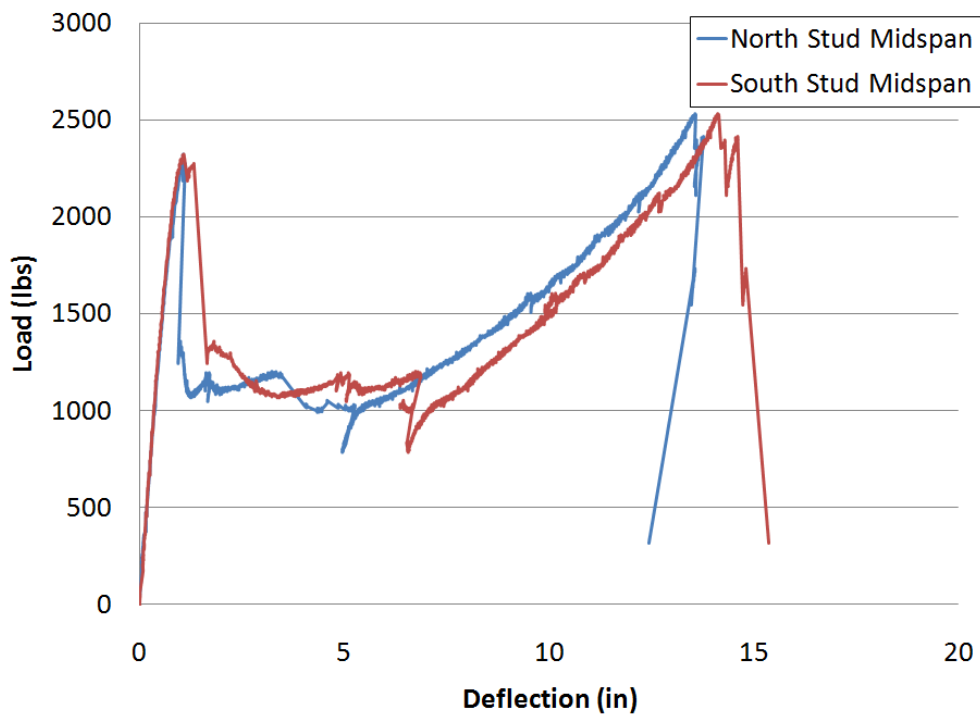


Figure B-40. Full-Length Sample 54 Load-Displacement Plot



Figure B-41. Full-Length Sample 67 after Failure



Figure B-42. Full-Length Sample 67 after Failure

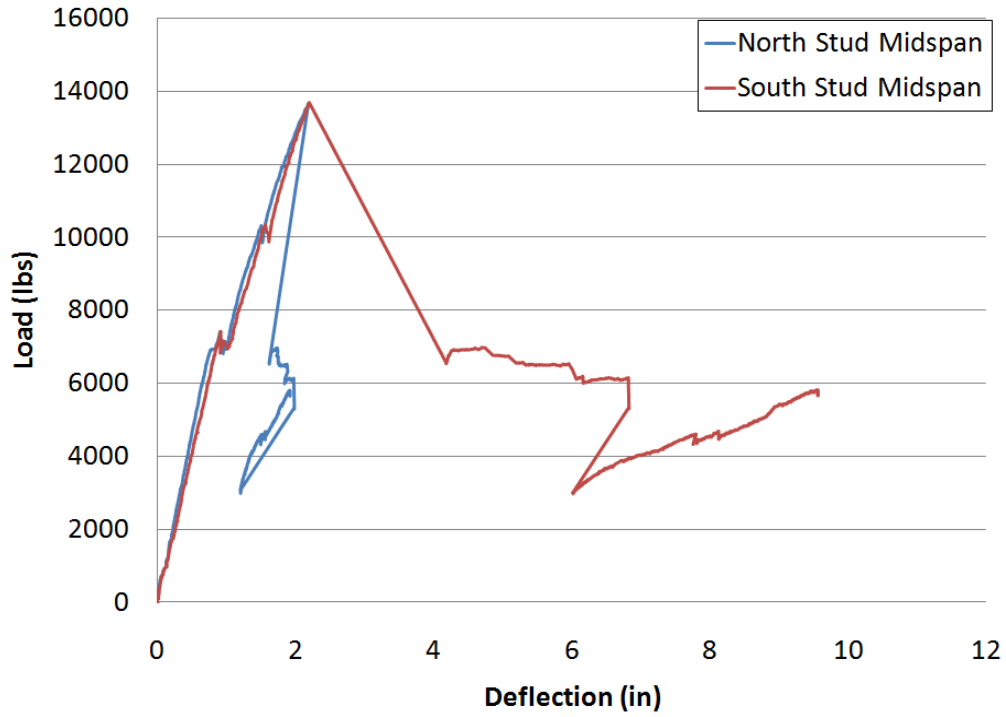


Figure B-43. Full-Length Sample 67 Load-Displacement Plot



Figure B-44. Full-Length Sample 68 after Failure

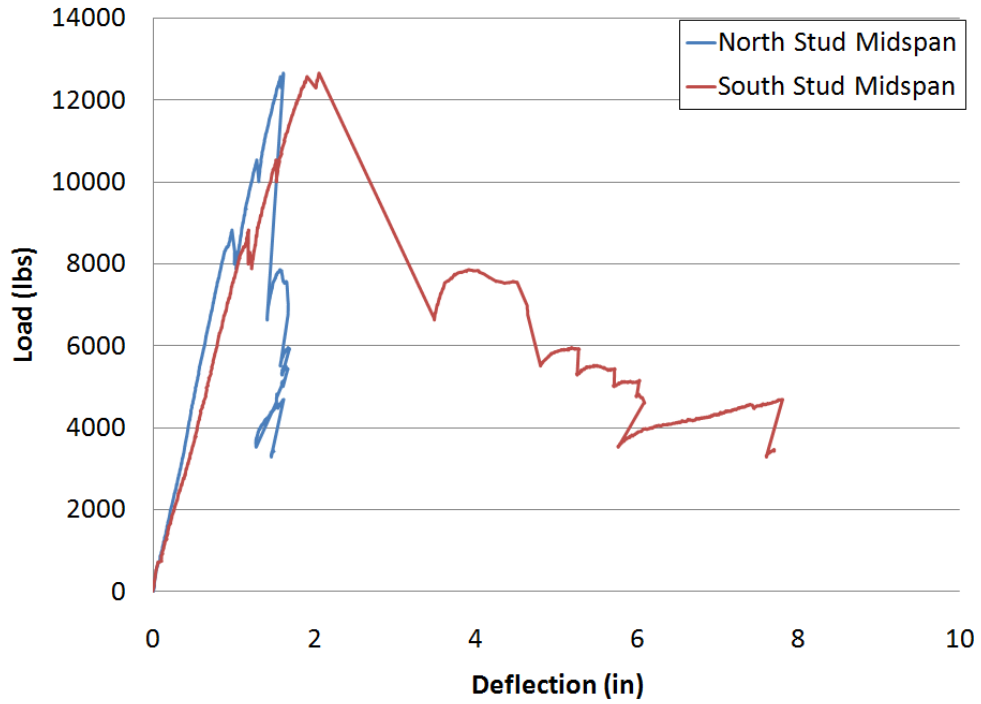


Figure B-45. Full-Length Sample 68 Load–Displacement Plot

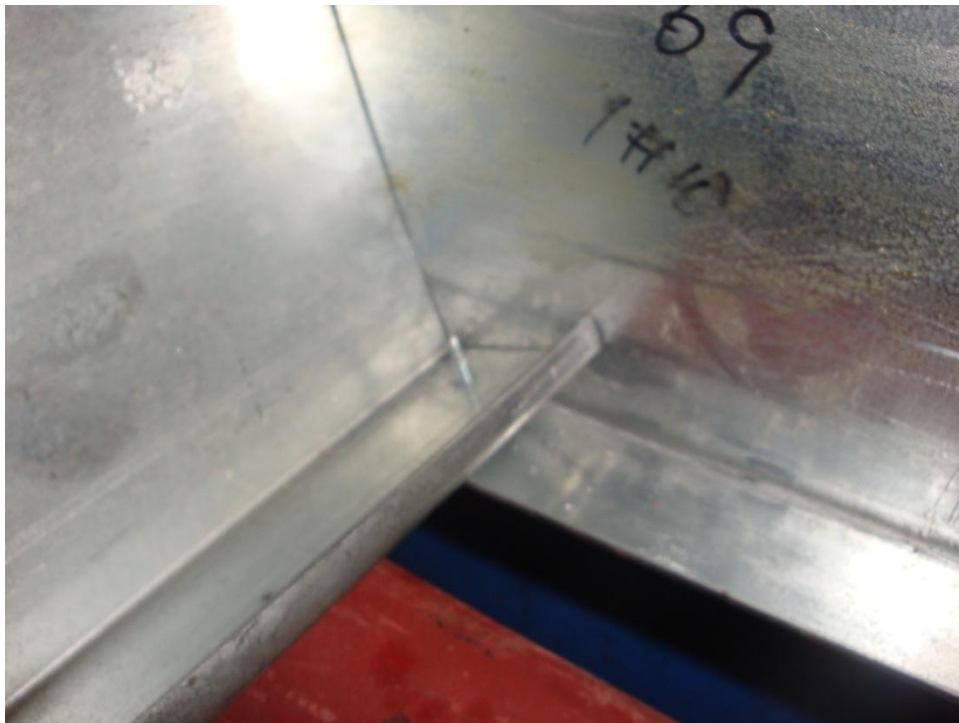


Figure B-46. Full-Length Sample 69 after Failure

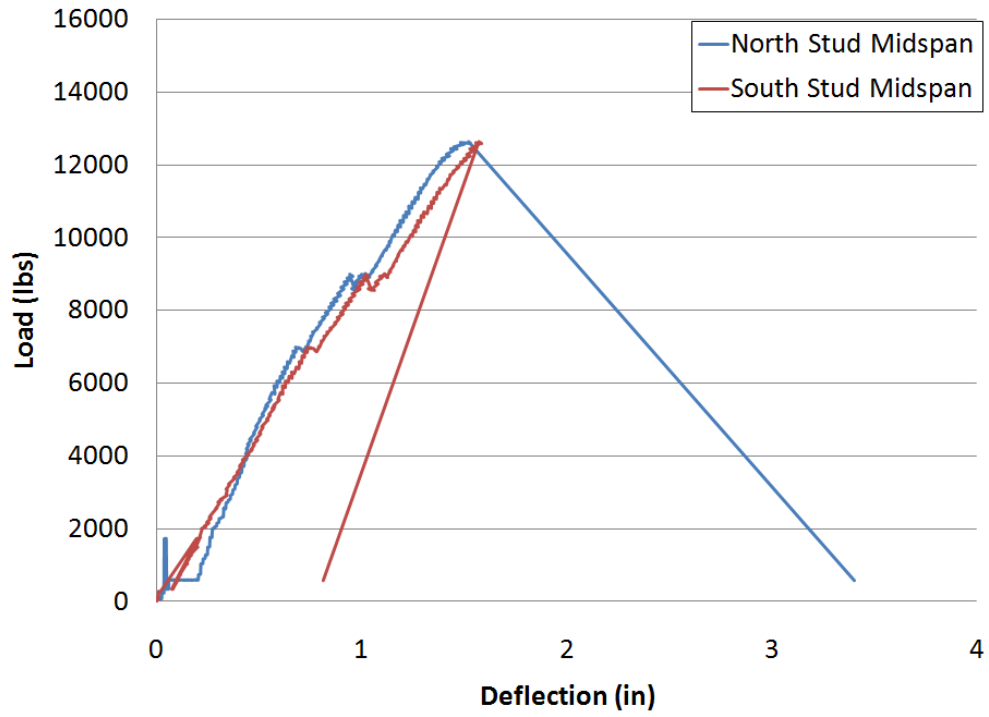


Figure B-47. Full-Length Sample 69 Load–Displacement Plot

Appendix C: Allowable Response Limits (developed by US Army Corps of Engineers, PDC)

Response Limits Summary Sheet	Dynamic Analysis Response Limits									
	HLOP		MLOP		LLOP		VLOP		Note #	
	μ	θ	μ	θ	μ	θ	μ	θ		
Reinforced Concrete										
Slab and Beams in Flexure										
No Tension Membrane										
Single-Reinforced or Double-Reinforced w/o Shear Reinforcing	1	-	-	1	-	2	-	3	1	
Double-Reinforced w/ Shear Reinforcing	1	-	-	1	-	4	-	6	2	
With Tension Membrane										
Normal Proportions (L/h>=5)	1	-	-	1	-	12	-	20		
Deep Proportions (L/h<5)	1	-	-	1	-	8	-	12		
Compression Members										
Walls & Seismic Columns	0.9	-	1	-	2	-	3	-	3, 4	
Non-Seismic Columns	0.7	-	0.8	-	0.9	-	1	-	4	
Structural Steel (hot rolled)										
Beams - Seismic Section	2	1	4	2	10	6	20	12		
Beams - Compact Section	1	-	2	-	3	-	5	-		
Beams - Noncompact Section	0.7	-	0.85	-	1	-	1.2	-		
Plates	4	1	8	2	20	6	40	12		
Columns & Beam Columns	0.9	-	1.3	-	2	-	3	-		
Wood										
Walls	0.5	-	-	1.6	-	2.3	-	5.1		
Roofs	0.5	-	-	1.0	-	1.4	-	3.2		
Beams	0.5	-	-	1.2	-	1.7	-	3.7		
Exterior Columns - Flexural Mode	0.5	-	-	1.2	-	1.7	-	3.7		
Interior Columns - Buckling	-	-	-	-	-	-	1	2.4		
Prestressed Concrete										
Slab and Beams in Flexure										
$\omega_p > 0.30$	0.7	-	0.8	-	0.9	-	1	-	5, 6	
$0.15 < \omega_p < 0.30$	0.8	-	$0.25/\omega_p$	1	$0.29/\omega_p$	1.5	$0.33/\omega_p$	2	5	
$\omega_p < 0.15$	1	-	-	1	-	2	-	3	5, 7	
With Tension Membrane										
Normal Proportions (L/h >= 5)	1	-	-	1	-	6	-	10		
Steel Joist										
Flexural Response - downward loading	1	1	2	2	5	3	10	4	8	
Shear Response	0.7	-	0.8	-	0.9	-	1	-	9	
Flexural Response - upward	1	-	1.5	-	2	-	3	-		
Masonry										
Unreinforced	1	-	-	0.5	-	1	-	2	10	
Reinforced	1	-	-	0.5	-	2	-	7	11	
Cold Formed Steel										
Girts and Purlins	0.5	-	1	0.5	2	2	5	5		
Metal Studs										
with full tensile membrane capacity	0.5	-	1	0.5	2	2	5	5		
with studs connected top and bottom	0.5	-	1	0.5	1.8	1.3	3	2		
with sliding connection	0.5	-	0.75	-	0.9	-	1	-		
Corrugated Metal Deck										
with some tensile membrane capacity	1	-	-	1.0	-	4.0	-	8.0		
with limited tensile membrane capacity	1	-	1.8	1.3	3	2.0	6	4.0		
Standing Seam Metal Deck	1	-	1.8	1.3	3	2.0	6	4.0		
Doors										
Structural Steel (hot rolled)										
Built-up (composite plate & stiffeners)	3	1	10	6	20	12	NA	NA	12	
Plate (solid)	3	1	20	6	40	12	NA	NA	12	
Hollow Metal Doors Seating into Stops										
3X7 Single Leaf Common										
6X7 Double Leaf Common										

Note: μ = ductility; θ = end rotation; HLOP = High Level of Protection; MLOP = Medium Level of Protection; LLOP = Low Level of Protection; VLOP = Very Low Level of Protection

LIST OF SYMBOLS, ABBREVIATIONS, AND ACRONYMS

AFRL	Air Force Research Laboratory
A_g	gross cross-sectional area
A_w	area of web element
BREW	blast-resistant exterior wall
c	damping coefficient
C	coefficient from cold-formed steel design manual
C_h	web slenderness coefficient from cold-formed steel design manual
C_N	bearing length coefficient from cold-formed steel design manual
C_R	bend radius coefficient from cold-formed steel design manual
d	screw diameter
d'_w	washer diameter
E	modulus of elasticity of steel
F_d	distortional buckling stress
$F(t)$	load as a function of time, t
F_u	ultimate stress
F_v	nominal shear stress
F_y	yield stress
h	flat dimension of web measured in plane of web
k	stiffness
k_v	shear buckling coefficient
M	mass
N	bearing length
P	pressure
P_n	nominal axial strength
P_{ns}	nominal shear strength per screw
P_s	peak pressure
R	static resistance function (Eq. 3)
R	inside bend radius (Eq. 4)
t	thickness
t	time
t_d	time duration of the blast
θ	angle between plane of web and bearing surface
μ	Poisson's ratio
UFC	Unified Facilities Criteria
V_n	nominal shear strength
WCA	web crippling action
y	deflection at a specified point